ADAPTIVE OBSERVER DESIGNS FOR FRICTION ESTIMATION IN POSITION CONTROL OF SIMPLE MECHANICAL SYSTEMS WITH TIME DELAY

A DISSERTATION SUBMITTED TO

THE GRADUATE SCHOOL OF ENGINEERING AND SCIENCE

OF BILKENT UNIVERSITY

IN PARTIAL FULFILLMENT OF THE REQUIREMENTS FOR

THE DEGREE OF

DOCTOR OF PHILOSOPHY

IN

ELECTRICAL AND ELECTRONICS ENGINEERING

By

Caner Odabaş

September 2021

ADAPTIVE OBSERVER DESIGNS FOR FRICTION ESTIMATION IN POSITION CONTROL OF SIMPLE MECHANICAL SYSTEMS WITH TIME DELAY

By Caner Odabaş

September 2021

We certify that we have read this dissertation and that in our opinion it is fully adequate, in scope and in quality, as a dissertation for the degree of Doctor of Philosophy.

Ömer Morgül(Advisor)

Hitay Özbay

Melih Çakmakcı

Kemal Leblebicioğlu

Coşku Kasnakoğlu

Approved for the Graduate School of Engineering and Science:

Ezhan Karaşan
Director of the Graduate School

ABSTRACT

ADAPTIVE OBSERVER DESIGNS FOR FRICTION ESTIMATION IN POSITION CONTROL OF SIMPLE MECHANICAL SYSTEMS WITH TIME DELAY

Caner Odabaş
Ph.D. in Electrical and Electronics Engineering
Advisor: Ömer Morgül
September 2021

Friction force/torque is a well known natural effect that can cause performance degradation or even instability in mechanical systems, although it sometimes can be disregarded in closed loop feedback design phase. Hence, friction modeling and cancellation methods can be vital to achieve desired robustness and performance criteria in position control problems.

Basically, the topic of friction cancellation is divided into two main categories named model based and non-model based methods. Friction modeling is a broad area of research and there are lots of different modeling approaches in various complexities. Among these approaches, Coulomb Model is one the simplest yet fundamental models. Nevertheless, in some cases, being a classical static model, it is inadequate to exhibit the dominant friction components occurring at different motion stages such as break-away force, stick-slip motion, pre-sliding behavior or friction lag. Generally, dynamical models, i.e. LuGre Model, are more advanced as a result, they are better to describe such friction effects. Unfortunately, for these cases, the number of friction parameters are increased. In fact, there is a trade-off between model complexity and parameter identification. A desired system response may not be achieved when model parameters do not coincide with the existing friction coefficients. In this manner, precise identification of each parameter can be challenging when there are many of them. Besides, some of these parameters might be time varying due to environment, temperature, material properties, position, etc. Therefore, non-model based adaptive schemes are prevalent in the literature since these methods do not require any parameter identification.

In this study, we focus on adaptive observer based friction compensation techniques and provide some stability conditions. First, we consider simple second order mechanical systems with or without time delay under Coulomb friction. To estimate the Coulomb friction, we first consider Friedland-Park observer. Then,

some necessary conditions are stated to extend the estimation function in the observer structure to a larger class of functions. Especially measurement delay can be significant since observers estimate friction based on the velocity measurements. Therefore, it is proposed to employ a velocity predictor either based on numerical differential equation solvers or inverse Pade approximant when the existing time delay is large. What is more, a new observer design that considers friction and velocity error dynamics together is proposed as a novel contribution. Extensive MATLAB simulations are conducted to investigate the performances of proposed observers in a closed loop position control system with and without delay. To this end, Smith predictor and ITAE index-based designs are considered to utilize a position controller. In some of these simulations, LuGre model is preferred to mimic the actual friction instead of Coulomb friction in order to observe the effects of dynamic parameters. Moreover, some experiments are performed on DC motor platform driven by Arduino Uno microcontroller. Under the light of acquired results, observer based friction compensation improves the system performance even existing friction cannot be confined to Coulomb coefficient, especially when the implemented controller has low bandwidth. Also, in terms of practicability, it is an advantage that these observer structures do not require any parameter identification.

Keywords: Friction observer, Time delay, ITAE Index, Smith predictor, Controller Parametrization, Position Control, Adaptive Control, Dwell Time, Numerical Differential Equation Solvers, Pade Approximation.

ÖZET

ZAMAN GECİKMELİ BASİT MEKANİK SİSTEMLERİN POZİSYON KONTROLÜNDE SÜRTÜNME KESTİRİMİ İÇİN ADAPTİF GÖZLEMCİ TASARIMLARI

Caner Odabaş
Elektrik ve Elektonik Mühendisliği, Doktora
Tez Danışmanı: Ömer Morgül
Eylül 2021

Sürtünme kuvveti/torku bazen kapalı döngü kontrol sistemlerinin tasarlanmasında ihmal edilmesine karşın sistemin performansında düşüşlere ve hatta kararsızlığa sebep olabilen en çok bilinen doğrusal olmayan bozucu etkenlerden biridir. Bu sebeple, sürtünmenin modellenmesi ve giderimi istenilen gürbüzlük ve performans ölçütlerine ulaşabilmek için önem arz edebilmektedir.

Temel olarak, sürtünme giderimi model tabanlı ve model tabanlı olmayan yöntemler olarak iki gruba ayrılmaktadır. Sürtünmenin modellenmesi oldukça geniş bir araştırma alanı olup bu konuda farklı karmaşıklıklarda yaklaşımlar bulunmaktadır. Bunlar arasında Coulomb Modeli basit ama en temel yaklaşımlardan biridir. Fakat bazı durumlarda statik bir sürtünme modeli olarak, Coulomb Modeli hareketin farklı fazlarında dominant hale gelen kopma kuvveti, kayma-yapışma hareketi, kayma öncesi davranış ve sürtünme hafızasına bağlı gecikme gibi sürtünme etkilerini kapsamakta yetersiz kalabilmektedir. Genellikle LuGre Modeli gibi dinamik modeller daha kompleks olmalarının sonucu olarak bu etkileri tanımlamakta daha faydalı olmaktadırlar. Öte yandan, kullanılan sürtünme parametrelerinin sayısı bu durumlar için artmaktadır. Gerçekte modelin karmaşıklığı ve model parametrelerinin çıkarımı arasında bir ödünleşim vardır. Modeldeki parametreler ve sürtünme katsayıları örtüşmediği durumlarda istenilen sistem tepkileri elde edilemeyebilmektedir. Bu anlamda her bir model parametresinin hassas bir şekilde çıkarımının yapılması kullanılacak parametrelerin sayısı arttıkça zorlayıcı bir hal almaktadır. Üstelik bu parametrelerin bazıları ortam, sıcaklık, malzeme özellikleri ve pozisyon gibi sebeplerden ötürü zamanla değişebilmektedir. Bu nedenle model tabanlı olmayan adaptif yöntemler herhangi bir parametre tanılaması gerektirmedikleri için litaratürde oldukça popülerdir.

Bu çalışmada gözlemci tabanlı sürtünme giderim yöntemleri üzerine yoğunlaşılmış ve bunlarla ilgili olarak kararlık şartları sunulmuştur. İlk olarak tanınan bir örnek olarak Friedland-Park Gözlemcisi sistemde zaman gecikmesinin olduğu ve olmadığı durumlar için ele alınmıştır. Sonrasında gözlemcinin kullandığı kestirim fonksiyonunun daha geniş bir kümeden seçilebilmesi için gerekli bazı koşullar belirtilmiştir. Gözlemciler sürtünme kestirimini hız ölçümlerini baz alarak yaptığı için özellikle bu ölçümlerin gecikmesi önemli olabilmektedir. Bu sebeple büyük gecikmeler için sayısal diferansiyel denklem çözümlerine veya Pade Benzetiminin tersine dayanan bir hız kestirimi yapısının kullanımı önerilmektedir. Ek olarak, hız ve sürtünme hatası dinamiklerinin beraber kullanıldığı yeni bir gözlemci tasarımı da özgün bir katkı olarak sunulmaktadır. Önerilen gözlemcilerin zaman gecikmeli ve zaman gecikmesiz kapalı pozisyon döngülerindeki performasını incelemek için MATLAB ortamında kapsamlı benzetim çalışmaları yapılmıştır. Bu amaçla, Smith kestirimi ve ITAE Endeksi tabanlı tasarımlar kullanılacak pozisyon kontrolcüsü için göz önünde bulundurulmuştur. Ayrıca, simülasyonların bazılarında dinamik parametrelerin etkisini görebilmek adına ortamdaki sürtünmeyi taklit etmesi amacıyla Coulomb modeli yerine LuGre modeli tercih edilmiştir. Bunların yanında, Arduino Uno mikrodenetleyecisi ile sürülen DC motor platformunda bazı deneyler yapılmıştır. Elde edilen sonuçların ışığında gözlemci tabanlı sürtünme giderimi özellikle gerçeklenen kontrolcü düşük bant genişliğine sahip olduğunda sistemin performansını arttırmaktadır. Ayrıca, bu gözlemci yapılarının herhangi bir parametre tanılaması gerektirmemeleri de uygulanabilirlik açısından bir avantajdır.

Anahtar sözcükler: Sürtünme Gözlemcisi, Zaman Gecikmesi, ITAE Endeksi, Smith Kestirimi, Kontrolcü Parametrizasyonu, Pozisyon Kontrolü, Adaptif Kontrol, Durma Zamanı, Diferansiyel Denklemlerin Sayısal Çözümü, Pade Yakınsaması .

Acknowledgement

First of all, I would like to express my sincere gratitude to my supervisor, Prof. Ömer Morgül for his patience, guidance, suggestions and support throughout my university life. It is definitely a privilege to be part of his research group.

I would also like to thank Prof. Hitay Özbay triggering my enthusiasm in systems and control theory. He also gave me an opportunity to work in two of his joint research projects with Aselsan Inc. laying the foundations of this dissertation.

I am indebted to Assist. Prof. Melih Çakmakcı, Prof. Kemal Leblebicioğlu and Prof. Coşku Kasnakoğlu for accepting to serve as jury members in my PhD thesis defense and their valuable feedback.

I kindly appreciate every piece of knowledge and support from all my instructors in my undergraduate and graduate studies. Especially, I am thankful to Prof. Orhan Arıkan and Prof. Ezhan Karaşan, without their encouragement, I may not have ended in the finish line.

Next comes current and former members of our research group. İsmail Uyanık, Ali Nail İnal, Dilan Öztürk Şener, Elvan Kuzucu Hıdır, Hasan Eftun Orhon, Mustafa Oğuz Yeğin, Ahmet Safa Öztürk, Mustafa Gül, Hasan Hamzaçebi and Burak Çatalbaş; thank you all for productive and fruitful conversations where I have always been inspired. I express my special thanks to Bahadır Çatalbaş. We have achieved lots of things together, including my PhD Qualifying Exam.

Another appreciation goes to my friends Memet Fatih Öndül, Deniz Gültek, Emir Çağrı Ertürk, Onur Sinan Köksaldı, Mohammad Tofighi, Damla Sarıca Çifçi, Serkan Sarıtaş, Ahmet Dündar Sezer, Burak Şahinbaş, Volkan Açıkel, Elif Aydoğdu Doğru and Oğuz Kaan Karakoyun. Doing a PhD is the biggest challenge in my life, both in academic and social sense. During these hard times throughout my journey, I have these precious friends paving the way for me.

I also want to express my appreciation for Bilkent University Electrical and Electronics Engineering Department for financial support in addition to its high quality teaching and ASELSAN for giving me an opportunity to complete my PhD. Also, I would to declare my gratitude to my colleagues in ASELSAN for their understanding and cooperation.

Last but not least, I am grateful to my parents Ozan, Candan and my brother İlker for their unconditional love and endless support throughout my life. I feel so fortunate to be part of this family.

To my family, with love and gratitute...

Contents

List of Figures

List of Tables

Chapter 1

Introduction

Stable and precise control of position is one of the main objectives in many engineering applications. To this end, system modeling and identification play an essential role in the performance of mechanical systems. In fact, unmodelled system nonlinearities may cause instability of closed loop feedback systems eventually. Friction force/torque is one of these effects which exists in almost every moving mechanism. Basically, friction is a natural phenomenon resulting from the complex interaction between two surfaces in contact. Although the definition of friction is pretty straightforward, its behavior may alter according to motion, material properties, or environment. Therefore, there are lots of different approaches for friction modeling, identification, and compensation.

1.1 Background and Motivation

Mainly, friction models can be categorized as static and dynamic models in the literature. Among the static models, Coulomb friction is a simple well-known model which expresses the fundamental and dominant component of friction at

the steady-state. According to this model, friction opposes the motion and depends mainly on the sign of the velocity. Therefore, this behaviour can be described as follows,

$$F = Ma_c sgn(v). \tag{1.1}$$

where F, M and a_c correspond to friction force, mass and Coulomb coefficient respectively and $sgn(v)$ is signum function, which is defined below.

$$sgn(v) = \begin{cases} 1, & v > 0, \\ 0, & v = 0, \\ -1, & v < 0. \end{cases} \tag{1.2}$$

What is more, it is possible to improve this model by adding a damping term so-called viscous coefficient denoted by F_v. Since this term is related to velocity, v, (1.1) can be rewritten as follows.

$$F = Ma_c sgn(v) + F_v v. \tag{1.3}$$

Generally, friction force at rest is higher than the Coulomb friction level. This component is called stick friction or stiction. Therefore, one should apply a force greater than the stiction level in order to trigger the motion; otherwise, the system preserves its position and practically, the amplitude of friction becomes equivalent to the applied force. However, even in the sticking regime, microscopic motion occurs. This behavior is called as pre-sliding motion and the minimum force required to generate movement is named as break-away force. To get a more realistic and continuous friction model, it is better to include Stribeck effect [4]. This component is dominant at low velocities and becomes minimal at a specific velocity called Stribeck velocity. According to this model, friction decreases continuously starting from stiction level while velocity increases. Hence, (1.3) becomes,

$$F = [Ma_c + (F_s - Ma_c)e^{-|v/v_s|^{\delta_s}}]sgn(v) + F_v v. \tag{1.4}$$

where F_s and v_s are stiction and Stribeck velocity respectively. In the model, δ_s is a parameter which is equal to 1 typically. Pictorially, distinctions among these models are depicted in Figure 1.1.

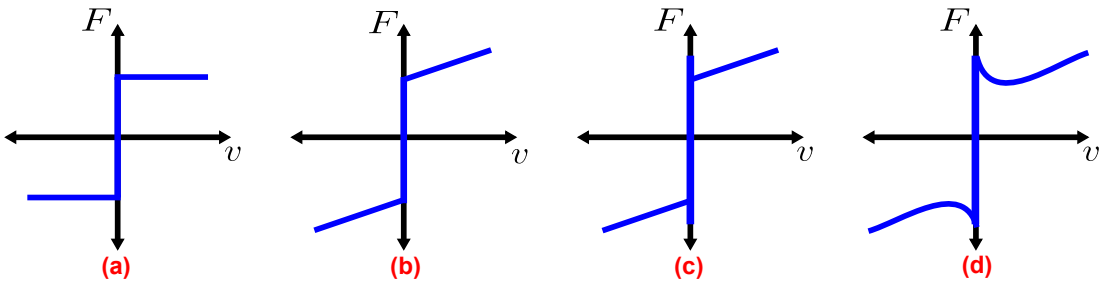

Figure 1.1: Friction curves of different static models. (a): Colomb, (b): Coulomb+Viscous, (c): Coulomb+Viscous+Stiction, (d): Stribeck Model.

Some friction terms may be dominant components at different stages of the motion. Static friction models generally portray the sliding phase, which can be treated as steady-state characteristics of friction well. On the other hand, dynamic models can express the pre-sliding phase of motion to a better extend compared to static models thanks to time varying model parameters. Moreover, Hess and Soom observed that dynamics of friction are important to explain the hysteresis behavior named friction lag [5]. In 1968, Dahl developed a dynamic model for sliding and rolling friction that can be used in simulations, especially for aerospace applications. Dahl assumes that the origin of friction is in quasi-static contact bonds that are formed and subsequently broken in a repetitive way [6]. According to the model, friction force is only a function of the displacement and the sign of velocity. This property is called rate independence and provides an advantage to model hysteresis and pre-sliding displacement. A General form of Dahl's model is given by

$$\frac{dF}{dp} = \sigma_0 \left| 1 - \frac{F}{Ma_c} sgn\left(\frac{dp}{dt}\right) \right|^i sgn\left(1 - \frac{F}{Ma_c} sgn\left(\frac{dp}{dt}\right)\right). \tag{1.5}$$

where p and σ_0 correspond to position and stiffness. Exponent i is a model parameter typically set to 1. Note that (1.5) does not include, Stribeck effect and viscous friction. Therefore, Bliman and Sorine developed a model based on linear space invariant differential operators to eliminate these drawbacks of Dahl Model [7]. To this end, time variable t is replaced by a space variable s with the following transformation.

$$s = \int_0^t |v(\tau)|\, d\tau. \tag{1.6}$$

Then, a first order model can be defined as

$$\frac{dF}{ds} = -\sigma_0 \frac{F}{Ma_c} z + \sigma_0 sgn(v). \tag{1.7}$$

This first order model can be extended to a second order model as below aiming, at imitation of Stribeck effect.

$$\frac{d^2F}{ds^2} + 2\zeta w \frac{dF}{ds} + w^2 F = w^2 Ma_c sgn(v). \tag{1.8}$$

where ζ and w denote damping coefficient and angular frequency respectively. Actually, this second order model includes two first order models in parallel, see [3, 7, 8] for details. Unfortunately, this second order model provides a transient Stribeck effect since it is not exhibited in the steady-state relation between velocity and friction force. Another extension of Dahl model is developed by the universities of Lund and Grenoble that is why it is named LuGre Model [2]. According to this model, moving object and asperities are connected through elastic bristles. When a tangential force is applied, these bristles start to bend as if a spring mass system. If the force is sufficiently large, deflected bristles slip off each other randomly. During the motion, new contacts are formed and slipped off repetitively and this results in friction generation. The average deflection of the asperities can be introduced through a new state variable z_d. Then, friction dynamics become

$$\frac{dz_d}{dt} = v - \frac{|v|}{h(v)} z_d, \tag{1.9}$$

$$F = \sigma_0 z_d + \sigma_1(v) \frac{dz_d}{dt} + F_v v. \tag{1.10}$$

where σ_0, σ_1 are model parameters and $h(v)$ is an appropriately chosen function to capture Stribeck effect. A well known candidate of $h(v)$ is given as follows.

$$h(v) = \frac{1}{\sigma_0} \left(Ma_c + (F_s - Ma_c) e^{-(v/v_s)^2} \right). \tag{1.11}$$

Note that when $\frac{dz_d}{dt} = 0$, system reaches steady state and LuGre Model converges to classical friction model given in (1.4). Furthermore, as it can be seen in (1.10), the inclusion of viscous friction and Stribeck effect at the same time is the main advantage of LuGre model compared to the aforementioned Dahl and Bliman-Sorine dynamic models. With LuGre Model, we conclude our discussion

on friction modeling. Certainly, there are many other models present in the literature. Interested readers may refer to [9] and the references therein.

After this brief introduction about modeling, we will move on to friction identification and compensation. Fundamentally, friction compensation approaches are grouped under two headings as model based and non-model based techniques. As the name implies, model based methods rely on accurately identified model parameters. Then, using these parameters, friction can be estimated and superposed via either feedback or feedforward to control input delivered to the plant. Therefore, if estimated friction is well enough, it cancels out existing friction dynamics and control input generated by a controller is completely directed to the plant. As mentioned before, friction regimes are different in the pre-sliding and sliding phases. Actually, the steady state characteristics of friction depend on velocity, while dynamic characteristics depend on position. Hence, viscous coefficient, Stribeck velocity, Coulomb and stiction coefficients can be determined using constant velocity tests. In these tests, force/torque generated by the controller will be equal to friction force/torque itself since acceleration is zero. Aiming at zero steady state velocity error, it is better to employ a basic PI controller during these tests. Then, one can have a friction-velocity mapping for the sliding regime and apply curve-fitting techniques in order to determine static friction parameters. On the other hand, dynamic characteristics of the friction in the presliding stage are a function of position; therefore, micro motion can produced by applying a ramp input with a low slope in order to obtain a friction-position mapping [10]. Nevertheless, parameter identification for the pre-sliding phase is challenging compared to the sliding phase. Revisiting (1.10), we can conclude that accurate identification of dynamics coefficients σ_0 and σ_1 is challenging due to complexity of LuGre model and immeasurable internal state variable z_d. Hence, there are some studies to improve the accuracy of dynamical parameter identification. For instance, inspired by biological theories, [11] and [12] utilize Genetic Algorithm and Novel Evolutionary Algorithm (NEA). In another approach, two linear controllers having strictly positive real transfer functions are utilized to adapt partially known friction parameters to normal force variations and temperature changes [13]. In [14], a sliding-mode observer is designed to estimate

the internal state z_d in LuGre model. Then, an adaptive controller drives the position and velocity of a motor to track the reference signals using estimations of z_d. Similarly, [15] employs a Q filter-based disturbance observer to compensate the differences between existing friction and nominal model. In this study, a feedforward static friction compensation is applied and taking velocity feedback, the observer regards unmodelled friction dynamics as a disturbance applied to the system. Likewise, [16], proposes an observer design aiming at minimization of modeling errors. Here, the observer is distinctively designed based on LuGre friction and model parameters are tuned adaptively using velocity feedback. Lastly, [17] proposes three different methods for friction identification. One of them is to construct a two layer neural network in order to obtain precise and offline estimation using the Extended Kalman Filter (EKF). Secondly, a polytopic model consisting of several locally valid friction models is suggested for a better parameter identification. These two methods are categorized as grey-box models and apart from them, [17] provides a frequency domain identification as a third alternative. Therefore, according to the third method, a system can be excited with random noise in a single experiment aiming at parameter identification, while grey-box models require several experiments.

Parameter identification can be time consuming and challenging since it requires an appropriate measurement setup and process. Furthermore, estimated parameters might tend to vary due to environmental properties such as temperature, liquidity, load, etc. [18] that is why nonmodel based approaches are prevalent in the literature as alternatives. For instance, in [19], it is proposed to utilize an Extended Kalman-Bucy Filter (EKBF) assuming friction torque is an unknown. Similarly, [20] has designed a disturbance observer for pivot friction compensation in a hard disk drive using Kalman Filter framework and [21] has designed a controller unit consisting of a low pass PD controller and Extended Kalman Filter to enhance the position performance of the system under friction. In [22], a robust sliding mode controller design is developed as a nonmodel based cancellation method. Furthermore, there are several different observer designs that do not require any friction modeling in the literature. For instance, separate

velocity and momenta observers are employed together using position measurements to eliminate disturbances including friction in [23]. Also, for a multilink robotic manipulator, a nonlinear disturbance observer is designed in [24]. Although the main purpose of this observer is to estimate constant disturbance signals, it can also give promising results with time varying disturbance. Therefore, it can be employed to satisfy different design purposes such as independent joint control, sensorless torque control, and fault diagnosis in addition to friction compensation. Again for a robotic platform controlled by passivity based multi input multi output (MIMO) controller, an observer operating as an integrator and driving the steady state error to zero is introduced in [25]. Of course, there are plenty many observer designs implemented for nonmodel based friction compensation in the literature. As the last example, we would like to mention Friedland-Park observer. Although this is an adaptive observer aiming Coulomb coefficient estimation, simulations and experiments reveal that it may still perform satisfactorily even actual friction is not confined Coulomb friction only [26]. Inspired by its simple structure and performance, we made some further analysis and extensions on the observer design which will be expressed in the subsequent chapter.

Motivated by all of these facts and justifications, we consider adaptive observer designs which do not require any parameter identification for friction cancellation in a position control system with one degree of freedom in the scope of our research. Therefore, it can move along only one axes. Note that the proposed methods in this study can be extended to the systems with multiple degrees of freedom. In this case, in addition to friction, systems include coupling forces and other nonlinearities which should be taken into account as well [27, 28, 29, 30]. A general block diagram of a one-degree position control system is displayed in Figure 1.2. Note that the inner loop which controls the velocity is optional. This structure is named a hierarchical closed loop position control system and is required if velocity control is also desired. When there are no design restrictions on velocity output or velocity is immeasurable, direct position control with a single closed loop is an alternative. Likewise, reference filter is another optional component in the position control problems. Although it may deteriorate the

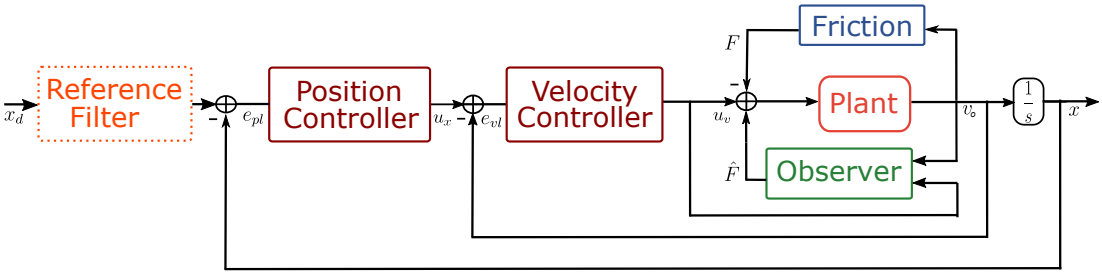

Figure 1.2: General representation of a hierarchical closed loop feedback system for position control under the presence of friction force

transient response of the system a little bit, it may be beneficial to obtain an improved steady state response. In later parts of this dissertation, all components of a position control system are explained in depth.

1.2 Key Contributions

One of the main contributions of this study is that we make performance and stability analysis of Friendland-Park observer to a broader extend. In real life position control applications, measurement delay may emerge due to sampling, data collection system/sensor design (i.e. encoder resolution, complex communication protocols etc.) and velocity estimation if direct measurement is not possible. This delay might deteriorate the system response and limit observer bandwidth significantly. For such cases, we show that velocity prediction is required in the presence of a large time delay in order to estimate the friction accurately. To this end, we propose different velocity predictor schemes to enhance the robustness and performance of the closed loop system.

Another novel contribution of our research is that we develop a novel adaptive observer design as an alternative. Parameters of Friedland-Park type observers are tuned somehow in a heuristic way, whereas in this new design, it may be possible to determine the observer parameters by considering overshoot and settling time properties of the friction estimation. Therefore, observer parameters may be determined by considering the damping ratio and natural frequency. Apart

from ease of its design, this new observer adopts both friction and velocity error dynamics which can improve the friction estimation performance in velocity uncertainties. This new observer has behavior as second order switching system. Furthermore, we provide a stability analysis for this new design. In addition to a numerical method based on linear matrix inequalities (LMI) to solve minimum dwell time, we have also stated some conditions for asymptotic stability. In addition to MATLAB simulations, we conduct some experiments on a DC motor application running by an Arduino Uno based platform. In these experiments, the system is delay free.; therefore, we tune the PID controller using the integral of the time-weighted absolute error (ITAE) index. Likewise, under the presence of measurement delay, this new observer design may work well enough without a separate velocity predictor since it also considers velocity error dynamics for friction estimation.

1.3 Organization of the Dissertation

This dissertation is organized as follows. In Chapter 2, different observer designs are discussed and stability analyses are presented. First, we revisit the original Friedland-Park Friction Observer for a delay free system and characterize a general class of nonlinear functions that could be used to estimate this observer. Friedland-Park type observers use both control input and velocity measurements for friction estimation. Therefore, the effects of actuation and measurement delay on observer estimation performance are investigated. For this purpose, some delay compensation techniques are discussed. To this end, several numerical differential equation solvers and inverse Pade Approximant based schemes are proposed to estimate the actual velocity based on delayed velocity measurements. Lastly, a new observer structure is provided as an alternative observer design.

Chapter 3 focuses on different controller design procedures to form a closed loop position with adaptive observers. At first, we simply consider a delay free system. An optimal PID controller can be obtained according to ITAE performance index considering bandwidth requirements in this scenario. However, designing

such optimal controllers for systems with delay can be challenging and might not provide the desired setpoint or robustness objectives. Therefore, we also consider a particular controller structure named Smith predictor. Smith predictor based controllers are highly preferred in the control of time delayed systems. This research utilizes pole placement and controller parametrization methods to design Smith Predictor-based velocity and position controllers.

In Chapter 4, we performed detailed simulations in MATLAB to observe the performance of the position control system. To this end, Coulomb and LuGre friction models have utilized to synthesis the disturbance signal arising from friction in the system. Motivated by simulation results, we also conduct some experiments on an Arduino Uno based DC motor platform to examine the effectiveness of proposed strategies.

Finally, in the Appendix, we present some concluding remarks in Chapter 6 and details of LMI based dwell time analysis and MATLAB Simulink block settings for Arduino Uno experiments.

Chapter 2

Friction Observer Designs

As mentioned in the introduction, different observer designs can be found in the literature. In this chapter, two main observer designs are discussed. We start with a well-known adaptive Coulomb Observer developed by Friedland and Park [26, 31]. Inspired by the proposed design, we provide some necessary conditions to acquire other candidate estimation functions for the observer. Furthermore, we propose some extensions and modifications for the plants which have a time delay. Ultimately, we propose a new observer design and provide a stability analysis based on an appropriate Lyapunov function.

2.1 Friedland-Park Observer design for delay free systems

A simple mechanical system can be modeled with a single mass equation. In this case, applied force/torque becomes control input, whereas position and/or velocity is the output. Assuming that the system is delay free, equations of

motion under the presence of friction can be written as follows

$$\dot{x} = v, \tag{2.1}$$

$$M\dot{v} = -F(v) + u. \tag{2.2}$$

where, M, u, x, v and $F(v)$ represent total mass, applied force, position, velocity and existing friction force respectively. Note that applied force/torque is directly generated by the controller itself when there is no friction compensation. However, when friction exists, control input cannot be fully transformed to desired $\dot{v}$ and the system begins to suffer from performance degradation due to friction force/torque, which is denoted by $F(v)$. Besides, stability issues may arise without any friction compensation. To this end, we adopt an observer based friction cancellation approach. In this case, applied force/torque becomes the sum of controller input, denoted by u_r and friction estimation of the observer $\hat{F}(v)$ as below.

$$u = \hat{F}(v) + u_r. \tag{2.3}$$

Assuming that observer estimation, $\hat{F}(v)$, perfectly matches to existing friction $F(v)$, force/torque sourcing from controller input can be effectively delivered to the system. Hence, any controller designed for a linear time-invariant system without any friction can be adopted for position control together with an appropriate observer. Certainly, friction cancellation eases the controller design process in this manner.

Similarly, equations of rotational motion can be derived as

$$\dot{\theta} = w, \tag{2.4}$$

$$J\dot{w} = -F(w) + u, \tag{2.5}$$

$$u = \hat{F}(w) + u_r. \tag{2.6}$$

where θ, w and J stand for angular position, angular velocity and moment of inertia of the system respectively.

In the literature, there are many different approaches to model the friction force; however, Coulomb friction is a common and fundamental component in

most of these models. Thus, observer depicted in Figure 2.1 mainly aims to estimate Coulomb component for friction cancellation. Consequently, existing and estimated friction can be formulated as $F(v, a_c) = Ma_c sgn(v)$ and $\hat{F}(v, \hat{a}_c) = M\hat{a}_c sgn(v)$, where a_c and $\hat{a}_c$ represent Coulomb friction coefficient and its estimation, both respectively.

To design the observer, let $g(v) : \mathbf{R} \mapsto \mathbf{R}$ be an appropriate differentiable function yet to be determined. Inspired by [26], we propose an extended adaptive friction observer given by

$$\dot{z} = g'(v)\frac{u}{M}, \tag{2.7}$$

$$\hat{a}_c = z - g(v). \tag{2.8}$$

Here, z is an internal state of the observer and $\hat{a}_c$ is the estimation of Coulomb friction coefficient. To analyze the performance of the observer given by (2.7) and (2.8), let us define the estimation error as:

$$e = a_c - \hat{a}_c. \tag{2.9}$$

Then, we can conclude that $\dot{a}_c = 0$ if we assume that a_c is constant. This leads

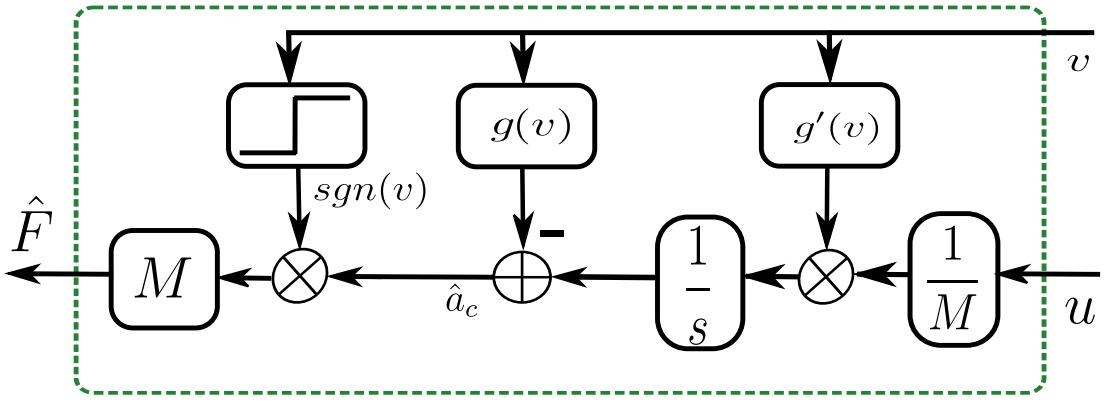

Figure 2.1: Structure of a generalized Friedland-Park observer

error dynamics to become

$$\begin{aligned}
\dot{e} &= -\dot{\hat{a}}_c \\
&= -\dot{z} + g'(v)\dot{v} \\
&= -\frac{g'(v)u}{M} + \frac{g'(v)[\hat{F}(v,\hat{a}_c) - F(v,a_c) + u]}{M} \\
&= -\frac{g'(v)}{M}[F(v,a_c) - \hat{F}(v,\hat{a}_c)] \\
&= -g'(v)sgn(v)e. \qquad (2.10)
\end{aligned}$$

Remark 1. *If $g'(v)sgn(v) \geq 0\ \forall v \neq 0$, then under some conditions one can show the asymptotic stability of the error dynamics given by (2.10). Indeed, there is a quite large class of functions $g(\cdot)$ which satisfy these conditions. To characterize these, let us define the following class of functions. Consider a function $h : \mathbf{R} \mapsto \mathbf{R}$ which satisfies the following condition*

$$\alpha v^2 \leq vh(v) \leq \beta v^2 \qquad \forall v \qquad (2.11)$$

where $\beta \geq \alpha$. Such functions have a graph in Cartesian axes whose boundaries are given by the lines $y = \alpha v$ and $y = \beta v$ and we say in such a case that $h(\cdot)$ belongs to a sector $[\alpha, \beta]$, or simply $h \in [\alpha, \beta]$, see [32] for more details. Note that if $\alpha = 0$, $\beta = \infty$, then the functions $h \in [0, \infty]$ have a graph which lies entirely in first and third quadrant of Cartesian axes. Since $sgn(\cdot) \in [0, \infty]$, it is clear that for any function g such that $g'(\cdot) \in [0, \infty]$, we will have $g'(v)sgn(v) \geq 0\ \forall v$. Clearly, a large class of functions $g(\cdot)$ satisfy this condition. For example, if we choose $g(v) = \frac{1}{2}kv^2$, then $g'(v) = kv$ which belongs to sector $[0, \infty]$ when $k > 0$. Indeed, in this case we have $g'(v)sgn(v) = k|v| \geq 0$. Another candidate function is $g(v) = kln(cosh(\alpha v))$ where $k > 0$ and $\alpha > 0$ are arbitrary constants. In this case, $g'(v) = k\alpha tanh(\alpha v) \in [0, \infty]$. For the choice of $g(v) = k \mid v \mid$, $k > 0$, we have $g'(v)sgn(v) = k$ and in this case the error equation given by (2.10) has the solution $e(t) = e^{-kt}e(0)$, provided that $v \neq 0$. In [26], the function $g(v) = k|v|^\mu$ is utilized, which yields $g'(v) = k\mu|v|^{\mu-1}sgn(v) \in [0, \infty]$ for any positive constants k and μ. □

Note that although for the particular choice of $g(v) = k|v|^\mu$, the well known

observer given in [26] will be attained, as a novel contribution, we also show that it is possible to use other alternatives of $g(v)$ as far as they satisfy Lemma 1.

Under certain mild assumptions, one can show the stability of the error dynamics given by (2.10) by using the standard Lyapunov stability analysis.

Lemma 1. *Consider the system given by (2.1)-(2.10). Assume that* $g(v) : \mathbf{R} \to \mathbf{R}$ *is a differentiable function which satisfies* $g'(v) \in [0, \infty)$, $g(v) \neq 0$ *and* $g'(v) \neq 0$ *for* $v \neq 0$. *Under these constraints, if* $|v| \geq \alpha \ \forall t$, *then the error dynamics given by (2.10) is exponentially stable, i.e.* $e(t) \longrightarrow 0$ *with an exponential decay.*

Proof. Note that $g'(v)sgn(v) \geq 0$ and with the given assumptions it easily follows that if $|v| \geq \alpha > 0$ then, $g'(v)sgn(v) \geq \beta$ for some $\beta > 0$. Let us define the following Lyapunov function

$$V(e) = \frac{1}{2}e^2 \tag{2.12}$$

By differentiating (2.12) and using (2.10) we obtain

$$\dot{V} = e\dot{e} \leq -\beta e^2 = -2\beta V \tag{2.13}$$

Hence, $V(t) \leq e^{-2\beta t}V(0)$ and therefore we have

$$|e(t)| \leq e^{-\beta t} |e(0)| . \quad \square \tag{2.14}$$

$\square$

Remark 2. *Although the applicability of Lemma 1 seems to be limited since it requires that* $|v| \geq \alpha > 0$*; nevertheless, it could be utilized in various meaningful applications such as unit step tracking in velocity loop, ramp tracking in position loop. Note that in these cases, it is expected that condition* $|v| \geq \alpha$ *hold sufficiently long period of time. Indeed, if we choose* $g(v) = kv^2$, *then we have* $g'(v)sgn(v) = 2k|v|$, *hence for* $|v| > \alpha$, $g'(v)sgn(v) \geq \beta$ *is satisfied with* $\beta = 2k\alpha$. $\square$

A somewhat less restrictive assumption on $v(t)$, which could be related to the persistency of excitation [33], could be given as below.

Lemma 2. *Let $v(t)$ be the solution of (2.1)-(2.10) and let us define*

$$G(t) = g'\left(v(t)\right) sgn\left(v(t)\right). \tag{2.15}$$

Assume that there exist some $\alpha>0$ and $T>0$ such that the following holds

$$\int_t^{t+T} \mathrm{G(s)}\,\mathrm{d}s \geq \alpha, \qquad \forall t \geq 0 \tag{2.16}$$

Then for the error dynamics given by (2.10), $e(t) \to 0$ as $t \longrightarrow \infty$; moreover, the decay is exponential.

Proof. Note that the solution of (2.10) is given as

$$e(t) = e^{-\int_0^t \mathrm{G(s)}\,\mathrm{d}s} e(0). \tag{2.17}$$

Since the exponential term is always positive, (2.17) can be rewritten as

$$|e(t)| = e^{-\int_0^t \mathrm{G(s)}\,\mathrm{d}s} |e(0)|. \tag{2.18}$$

Let $t = nT + \tau$ for some integer $n \in Z^+$ and $0<\tau<T$. Then,

$$\int_0^t \mathrm{G(s)}\,\mathrm{d}s = \int_0^{nT} \mathrm{G(s)}\,\mathrm{d}s + \int_{nT}^{nT+\tau} \mathrm{G(s)}\,\mathrm{d}s \geq n\alpha. \tag{2.19}$$

where the fact that $G(s) \geq 0$ is used. Inserting (2.19) into (2.18) leads to

$$|e(t)| \leq e^{-n\alpha} |e(0)|. \tag{2.20}$$

As $t \longrightarrow \infty$, $n \longrightarrow \infty$ as well; hence, $|e(t)| \longrightarrow 0$. As it can be seen from (2.20), the decay is exponential. In fact, since $n = \frac{t-\tau}{T}$ and $\tau < T$,

$$|e(t)| \leq e^{\alpha} e^{-\frac{\alpha t}{T}} |e(0)|. \quad \square \tag{2.21}$$

$\square$

Remark 3. *Note that when $|v(t)| \geq \alpha>0$, the condition given by (2.15) also holds. On the other hand, when the signals are in the sinusoidal form, the condition $|v(t)| \geq \alpha$ may not hold whereas (2.15) may hold. Hence, Lemma 2 could be utilized in the sinusoidal signal tracking and/or rejection. Indeed, if we choose $g(v) = kv^2$, then $G(t)$ given by (2.15) satisfies $G(t) = 2k|v|$. If $v(t) = \sin\omega t$, then (2.16) is satisfied with $T = \pi/\omega$ and $\alpha = 2k/\omega$.* $\square$

Although Remark 1 sets a condition for estimation function $g(v)$, the relationship between convergence rate of the observer response to existing friction and parameter selection of $g(v)$ remains implicit. Specifically in original Friedland-Park observer where $g(v) = k|v|^{\mu}$, design parameters k and μ are generally chosen in a heuristic way. In other words, [26] claims that estimation error convergences to zero asymptotically and rate of convergence becomes faster when either observer gain k or design exponent μ is increased. However, it is not clear that how k and μ should be chosen to obtain desired observer bandwidth. To overcome this parameter selection issue, [34] makes a linear approximation for the pole location of Friedland-Park observer, assuming that desired velocity signal is sinusoidal. Before moving forward on the computation of approximate pole location, note that in Friedland-Park observer case (2.10) can be rewritten as

$$\dot{e} = -k\mu|v|^{\mu-1}e. \tag{2.22}$$

Hence, for an initial condition $e(0)$ explicit solution of the error function at time T can be acquired as

$$e(T) = e(0)e^{-k\mu\int_0^T |v|^{\mu-1}dt}. \tag{2.23}$$

To establish an analogy with first order linear time invariant observer, this solution can be rewritten such that

$$e(T) = e(0)e^{\sigma(T)T}. \tag{2.24}$$

where $\sigma(T) = -k\mu\big[\frac{1}{T}\int_0^T |v|^{\mu-1}dt\big]$. Then, at the steady state, approximate pole location can be computed as

$$p = -k\mu\overline{|v|^{\mu-1}} \tag{2.25}$$

where $\overline{(.)}$ denotes the mean value ofthe corresponding variable. Note that (2.25) can be generalized as

$$p = -\overline{g'(v)} \tag{2.26}$$

Under this assessment, parameters can be set to satisfy desired pole placement of the observer. Nevertheless, to compute the pole location, we still need to

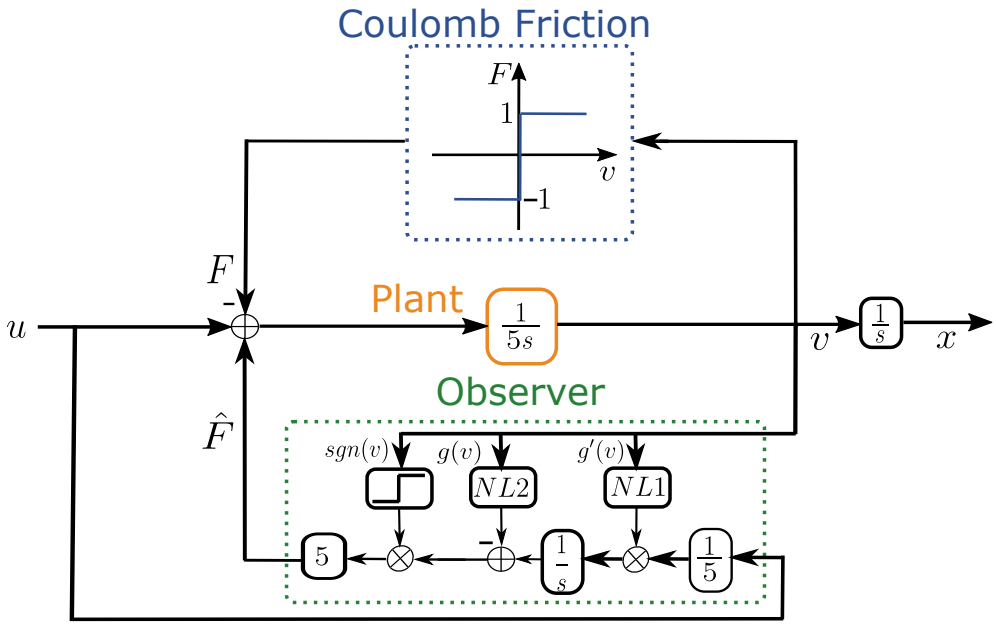

Figure 2.2: Block diagram of the open loop system formed by plant and adaptive observer under Coulomb Friction.

know velocity response of the system beforehand. Based on some assumptions [34] makes a velocity estimation based on a desired sinusoidal position response. However, foreseeing velocity to observer design can be problematic if there are some unmodelled dynamics due to nonlinearities, disturbances or time delay in the system. What is more, when position reference does not have a periodic trajectory, it may be difficult to use velocity for observer characterization and this may lead to poor friction canceling. Moreover, a particular pole placement can be achieved for different estimation functions $g(v)$ with appropriately tuned parameters. Consequently, how fast the observer estimation converges to friction existing in the system is not so obvious. For instance, in order to achieve a certain estimation error at time t with the original Friedland-Park observer, one should know $v(t)$ and carefully set k and μ in (2.23). Apart from these inferences, it is also remarked that original Friedland-Park observer becomes sensitive when high gain k is combined with a relatively high value of μ and as a result of this response tends to ring [26].

To gain a deeper understanding of this issue, we conduct some open loop observer simulations. To this end, we design a system as in Figure 2.2 assuming

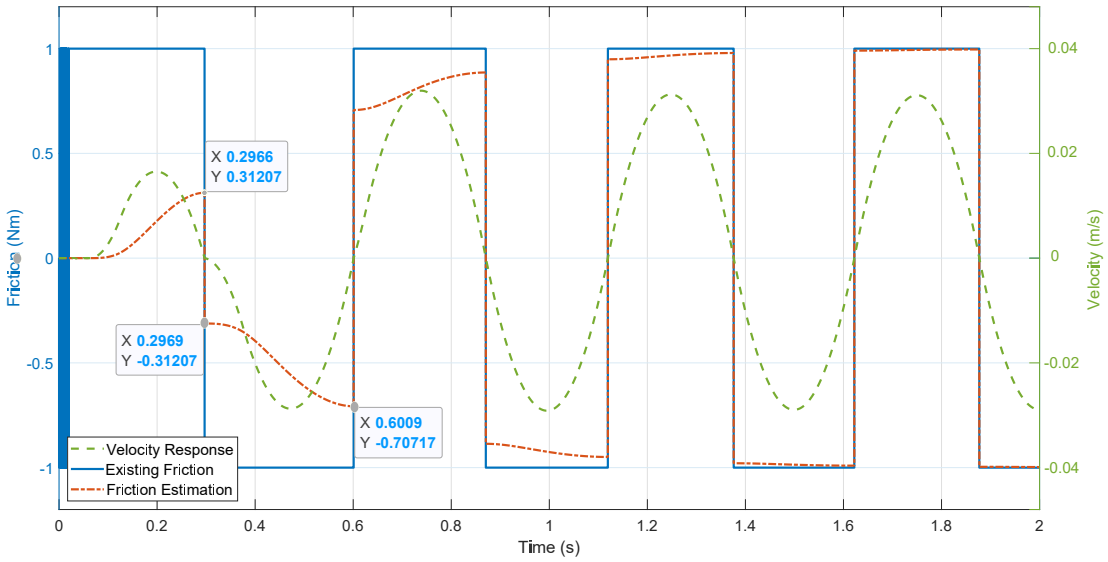

Figure 2.3: Friction estimation and velocity response of the open loop system for $g(v) = 100v^2$.

that $M = 5$ and $F(v) = sgn(v)$ in (2.2). Note that in this case Coulomb coefficient, a_c becomes 0.2. Then, we apply a control input, $u = 2\Lambda(2)$ where $\Lambda(f)$ denotes a zero mean periodic triangular signal with frequency f. We first consider $g(v) = k|v|^\mu$ for $k = 100$ and $\mu = 2$. In this case, the velocity response of the open loop system becomes periodic as in Figure 2.3. Then, the mean of absolute velocity at the steady state can be computed within a period 0.5 sec as below.

$$\begin{aligned} \overline{|v|} &= \tfrac{1}{2}\int_{2.5}^{3} |v|dt \\ &= 0.0836 \end{aligned} \tag{2.27}$$

Consequently, Referring to (2.25), pole location can approximated as $p \approx -16.72$. Furthermore, it is possible to friction estimation error at time t using (2.23). For instance, initially $e(0) = 0.2$ since system is in rest and $\hat{a}_c = 0$. For $t = 0.29$ sec., error and estimated Coulomb coefficient can computed using (2.23) such that $e(0.29) \approx 0.1376$ and $\hat{a}_c(0.29) = 0.0624$. By using these, the estimated friction becomes $\hat{F} = 0.312$ at $t = 0.29$ as in Figure (2.3). As another example, we can consider $t = 0.6$ case. Then, $e(0.6) = e(0)e^{-200\int_0^{0.6}|v|dt} \approx 0.06$ leads to $\hat{a}_c \approx 0.14$ $\hat{F} = -0.707$ due to $sgn(v) = -1$.

As stated previously, a similar estimation performance can be achieved for

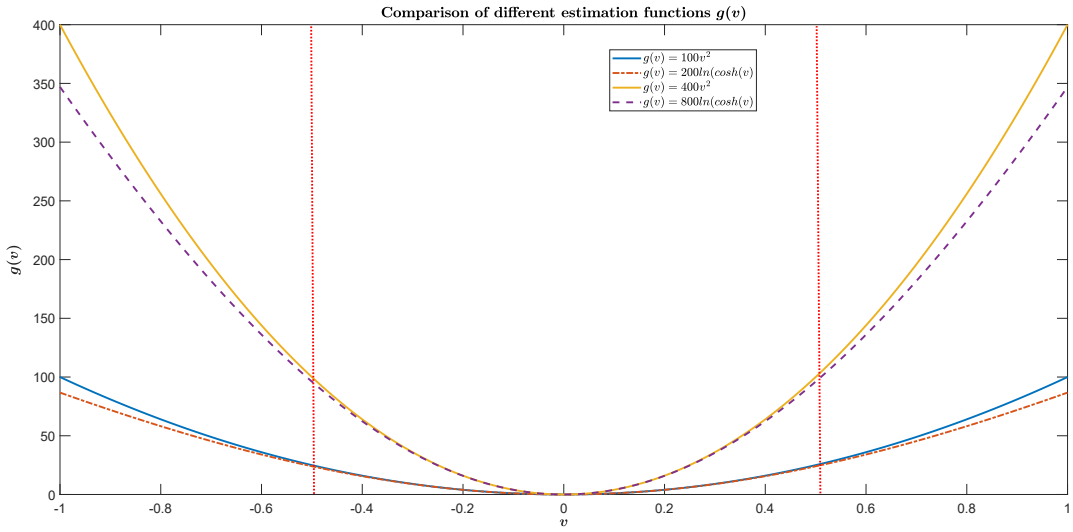

Figure 2.4: Characteristics of different observer estimation functions for pole locations at -16.72 and -66.88.

another $g(v)$. Again aiming a pole location $p = -16.72$, one can determine $g(v) = 200ln(cosh(v))$ since $\overline{tanh(v)} = 0.0836$. Note that although these two estimation function candidates are different, they have a similar graph in the interval [-0.5,0.5] and as a result, their estimations are the same as long as open loop velocity response stays inside the area designated by dotted red lines.

Moreover, functions corresponding to larger pole locations provide faster friction estimation response as shown in Figure 2.5. Consequently, although estimation functions used in the observer design have different characteristics, they can produce similar responses for the same pole locations. When a rapid convergence is desired, one should design an observer with a larger pole to increase its bandwidth. For instance, both $g(v) = 400v^2$ and $g(v) = 800ln(cosh(v))$ lead to a pole at approximately -66.88 for the same velocity signal in the previous case. Therefore, estimation converges to existing friction faster as in Figure 2.5. Considering (2.23), it is an expected result since k is larger and the average velocity integral is the same compared to the previous case. In other words, the observer has a larger pole in this case referring to (2.24). Mathematically speaking observer pole can be very large; however, performance problems may also arise in practice. For instance, in [26], it is stated that observer tends to ring when high k combined with relatively high μ. Probably, in this case, the observer becomes very sensitive

to velocity noise. In fact, these type observers assume that velocity information is present precisely since they do not perform a velocity estimation. Therefore, if direct velocity measurement is not available, a velocity predictor is required. However, this predictor can degrade friction performance. Similarly, if velocity measurements are acquired with a time delay, friction performance may again deteriorate that is why in the following sections, we will consider these issues in detail. Furthermore, we will also exhibit a new observer design including velocity dynamics for friction estimation.

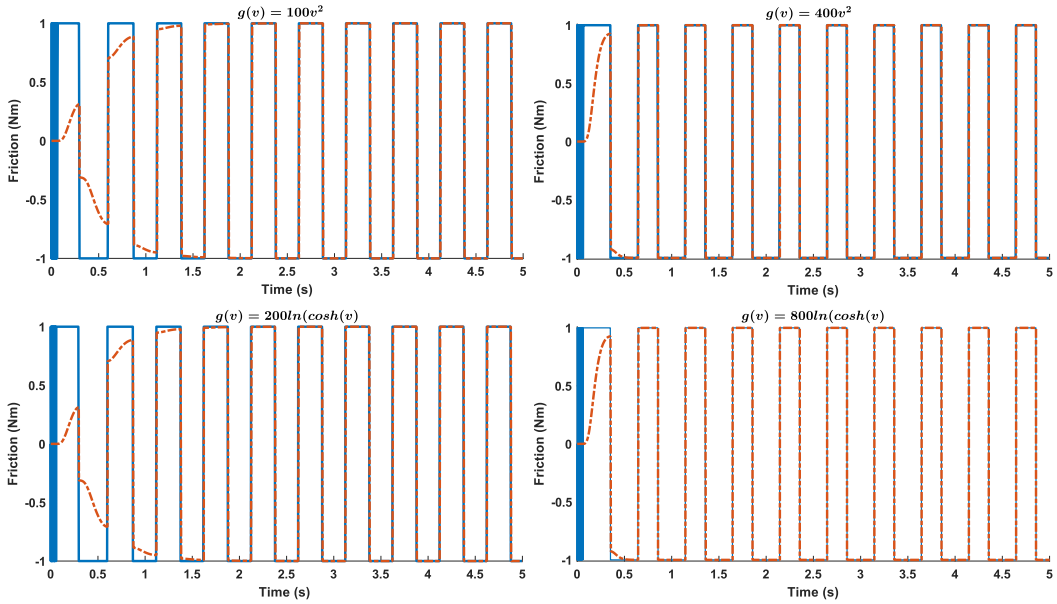

Figure 2.5: Friction estimation performances of Friedland-Park type observer designs having different $g(v)$. (Solid Blue: $F(v) = sgn(v)$, Dashed Orange: $\hat{F}(v)$)

2.2 Friedland-Park Observer design for systems with time delay

Previously, we have emphasized that Friedland-Park type observers count on control input and velocity measurements to estimate the friction. Hence, they can suffer performance degradation under the presence of time delay within the system. In such cases, time delay may exist as input and/or output delay and

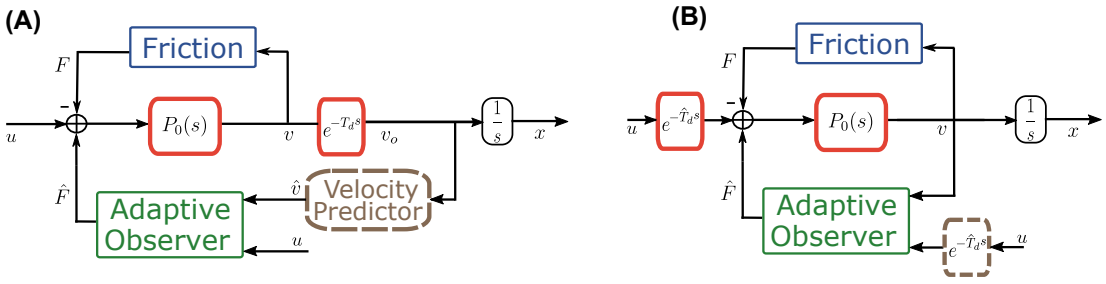

Figure 2.6: Time delay may emerge either in input or output ports of the plant. In case A, an output-delay model is used due to measurement issues whereas in case B, an input-delay model is used due to actuation issues.

require some delay compensation techniques, especially when it is large compared to observer bandwidth, see Figure 2.6. For our analyses in this thesis, we assume that open loop system has a fixed and known time delay. Although it is out of the main context of our study, time delay can be measured by considering system properties or inferred after some system identification techniques. Regarding this issue, interested readers can find further details in [35, 36].

Let us first start with considering input case which occurs actuation or process delay. In our previous work [37], a copy of the time delay is attached to the control input port of Friedland-Park observer as in Figure 2.6 B. This enables observer to make a fair computation using theoretical velocity derived from u and actual velocity v [37, 38]. To investigate the effect of input delay on the observer performance, we first revisit the system in Figure 2.2 with an input delay such that $T_d = 0.05$ and $T_d = 0.1$ seconds. For $g(v) = 100v^2$ and $g(v) = 400v^2$, estimation performances of the observers are given in Figure 2.7. Referring to the figure, it can be inferred that without any delay compensation observer performance deteriorates drastically. In fact, for $T_d = 0.1s$, it tends to make the system unstable since the direction of real friction and estimation becomes opposite due to large delay for each $g(v)$.

As stated in [16], an effective friction compensation scheme generally requires velocity measurements with a good resolution and small time delay. Mostly, measurement delay is introduced by sampling, data collection system/sensor design (i.e. encoder resolution, complex communication protocols, etc.) and velocity

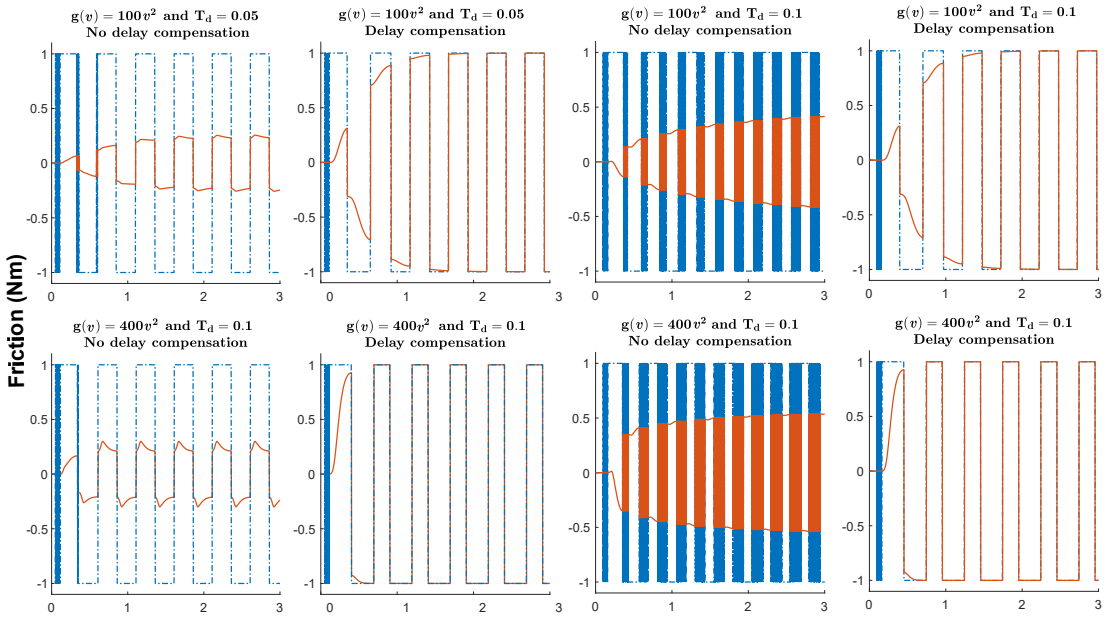

Figure 2.7: Friction estimation performances of Friedland-Park type observer designs with different estimation function and actuation delays. (Dashed Blue: $F(v) = sgn(v)$, Solid Orange: $\hat{F}(v)$)

estimation if a direct measurement of it is not possible. In this case, estimated friction becomes a function of delayed velocity measurements denoted by $v_o(t)$ while existing friction is a function of actual velocity $v(t)$, see Figure 2.6 A. In this case, friction cancellation is still achieved imperfectly if the time delay is small and $v_o(t)$ has similar behavior to $v(t)$. Otherwise, a velocity predictor as in Figure 2.6 A should be utilized in order to increase observer performance [39]. Hence, observer can estimate friction by (2.7)-(2.8) since both estimated and existing friction forces are functions of v. The relationship between the measured $v_o(t)$ and the actual velocity $v(t)$ can be formulated as:

$$v_o(t) = v(t - T_d). \tag{2.28}$$

where T_d stands for the time delay present in the system. Replacing t with $t + T_d$, we see that obviously it is required to have $v_o(t + T_d)$ to estimate the friction force accurately. Hence, the actual velocity $v(t)$ and observed velocity $v_o(t)$ are related as follows

$$v(t) = v_o(t + T_d). \tag{2.29}$$

Since we observe $v_o(t)$, but $v(t)$ is required to calculate the friction force, we need to estimate $v(t)$. Let us call $\hat{v}(t)$ as an estimation of $v(t)$, and define the velocity estimation error e_v as

$$e_v = v(t) - \hat{v}(t). \tag{2.30}$$

Due to the fact that measurement $v_o(t)$ is the delayed velocity of the actual velocity $v(t)$, we can only use the estimated velocity $\hat{v}(t)$ in the observer equations given by (2.7)-(2.8). In this case, the observer should be given as follows:

$$\begin{aligned} \dot{z} &= g'(\hat{v})\frac{u}{M} && (2.31)\\ \hat{a}_c &= z - g(\hat{v}) && (2.32) \end{aligned}$$

Then, the parameter estimation error $e(t) = a_c - \hat{a}_c$ dynamics is given as

$$\dot{e} = -g'(\hat{v})\frac{u}{M} + g'(\hat{v})\dot{\hat{v}}. \tag{2.33}$$

Defining the velocity estimation error e_v as given by (2.30), by using (2.31)-(2.32) we obtain

$$\begin{aligned} \dot{e} &= g'(\hat{v})(\hat{a}_c sgn(\hat{v}) - a_c sgn(v)) - g'(\hat{v})\dot{e}_v \\ &= -g'(\hat{v})sgn(\hat{v})e + g'(\hat{v})a_c(sgn(\hat{v}) - sgn(v)) \\ &\quad -g'(\hat{v})\dot{e}_v. \end{aligned} \tag{2.34}$$

If $sgn(\hat{v}) = sgn(v)$, which is satisfied when $|v| > |e_v|$, then the parameter error dynamics becomes:

$$\dot{e} = -g'(\hat{v})sgn(\hat{v})e - g'(\hat{v})\dot{e}_v. \tag{2.35}$$

Note that with velocity estimation error e_v satisfying $e_v = 0$, we have $v = \hat{v}$, and (2.35) becomes the same as (2.10). When $e_v \neq 0$, the perturbation term $g'(\hat{v})\dot{e}_v$ could be considered as a disturbance acting on an exponentially stable system. Since exponentially stable systems are robust to perturbations, we could expect stable (may not be necessarily asymptotically stable) error dynamics in (2.35). Consequently, in the presence of time delay, when the conditions stated in Lemma (2) are satisfied and velocity error and time delay are small enough, it is expected to have stable error dynamics as in delay free design. The following lemma clarifies this point.

Lemma 3. *Consider the system given by (2.1)-(2.2). Assume that $\hat{v}$ is the estimation of $v(t)$ (see Figure 1.2) and that the observer is given as (2.31)-(2.32), where $g(v) : \mathbf{R} \mapsto \mathbf{R}$ satisfies the conditions stated in Lemma 1 (or lemma 2). Furthermore assume that $sign(\hat{v}) = sign(v)$. Under these conditions, if $|g'(\hat{v})\dot{e}_v| < m$ for some $m > 0$, then the parameter estimation error e given by (2.10) is bounded as well. Furthermore, if $m \to 0$, then $|e| \to 0$ as well.*

Proof. Note that when $e_v = 0$, i.e. $\hat{v}(t) = v(t)$, then the parameter error satisfies (2.10), which is shown to be exponentially stable in Lemma 1 or Lemma 2. Then by classical converse theorems of Lyapunov stability theory, there exists a Lyapunov function $V : \mathbf{R}_+ \times \mathbf{R} \mapsto \mathbf{R}_+$ which satisfies the following

$$n_1\|e\|^2 \leq V(t,e) \leq n_2\|e\|^2 \tag{2.36}$$

$$\frac{\partial V}{\partial t} + \frac{\partial V}{\partial e}[-g'(\hat{v})sgn(\hat{v})e] \leq -n_3\|e\|^2 \tag{2.37}$$

$$\left\| \frac{\partial V}{\partial e} \right\| \leq n_4\|e\| \tag{2.38}$$

for some positive constants $n_1,\ n_2,\ , n_3,\ n_4$, see [32]. By using this function from (2.35) we obtain

$$\dot{V}(t,e) = \frac{\partial V}{\partial t} + \frac{\partial V}{\partial e}[-g'(\hat{v})sgn(\hat{v})e] - \frac{\partial V}{\partial e}(g'(\hat{v})\dot{e}_v) \tag{2.39}$$

$$\leq -n_3\|e\|^2 + n_4\|e\|m \tag{2.40}$$

$$\leq -n_3\|e\|\left(\|e\| - \frac{n_4}{n_3}m\right) \tag{2.41}$$

clearly, if $\|e\| \geq \frac{n_4}{n_3}m$, then $\dot{V} < 0$ and by (2.36), $\|e\|$ is bounded. By using standard Lyapunov Theory arguments it follows that the error is bounded [32]. In fact, $\lim_{t\to\infty} \|e(t)\| < \frac{n_4}{n_3}m$. Clearly as $m \to 0$, we have $e \to 0$ as well. □

Remark 4. *Lemma 1 and 2 show that when the measurements are not delayed, the observer structure given by (2.7)-(2.8) achieves exact friction cancellation since the parameter error dynamics is exponentially stable. When there is a measurement delay, obviously, we need to estimate $v(t)$ for exact friction cancellation.*

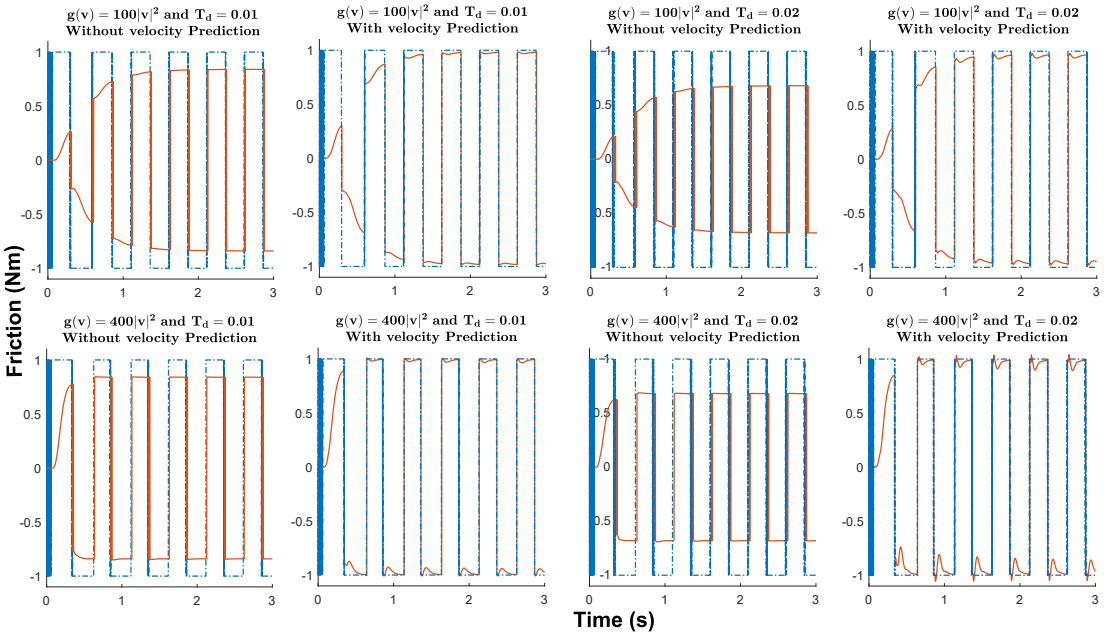

Figure 2.8: Friction estimation performances of Friedland-Park type observer designs with different estimation function and measurement delays.(Dashed Blue: $F(v) = sgn(v)$, Solid Orange: $\hat{F}(v)$)

In such a case, we need a method to estimate $v(t)$ based on the delayed measurements $v_o(t)$. If the methodology chosen for such an estimation yields small errors, then Lemma 3 guarantees that the friction parameter estimation error also remains small. This point will be clarified in the sequel, see Remark 5. □

In order to investigate the effects of output delay, we revisit the system in Figure 2.2 one more time and apply $u = 2\Lambda(2)$ to open loop system with adaptive estimation function $g(v) = 100v^2$ and $g = (v)400v^2$ for $T_d = 0.01$ and $T_d = 0.02$ seconds. In this case, estimation performance deteriorates even under small measurement delays compared to the input delay case. Moreover, without any predictor, there will be time lag equal to T_d between actual and estimated frictions as shown in Figure 2.8. Motivated by this, we will mainly consider measurement delay in the remaining chapters of the thesis since estimation performance may dramatically become poor under this type of delay. To this end, we will exhibit different velocity predictor designs to compensate for hindering measurement delay effects on friction estimation. However, here we present some results for observer response when a velocity predictor based on Heun Method is

employed to conclude our discussions on output delay , which will be explained in the following section. As shown in Figure 2.8, friction estimation matches with the existing friction pretty well thanks to Heun Method based predictor. We can conclude that minor mismatches between actual and inferred time delays can slightly affect the robustness of the controllers.

2.2.1 Velocity prediction via delayed measurements

For velocity prediction, we propose two different approaches. The first one is based on the numerical solution of Ordinary Differential Equations (ODEs). Although we mention some of the well known numerical solvers in this thesis, a numerical derivation is a broad research area and one can find some other advanced solvers to enhance the accuracy of prediction. In the second approach, we approximate the time delay as a rational function. Thus, the inverse of this rational function can be utilized to compensate for the effect of measurement delay on velocity signal.

Obviously, better velocity estimation schemes will yield better friction compensation performance. Two main approaches, which will be explained in this section, provide a sufficient velocity prediction in order to extend an adaptive observer to applications with measurement delay within the scope of our research; however, there might be other estimation schemes giving better velocity prediction error bounds in the literature. Indeed, this issue requires and deserves further investigation.

2.2.1.1 Numerical ODE Solver based approaches

As a first alternative to predict $v_o(t + T_d)$, one can simply utilize the definition of derivative as given below.

$$\dot{v}_o(t) = \lim_{T_d \to 0} \frac{v_o(t + T_d) - v_o(t)}{T_d}. \tag{2.42}$$

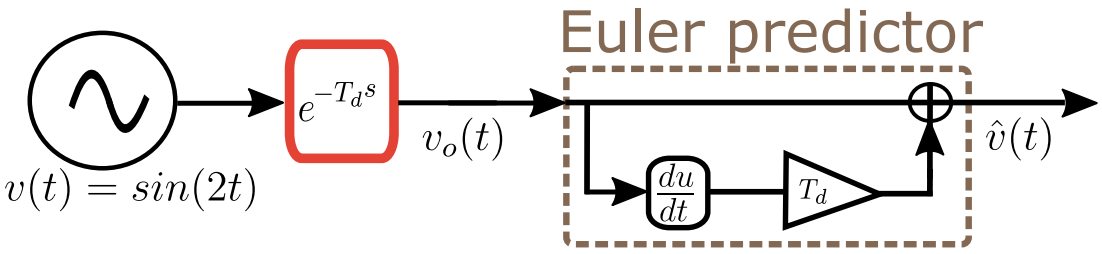

Figure 2.9: The Euler Approximation based velocity predictor.

Note that $\dot{v}_o(t)$ can be easily found since past velocity measurements have already been available. Then, $\hat{v}(t)$ can be estimated by using current value of $v_o(t)$ and its derivative $\dot{v}_o(t)$. By using this approach, which is well known as Euler approximation, we can approximate $\hat{v}(t)$ as follows

$$v(t) = v_o(t + T_d) \approx v_o(t) + T_d \dot{v}_o(t). \tag{2.43}$$

By considering $\hat{v}(t)$ is the estimation of $v(t) = v_o(t + T_d)$, we may utilize the following

$$\hat{v}(t) = v_o(t) + T_d \dot{v}_o(t). \tag{2.44}$$

Now from (2.42) it follows that the predicted velocity error e_v will be small if the time delay T_d is sufficiently small. To test this assumption, we apply a delayed sinusoidal input (u) to Euler Approximation based predictor as in Figure 2.9. As can be seen in Figure 2.10, the proposed method predicts $v(t)$ based on delayed measurements $v_o(t)$ with sufficient accuracy.

Remark 5. *Velocity estimation error bounds for Euler approximation can be obtained theoretically as well. Note that Taylor series expansion of a function* $f : \mathbf{R} \mapsto \mathbf{R}$ *can be given as follows:*

$$f(t + T_d) = f(t) + T_d \dot{f}(t) + \frac{1}{2} T_d^2 \ddot{f}(\xi) \tag{2.45}$$

where $t < \xi < t + T_d$*, see [40]. Now if we choose* $f(t) = v_o(t)$ *in (2.45), we obtain*

$$v_o(t + T_d) = v_o(t) + T_d \dot{v}_o(t) + \frac{1}{2} T_d^2 \ddot{v}_o(\xi) \tag{2.46}$$

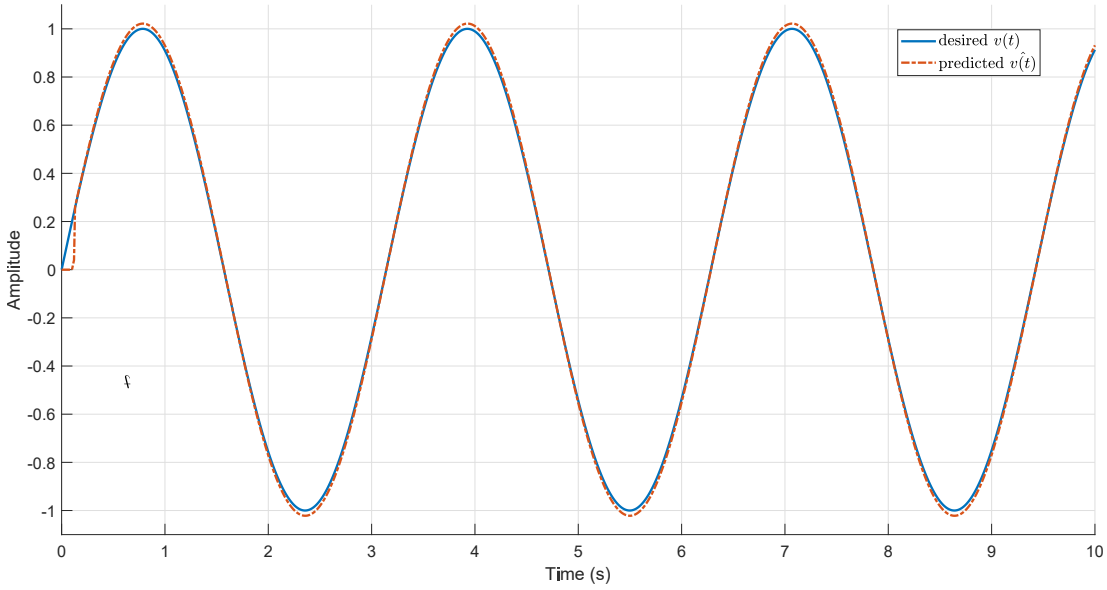

Figure 2.10: Performance of the Euler when desired velocity is $v(t) = sin(2t)$ and $T_d = 0.1$ second.

where $t < \xi < t + T_d$. *We note that the last term in (2.46) is called as the discretization or truncation error of Euler Method [40]. By using (2.29) and (2.44) in (2.46), we obtain*

$$v(t) = \hat{v}(t) + \frac{1}{2}T_d^2 \ddot{v}_o(\xi) \tag{2.47}$$

By using (2.30) we easily obtain

$$|e_v| = |v(t) - \hat{v}(t)| \leq \frac{1}{2}T_d^2 \hat{m}_1 \tag{2.48}$$

where $\hat{m}_1 = \max_t \ |\ddot{v}_o(t)|$. *Similarly, if we use* $f(t) = \dot{v}_o(t)$ *in (2.45) we obtain*

$$|\dot{e}_v| < \frac{1}{2}T_d^2 \hat{m}_2 \tag{2.49}$$

where $\hat{m}_2 = \max_t \ |\dddot{v}_o(t)|$. *Clearly, if* T_d *is sufficiently small, then the conditions of Lemma 3 are satisfied and subsequently the performance of the proposed friction compensation scheme will be satisfactory.* □

Note that Euler method is a first order approximation and there are some higher order methods such as Runge-Kutta, midpoint etc. [41]. For instance,

Heun Method, a particular choice of Runge-Kutta Method, is a second order technique that uses Euler approximation at the initial step, i.e.

$$v_o^i(t+T_d) = v_o(t) + T_d\dot{v}_o(t) \tag{2.50}$$

$$v_o(t+T_d) = v_o(t) + \frac{T_d}{2}\left(\dot{v}_o(t) + \dot{v}_o^i(t+T_d)\right). \tag{2.51}$$

In these equations, the initial estimation process is also called the predictor part. Together with finalized $v_o(t+T_d)$ computation, whole process is called predictor-corrector approach. Unfortunately, numerical derivative operation adds both positive and negative errors at the end of each step; therefore, it tends to be unstable. Although higher order approximations may provide better accuracy in the computation of derivative numerically, they become more sensitive to input uncertainties. In contrast to numerical integration, differentiation is an ill-conditioned process. Conditioning or condition number is a definition to measure amplification of the input perturbation at the output. Since high order numerical derivatives tend to provide larger condition numbers, they become vulnerable to input uncertainties as well [42]. Hence, in practice, filters are utilized to prevent large oscillations at the input of derivative action [43]. Practically, a simple low pass filtered differentiator, $L(s)$ is designed for the scope of this paper; however, filtering is a wide research area and one can find various filter designs in the literature for that purpose. Similarly, [34, 44] employ our proposed low pass filtered differentiator $L(s)$ aiming at a velocity prediction from position measurements. Distinctively, here in this study, we have employed a filter to predict velocity based on delayed velocity measurements. Certainly, it is also possible to use such a filter for velocity prediction from delayed position measurements in the absence of direct velocity output. Thus, we may use the following high-pass filter as a differentiator

$$L(s) = \frac{sN}{s+N}. \tag{2.52}$$

where N is high-pass filter coefficient. As N increases, filter behavior converges to ideal derivative operation. Nevertheless, in this case, filter gain becomes larger for high frequency signals and generates larger variations. Hence, the choice of N should be made carefully to realize this trade-off. Note that MATLAB also utilizes the same filtering to generate PID controllers.

Note that Euler Method is also a single step method because it refers to only one previous point and its derivative to determine the function's current value. Higher order methods such as Runge-Kutta take some intermediate steps. Alternatively, there are multi step methods utilizing more than one previous point to compute the function's current value. For instance, any two step linear multi step solver needs two past values to compute the current value of a function. In order to stay in the main scope of this thesis, we study two widely known two-step methods called Adams-Bashforth and Adams-Moulton. Interested readers can find further details about multi-step methods in [40, 41]. Two-step Adams-Bashforth Method is given as

$$v_o(t+T_d) = v_o(t) + \frac{T_d}{2}(3\dot{v}_o(t) + \dot{v}_o(t-T_d)). \tag{2.53}$$

Smilarly, two-step Adams-Moulton is given as

$$v_o(t+T_d) = v_o(t) + \frac{T_d}{2}(\dot{v}_o(t) + \dot{v}_o^i(t+T_d)). \tag{2.54}$$

Note that, like Heun Method, two-step Adams-Moulton Method is an implicit method. Therefore, a predictor-corrector approach should be utilized in order to compute an initial $\dot{v}_o^i(t+T_d)$. To this end, again, a simple solution is to utilize Euler Approximation. Nevertheless, when the number of steps increases, such solvers need further past values for numerical computation. What is more, they require a single step method such as Euler predictor to calculate some of their initial conditions. Therefore, single methods have some advantages over multi step methods in terms of practicability.

2.2.1.2 Inverse Pade Approximant based approaches

Irrational $e^{-T_d s}$ can be approximated by a rational function using Pade approximation such that

$$e^{-T_d s} \approx R(s) = \frac{\sum_{k=0}^{n} (-1)^k c_k T_d^k s^k}{\sum_{k=0}^{n} c_k T_d^k s^k} \tag{2.55}$$

where n is the order of approximation and coefficients are

$$c_k = \frac{(2n-k)!n!}{2n!k!(n-k)!}, \quad k = 0, 1, ..., n. \tag{2.56}$$

Typically, as delay increases, n should be increased as well to keep approximation error low. On the other hand, for substantial values of n, the relative magnitude c_0/c_n of the coefficients in (2.55) become very large; therefore, some numerical analysis/simulation difficulties can arise [45]. Furthermore, a high order approximation may produce clustered poles in the transfer function that makes the system sensitive to perturbations again. Aiming at delay cancellation, the inverse of Pade approximation should be cascaded to velocity output for prediction; however, note that (2.55) is a nonminimum phase system; hence its inverse is unstable. Therefore, another rational function approximation with zero numerator dynamics is used by taking the first n-terms of Maclaurin series [46]. Although this approach provides a coarse approximation compared to the standard Pade approximation, it is implementable. In this case (2.55) and (2.56) become

$$e^{-T_d s} \approx R(s) = \frac{1}{\sum_{k=0}^{n} c_k s^k} \tag{2.57}$$

$$c_k = \frac{T_d^k}{k!}, \quad k = 0, 1, ..., n. \tag{2.58}$$

Then, for an n^{th} order velocity prediction, it is sufficient to multiply velocity measurement with

$$R(s)^{-1} \approx 1 + T_d s + \frac{T_d^2}{2} s^2 + .. + \frac{T_d^n}{n!} s^n \tag{2.59}$$

Consequently, it is observed that either inverse of first order Pade approximation or Euler method can perform adequately for velocity prediction when the delay is not large compared to the system's bandwidth. The general representation of an n^{th} order predictor is illustrated in Figure 2.11. Note that both first order predictors have the same structure. Particularly, Euler method and first order inverse Pade approximant have the same structure as in Figure 2.11 with different c_1 coefficients. In Figure 2.12, a comparison of predictor errors of different velocity predictors can be found. In all predictors, initially estimation error,

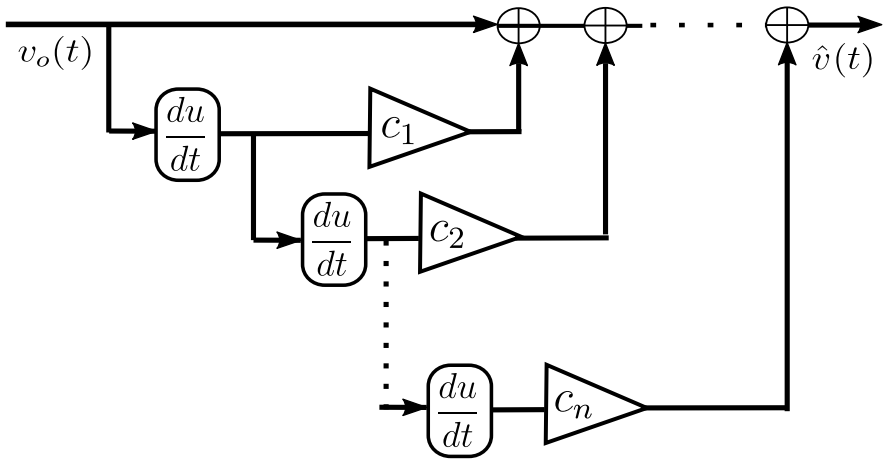

Figure 2.11: The general structure of a n-th order predictor

$e_v(0)$ is large due to time delay; however, it decreases after a while. In fact, all predictor schemes can be utilized to estimate the delay free velocity $v(t)$ since estimation error becomes smaller than its initial value. In this sense, using delayed measurements $v(t - T_d)$, their prediction $\hat{v}(t)$ converges to actual $v(t)$. Although the performance of Euler approximation is the worst among these predictors, its accuracy is still acceptable. Moreover, its simplicity is an advantage compared to other methods.

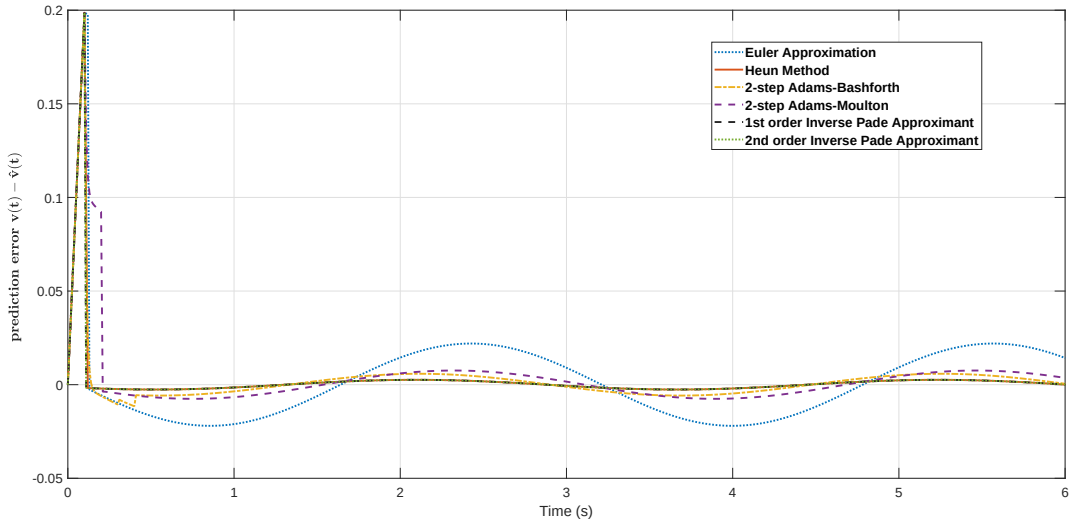

Figure 2.12: Prediction performances of different types of velocity predictors when $T_d = 0.1$s and $v(t) = sin(2t)$.

2.3 A New Observer design

In Section 2.1, we introduced a generalization of Friedland-Park observer to estimate the Coulomb Friction for simple mechanical systems without delay. Then, in Section 2.2, we modified this observer for the time delay case by introducing various velocity prediction schemes. Similar to Section 2.1, in the sequel, we will introduce a novel friction observer for simple mechanical systems for delay free case. Let us rewrite the simple mechanical systems given by (2.2) as below.

$$M\dot{v} = -Ma_c sgn(v) + u. \tag{2.60}$$

Assuming that v is measured, we first consider the following observer for velocity estimation

$$M\dot{\hat{v}} = -M\hat{a}_c sgn(v) + KM(v - \hat{v}) + u. \tag{2.61}$$

where $\hat{v}$ is the estimated velocity, $\hat{a}_c$ is the estimated Coulomb friction constant and $K > 0$ is an observer gain. Since v is already measured, one may argue that the observer given by (2.61) is not necessary. However, as it will become clear in the sequel, it is instrumental in estimating the friction coefficient a_c. Now let us define the velocity error e_v and Coulomb friction parameter error e_a as follows

$$e_v = v - \hat{v}, \tag{2.62}$$

$$e_a = a_c - \hat{a}_c. \tag{2.63}$$

By using (2.60) (2.61), we obtain

$$M\dot{e}_v = -Me_a sgn(v) - KMe_v \tag{2.64}$$

For the stability analysis, let us define the following Lyapunov function V:

$$V = \frac{1}{2}e_v^2 + \frac{L_1}{2}e_a^2 \tag{2.65}$$

where $L_1 > 0$ is another observer gain. By taking the derivative of (2.65) and using (2.64), we obtain:

$$\dot{V} = e_v\dot{e}_v + L_1 e_a\dot{e}_a \tag{2.66}$$

$$= -e_v e_a sgn(v) + L_1 e_a\dot{e}_a - Ke_v^2 \tag{2.67}$$

If we choose the following adaptive law

$$\dot{e}_a = \frac{1}{L_1} e_v sgn(v) \tag{2.68}$$

then, (2.67) becomes

$$\dot{V} = -K e_v^2 \leq 0 \tag{2.69}$$

which proves that the error system given by (2.64) and (2.68) is stable. For time-invariant systems, using LaSalle's invariance principle, one could prove asymptotic and even exponential stability [32]. However, due to the term $sgn(v) \in \{-1, 1\}$, the error system is time-varying and LaSalle's argument cannot be applied directly [32, 47]. Moreover, the error system can be viewed as a switching system and in general, the stability properties may depend on the so-called dwell time [48, 49]. We will address these issues in the sequel. Note that, assuming that a_c is constant, (2.68) results in the following adaptive parameter update rule

$$\dot{\hat{a}}_c = -L e_v sgn(v) \tag{2.70}$$

where $L = 1/L_1$ and $L > 0$. Using (2.64) and (2.70) state space representation of error vector $e = [e_v \ e_a]^T$ can be obtained as

$$\frac{d}{dt}\begin{bmatrix} e_v \\ e_a \end{bmatrix} = \underbrace{\begin{bmatrix} -K & -sgn(v) \\ L sgn(v) & 0 \end{bmatrix}}_{A(v)} \begin{bmatrix} e_v \\ e_a \end{bmatrix} \tag{2.71}$$

Note that the sign of off diagonal terms in $A(v)$ changes according to sign of velocity. In this manner, $A(v)$ can be treated as a system switching between $A_1(v)$ and $A_2(v)$ based on velocity sign. To clarify, $A_1(v)$ is associated with $v > 0$ while $A_2(v)$ is associated $v < 0$. Then, under this statement, they become

$$A_1(v) = \begin{bmatrix} -K & -1 \\ L & 0 \end{bmatrix}, \qquad A_2(v) = \begin{bmatrix} -K & 1 \\ -L & 0 \end{bmatrix} \tag{2.72}$$

Note that $A_1(v)$ and $A_2(v)$ have very similar structure. In fact, they share same eigenvalues since $|sI - A_i(v)| = s^2 + Ks + L$ for $i = 1, 2$. This equation

can be linked to the characteristic equation of a second order systems which is $s^2 + 2w_n\zeta s + w_n^2$. Then,

$$L = w_n^2, \tag{2.73}$$

$$K = 2w_n\zeta. \tag{2.74}$$

where ζ and w_n stand for damping ratio and natural frequency of second order system. Moreover, settling time to within 2% desired output and percentage overshoot equations can be rewritten as below adopting the definitions given in [50].

$$settling\ time = -\frac{2ln(0.02\sqrt{1-\zeta^2})}{K} \tag{2.75}$$

$$\%\ overshoot = 100e^{-K\pi/\sqrt{4L-K^2}}. \tag{2.76}$$

To sum up, new observer parameters K and L can be determined by considering settling time and overshoot performance of the observer response. For different K and L values calculated settling time and overshoot are presented in Table 2.1. These theoretical values are compatible with the responses plotted in Figure 2.13 where again $u = 2\Lambda(2)$ is applied to open loop observer as in the previous section. However, there are some minor differences between theory and simulations. For instance, for $K = 10$ and $L = 90$, simulated settling time and percentage overshoot are 0.73 seconds and 16.47% which are slightly different in Table 2.1. This difference is mainly due to the switching and hence essentially the time varying nature of the underlying dynamics given by (2.71). If the switching becomes less frequent, which is related to the so-called dwell-time, one expects that these mismatches may diminish and the second order approximation becomes more accurate. Consequently, it seems that this new proposed structure can provide a good enough friction compensation performance while it is easy to design. Likewise, under the presence of time delay, observer performance degrades. However, the parameters of new observer can be tuned considering delay effects or similar input/output delay compensation methods proposed in the previous section can still be implemented in order to improve estimation response.

Table 2.1: The theoretical Settling time and overshoot values for different K and L parameters of the new adaptive observer

K	L	ζ	w_n	settling time (s)	% overshoot
10	90	0.53	9.49	0.81	14.25
40	800	0.71	28.28	0.21	4.32
80	1600	1	40	0.23	0

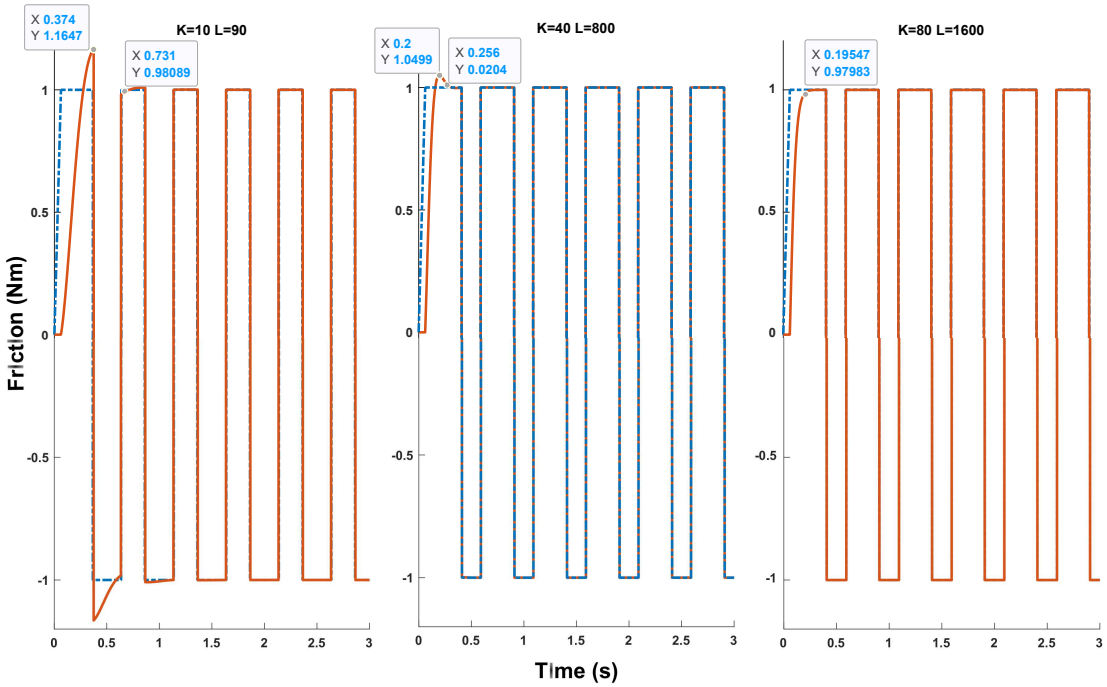

Figure 2.13: Friction estimation performance of the new observer design for different K and L values given in Table 2.1. (Dashed Blue: $F(v) = sgn(v)$, Solid Orange: $\hat{F}(v)$.)

2.3.1 Stability analysis of the new observer

As stated above, (2.69) proves the stability of the new observer, but not necessarily the asymptotic stability due to the switching nature of the whole system. The basic underlying reason is that LaSalle's Invariance Theorem is not directly applicable to our case due to the time-varying behavior of the switching signal. Nevertheless, as shown is [47], under certain cases, LaSalle's Invariance Principle can be applied to switching systems and asymptotic stability can be deduced under certain cases. This requires that the switching signal have certain properties,

depending on the so-called dwell-time. We will follow the methodology and results given in [47] in the sequel. To adopt the notation of [47], we first define the following quantities. Let $\sigma(.) : [0, \infty) \to \Sigma_2 = \{1, 2\}$ be a piecewise continuous function. Note that we will also refer to $\sigma(.)$ as the switching function. In our case, $\sigma(t)$ will depend on the sign of $v(t)$; i.e.

$$\sigma(t) = \begin{cases} 1, & v(t) \geq 0 \\ 2, & v(t) < 0 \end{cases} \tag{2.77}$$

Since $\sigma(.)$ is piecewise continuous, there exists a sequence $\{t_k \mid k = 0, 1, ...\}$ such that $t_{k+1} > t_k$ and $t_k \to \infty$ as $k \to \infty$. For simplicity, one may assume $t_0 = 0$. In our case, the instance t_k will denote the times that $v(t)$ changes the sign.

From a mathematical point of view, $\sigma(t)$ could be arbitrary, but if it has certain regularity, it was shown in [47] that LaSalle's Invariance Principle is applicable and one may deduce asymptotic stability. Next, we will give these regularity conditions.

We assume that $\sigma(t)$ satisfies the following properties:

A1) $\sigma(t) \in \Sigma_2$ and constant for $t_k < t < t_{k+1}, \ \forall k$.

A2) For any t and τ such that $t_k < t < t_{k+1} < \tau < t_{k+2}$, $\sigma(t) \neq \sigma(\tau), \ \forall k$.

A3) There exists a $\tau_D > 0$ such that $t_{k+1} - t_k \geq \tau_D, \ \forall k$.

Note that maximum $\tau_D > 0$ satisfying A3 is called dwell-time of the switching signal.

Now we consider the switching signals $\sigma(t)$ satisfying A1-A3, with the notations of [47]. This set contains sufficient regularity to prove asymptotic stability. For future reference, we define this set as follows;

$$\mathcal{S}_{ob} = \{\sigma : [0, \infty) \to \Sigma_2 | \sigma \ satisfies \ A1 - A3\} \tag{2.78}$$

Note that (2.65) could be written as follows

$$V = \frac{1}{2}e_v^2 + \frac{1}{2}L_1 e_a^2 = \frac{1}{2}\begin{bmatrix} e_v & e_a \end{bmatrix}\begin{bmatrix} 1 & 0 \\ 0 & L_1 \end{bmatrix}\begin{bmatrix} e_v \\ e_a \end{bmatrix} \tag{2.79}$$

Let us define the symmetric positive definite matrix P as

$$P = \begin{bmatrix} 1 & 0 \\ 0 & L_1 \end{bmatrix} \tag{2.80}$$

Clearly, by using (2.69), (2.71) and (2.72) we obtain

$$A_i^T P + P A_i = -\begin{bmatrix} 2K & 0 \\ 0 & 0 \end{bmatrix} \qquad i = 1, 2 \tag{2.81}$$

Next we define C_1 and C_2 as follows:

$$C_1 = C_2 = \begin{bmatrix} \sqrt{2K} & 0 \end{bmatrix} \tag{2.82}$$

From (2.81), it easily follows that

$$A_i^T P + P A_i = -C_i C_i^T \qquad i = 1, 2 \tag{2.83}$$

Moreover the pairs (C_i, A_i) are observable, $i = 1, 2$. Now we can state our main stability result.

Lemma 4. *Consider the observer system given by (2.71). Let $\sigma(t)$ be the switching signal for the velocity $v(t)$. We preset $\sigma(t) = 1$ when $v(t) \geq 0$ and $\sigma(t) = 2$ when $v(t) < 0$. Let $t_k,\ k = 0, 1, ..$ be the corresponding switching instants. Furthermore, assume that $\sigma(t)$ satisfies A1-A3. Under these conditions, the observer system given by (2.71) is exponentially stable.*

Proof. With the notation of [47], we have $\mathcal{S}_{ob} \subset \mathcal{S}_{dwell}$ i.e. the given conditions provide sufficient regularity for asymptotic stability, and the stability result follows from Theorem 4 of [47]. (For the definition of $\mathcal{S}_{dwell}$, see [47].) □

Remark 6. *We note that the essential part in the regularity conditions is the assumption that $t_{k+1} - t_k \geq \tau_D$. This implies that the switching frequency is finite. To demonstrate that this condition is essential, in [47] a switching system which*

is essentially the same as given by (2.72) is considered, and a special switching sequence for which $t_{k+1} - t_k \approx o(1/k)$ is constructed and it was shown that the system remains stable, but asymptotic stability does not hold. Note that for such a switching signal, the condition A3 is not satisfied, i.e. this switching signal does not have a nonzero dwell-time, and as a result, switching frequency does not remain finite.

Remark 7. *Previously, in Remark 2 and 3 we make some mild assumptions which are typical in adaptive control theory to guarantee the asymptotic stability of Friedland-Park type observers. Revisiting these remarks, we can state that it is necessary to satisfy either $|v| \geq 0$ or (2.16) for a sufficiently long period of time. Similarly, for the stability of the new observer structure, velocity switching frequency should be finite such that $t_{k+1} - t_k \geq \tau_D > 0$.*

2.3.2 Dwell time analysis for the new observer

Now consider the system given by (2.71). Let $\sigma(t)$ be the switching function related to the velocity $v(t)$, is indicated in Lemma 4 and let τ_D be the corresponding dwell-time. Note that both A1 and A2 given (2.72) are stable. Hence, according to the well known results, (2.71) is exponentially stable if τ_D is sufficiently large [51]. The minimum τ_D satisfying this result is also called minimum dwell-time for stability. Although an analytical solution of this minimum dwell time is not available, there are many efficient algorithms in the literature for the computation of τ_D [47, 48, 52, 53, 54].

In our case, subsystems $A_1(v)$ and $A_2(v)$ are all individually stable systems; therefore, a dwell time analysis is conducted to investigate the stability of the observer. For simplicity, we investigate delay-free dynamics. In the presence of delay, a velocity predictor proposed in the previous section can be utilized to diminish velocity error e_v. Alternatively, time delay can be injected in observer dynamics to get a switched delay system. However, dwell time analysis for switched delay systems is a vast research area; therefore, it is out of the main scope of the thesis, yet further interested readers in this subject may find some

inspiring details in [49, 55, 56].

Lemma 5. *Consider a class of switched delay system given by*

$$\dot{x}(t) = A_{\sigma(t)}x(t), \quad t \geq 0 \tag{2.84}$$

where $x(t) \in \mathbf{R}^n$ is the state vector and $\sigma(t)$ is the piecewise switching signal in a finite set $\mathcal{S} = 1, 2, ..., M$. Assume that, for given $T > 0$

$$\exists P_i : \begin{cases} P_i > 0, & \forall i \in \mathcal{S} \\ A_i' P_i + P_i A_i < 0, & \forall i \in \mathcal{S} \\ e^{A_i' T} P_j e^{A_i T} < P_i, & \forall i, j \in \mathcal{S}, \quad i \neq j. \end{cases} \tag{2.85}$$

Then, the system is exponentially stable for all $\sigma(t)$. Also, for switching instances t_k where $k = 1, 2, ..., M$, τ_D satisfying $t_{k+1} - t_k \geq \tau_D$ is called dwell time.

Interested readers can find further details and proof of the lemma in [57]. Also, note that this lemma provides a sufficient but not necessary condition for exponential stability. Therefore, the actual dwell time might be smaller than the solution found by Lemma 5 in practice. To compute the upper bounds of minimum dwell time, some advanced methods can be utilized. For instance, square matrix representation and Kronecker products based methods are proposed in [58]. However, observe that solutions of these methods coincide with Lemma 5 initially. In the light of this fact, we developed Matlab scripts given in Appendix A to minimize the solution LMI conditions given in Lemma 5 numerically for different K and L values. According to simulation results, minimum dwell time converges to zero for all K and L pairs in $[1, 10000]$. Note that this observation is in agreement with Lemma 4. Therefore, the new observer design is asymptotically stable. This can also be seen visually in Figure 2.14 within the interval $[1, 50]$. Certainly, in addition to stability concerns, one should also consider performance criteria. Previously, we state that friction estimation's percentage overshoot and settling time depend on parameters K and L. Therefore, when these parameters are large, undesired estimation responses can be acquired in an instantaneous interval and this can affect the performance of the overall closed loop feedback system.

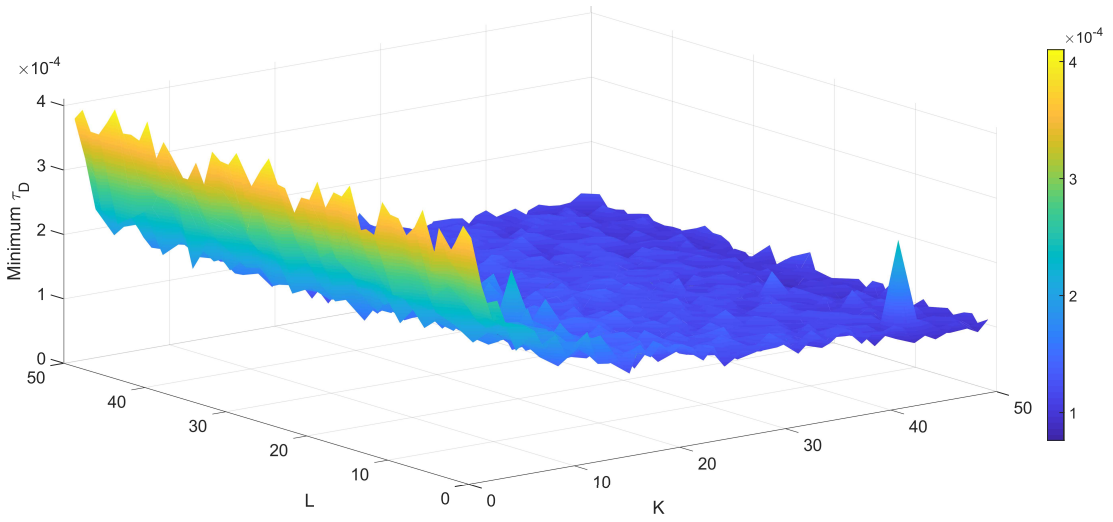

Figure 2.14: The minimum dwell time for different K and L values.

2.3.3 New observer with the delayed measurements

Similar to Section 2.2, next we will consider the effect of delayed measurements for the new observer. Note that in this case, we cannot measure the actual velocity $v(t)$, but only measure the delayed velocity $v_o(t) = v(t - T_d)$, see (2.28) and (2.29). Hence, the new observer equations should be modified as follows.

$$M\dot{\hat{v}} = -M\hat{a}_c sgn(\hat{v}) + KM(v_o - \hat{v}) + u. \tag{2.86}$$

By using (2.60), we obtain:

$$M\dot{\hat{v}} = -Ma_c sgn(v) + M\hat{a}_c sgn(\hat{v}) - KMe_v - KM(v_o - v). \tag{2.87}$$

If, as before, we assume that $sgn(v) = sgn(\hat{v})$, which is satisfied when $|v| > |e_v|$, we have the following

$$M\dot{e}_v = -Msgn(v)e_a - KMe_v - KM(v_o - v). \tag{2.88}$$

Note that apart from the last term, (2.88) is the same as (2.64). If we use the same adaptation rule as given by (2.68), the observer equation will become

$$\frac{d}{dt}\begin{bmatrix} e_v \\ e_a \end{bmatrix} = A(v)\begin{bmatrix} e_v \\ e_a \end{bmatrix} + \begin{bmatrix} -KM(v_o - v) \\ 0 \end{bmatrix} \tag{2.89}$$

In Remark 4, we conclude that when there is a measurement delay, it is required to design a velocity predictor for exact friction cancellation. If the time delay is small enough, a promising estimation performance can still be achieved without a velocity prediction for the cost of a negligible friction estimation error. Obviously, for large delay values, this error cannot be tolerated by the feedback system. Although new observer design include velocity error dynamics, a separate velocity prediction described in Section 2.2.1 may still be required to estimate friction precisely in systems with time delay. To investigate the delay effects on the estimation, we again revisit open loop system given in Figure 2.2. This time we utilize the new observer instead of a Fridlank-Park type observer in the simulations. As it is shown in Figure 2.15, Heun method based velocity predictor enhances the friction estimation performance. Furthermore, comparing Figure 2.13 and 2.15, we can observe that settling time and percentage overshoot slightly change when output delay is imposed. In fact, this is a conceivable outcome because delay term introduces infinitely many poles into the transfer function of the system. Hence, second order dynamics approximation changes. One should consider this to determine the observer parameters K and L. On the other hand, when velocity predictor as in Section 2.2.1 is utilized, the estimation response of the observe resembles to delay free case. Consequently, proposed velocity predictor schemes can be still employed together with the new observer structure in order to improve the friction estimation in systems with delay.

Remark 8. *Note that when $v_0 = v$, (2.89) reduces to (2.71), which is an exponentially stable system by Lemma 4. Hence, if $|v_o - v|$ is small, (2.89), similar to (2.33), becomes a bounded perturbation of an exponentially stable system. Hence if $|v_o - v| < m$, then we can state that $||e|| \leq Cm$ for some $C > 0$. Hence, as $m \to 0$, we have $||e|| \to 0$ as well. This property can easily be proven similar to Lemma 3. We also note that the perturbation term $v_o - v$ in (2.89) will be sufficiently small if the velocity prediction error is small as well, see (2.44)-(2.48).*

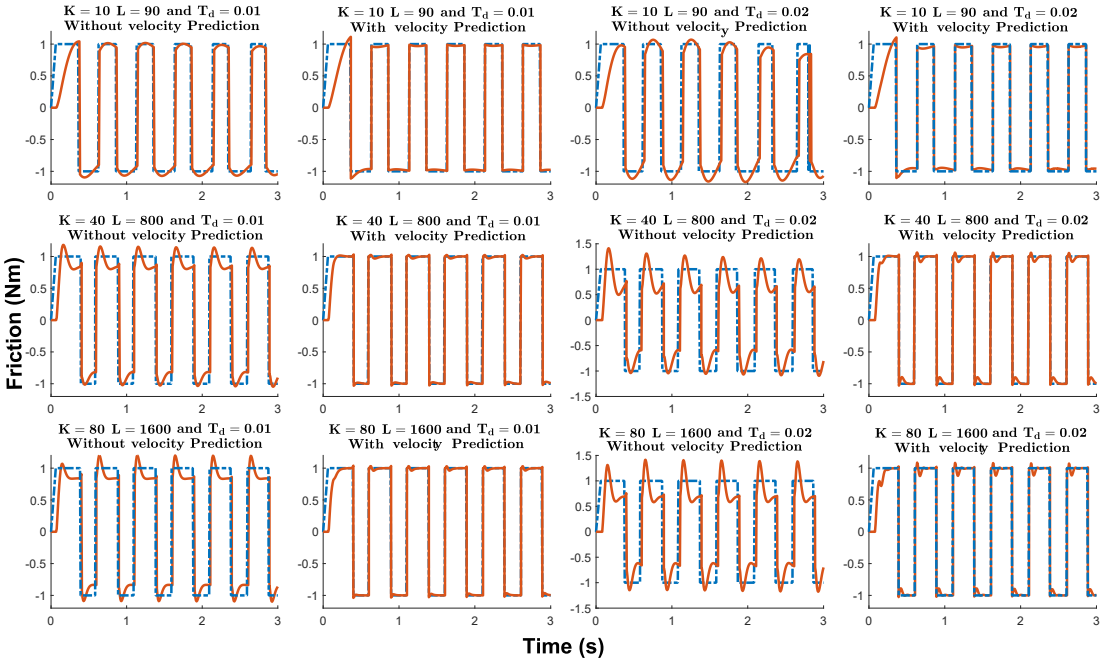

Figure 2.15: Friction estimation performances of the new observer design for different measurement delays and observer parameters. (Dashed Blue: $F(v) = sgn(v)$, Solid Orange: $\hat{F}(v)$)

Chapter 3

Controller Designs For Velocity and Position Loops

This dissertation investigates the effectiveness of adaptive observer based friction compensation approach for different controller implementations aiming at direct or hierarchical position control. To this end, we separately consider optimized PID controller designs based on the integral of time multiplied by absolute error (ITAE) for delay free systems and Smith Predictor based controller designs for systems with delay.

3.1 ITAE Index Based PID Controller Design

PID controllers are very popular in control theory. Roughly speaking, one can tune controller parameters to achieve desired performance metrics. While integral term denoted by K_i, improves steady state behavior and disturbance rejection, it also can lead to a larger settling time, overshoot and oscillatory response at the transient, which may even cause instabilities in some cases. On the other hand, the derivative term denoted by K_d, enhances transient response, provides shorter settling time and overshoot. In this case, derivative kicks due to large

derivative coefficients might be a drawback. Whenever the setpoint is adjusted, sudden changes in the error signal occur and as a result, the derivative of the error signal becomes very large instantaneously. This phenomenon is called derivative kick and may result in undesired saturation problems at the controller output. Lastly, the proportional gain denoted by K_p, can make the controller aggressive since the error signal is directly multiplied with it. In this sense, percentage overshoot may increase and steady state error may decrease when proportional gain is increased. In theory, the disturbance rejection performance is improved for larger K_p. However, in most of time, K_p alone is insufficient to eliminate steady state error completely because in real-world applications, there is an upper bound for K_p that can be set without causing instability. The system bandwidth and phase margin limit this bound. In conclusion, a good designer should recognize the trade-off among the parameters of a PID controller. In the literature, one can find many different algorithms for manual and auto tuning of PID controllers [59]. One popular approach among these algorithms is to define a performance index for controller optimization. For instance, integral of the square of the error (ISE), the integral of the absolute magnitude of the error (IAE), the integral of time multiplied by absolute error (ITAE), the integral of time multiplied by squared error (ITSE) are some of well known performance indices whose equations are given below.

$$ISE = \int_0^T e^2(t)\,dt, \tag{3.1}$$

$$IAE = \int_0^T |e(t)|\,dt, \tag{3.2}$$

$$ITAE = \int_0^T t|e(t)|\,dt, \tag{3.3}$$

$$ITSE = \int_0^T te^2(t)\,dt. \tag{3.4}$$

where e is the error is the difference between the reference input and the output of closed loop feedback system.

In theory, even a single proportional controller is sufficient to stabilize a feedback position control system designed for a first order plant transfer function without any position error when there is no friction. However, due to friction, a PID controller is required to satisfy performance criteria and eliminate steady

Table 3.1: Graham and Lathrop derived the set of normalized transfer function coefficients, minimizing the ITAE criterion for a step input.

$s + w_n$
$s^2 + 1.4w_n s + w_n^2$
$s^3 + 1.75w_n s^2 + 2.15w_n^2 s + w_n^3$
$s^4 + 2.1w_n s^3 + 3.4w_n^2 s^2 + 2.7w_n^3 s + w_n^4$
$s^5 + 2.8w_n s^4 + 5.0w_n^2 s^3 + 5.5w_n^3 s^2 + 3.4w_n^4 s + w_n^5$

Table 3.2: Graham and Lathrop derived the set of normalized transfer function coefficients, minimizing the ITAE criterion for a ramp input.

$s^2 + 3.2w_n s + w_n^2$
$s^3 + 1.75w_n s^2 + 3.25w_n^2 s + w_n^3$
$s^4 + 2.41w_n s^3 + 4.93w_n^2 s^2 + 5.14w_n^3 s + w_n^4$
$s^5 + 2.19w_n s^4 + 6.5w_n^2 s^3 + 6.3w_n^3 s^2 + 5.24w_n^4 s + w_n^5$

state error. To this end, we employ ITAE performance index to tune PID designed for position control. According to bandwidth requirements of desired PID controller, the optimum characteristic equation of closed loop feedback system for step input tracking is computed by Graham and Lathrop in [60] and presented in Table 3.1. Similarly, for ramp input tracking one can design an optimum PID using coefficients provided in Table 3.2 [59]. For instance, consider a plant transfer function $P(s) = K/Js$ where J denotes inertia. Then, a single closed loop position control system transfer function $T(s)$ can be derived as

$$T(s) = \frac{\frac{KK_d s^2}{J} + \frac{KK_p s}{J} + \frac{KK_i}{J}}{s^3 + \frac{KK_d s^2}{J} + \frac{KK_p s}{J} + \frac{KK_i}{J}}. \tag{3.5}$$

Afterwards, according to Table 3.1, controller parameters can optimized as given below.

$$1.75w_n = \frac{K_d}{J}, \tag{3.6}$$

$$2.15w_n^2 = \frac{K_p}{J}, \tag{3.7}$$

$$w_n^3 = \frac{K_i}{J}. \tag{3.8}$$

Similar to ITAE based position controllers, velocity controllers can be designed and employed for a hierarchical control loop. However, such a separate and

cascaded position and velocity controller designs are not very common in the literature. Also, since K_i is directly proportional with the cube of bandwidth, overshoot increases when controllers with large bandwidth are utilized. Therefore, in some applications, it is not an obligation but an option to design a pre-filter in order to improve the transient response of the feedback system as shown in Figure 1.2. One particular choice is to design a simple low-pass filter. A filter with a smaller cut-off frequency reduces the overshoot. However, diminution of the cut-off frequency affects the rising time negatively. In other words, system response slows down that is why cut-off frequency should be chosen according to the design requirements on overshoot and rise time of the system. Typically, it is chosen to cancel the fastest negative real axis zero of closed loop system [61]. In this case, the transfer function of this optional filter denoted by $H(s)$ can be written as follows

$$H(s) = \frac{K_i}{K_d s^2 + K_p s + K_i}. \tag{3.9}$$

3.2 Smith Predictor Based Controller Design

Generally, PID controllers are designed to track position input for delay free systems with friction in the literature [1, 3, 2]. On the other hand, Smith predictor controllers are very effective and easy to design to control systems with delay.

Time delay, also known as dead time or transport delay, may emerge due to signal transmission, communication, processing, analysis or measurement. Physical systems in the nature might have a significant amount of time delay making controller design challenging or causing performance and/or stability issues since time delay introduces infinitely many poles into closed loop transfer function. Motivated by this fact, [62] proposed a special predictor to the ease controller design process. In fact, although closed loop feedback system includes time delay physically, it is possible to remove this delay from the characteristic equation of the closed loop system mathematically as in Figure 3.1. In this case, it is possible to design a controller as if the plant is delay free. However, [63] proved that constant

disturbance rejection could not be achieved by using original the Smith predictor structure. Afterward, many other modifications have been made to improve the performance of Smith predictor in various application fields. For instance, [64] introduced a new form for the Smith predictor aiming at decoupling disturbance and set-point response from each other. In [65], an auto tuning algorithm is developed to estimate Smith predictor parameters; however, it requires no modeling error in the assumed plant transfer function. In reality, the perfect representation of the plant might not be always available; therefore, [66] has made an addition of extra feedback path from the difference of plant output and the model output to the control input aiming at higher order process control. Later, in [67], it is suggested to replace proportional controller in predictor structure with a lead/lag controller in order to have fast disturbance rejection. Furthermore, [68] studied a congestion control problem such that there is a bounded uncertainty in delay. For this problem, they utilized a geometric approach to design a Smith predictor plus proportional controller for the network system. For the control of a robot arm, [69] employs the internal model principle for Smith predictor based velocity and position controller design. The internal model control (IMC) principle implies that to reject impacts of disturbances and to track a reference signal, controller structure should include the copies of disturbance and reference signal generators [70]. Hence, [61] proposed a method to achieve desired set point tracking and robustness criterion based on IMC principle and calculate vector margin to analyze robustness to time delay perturbations.

To design a Smith Predictor based controllers, we utilized the technique developed by [69]. In this approach, it is possible to design a Smith predictor based controller using controller parametrization method given in [71] to place the poles of closed loop system to satisfy the required robustness and performance objectives. Indeed, applying the pole placement method based on the controller parametrization technique to both systems with and without time delay is possible. As another remark, it is possible to extend the idea given in this section to plant with any higher order transfer functions; however, we simply assume that plant has a first order transfer function including time delay. In this regard, it is worth reading the whole motivation presented in [61]. To start with, let the

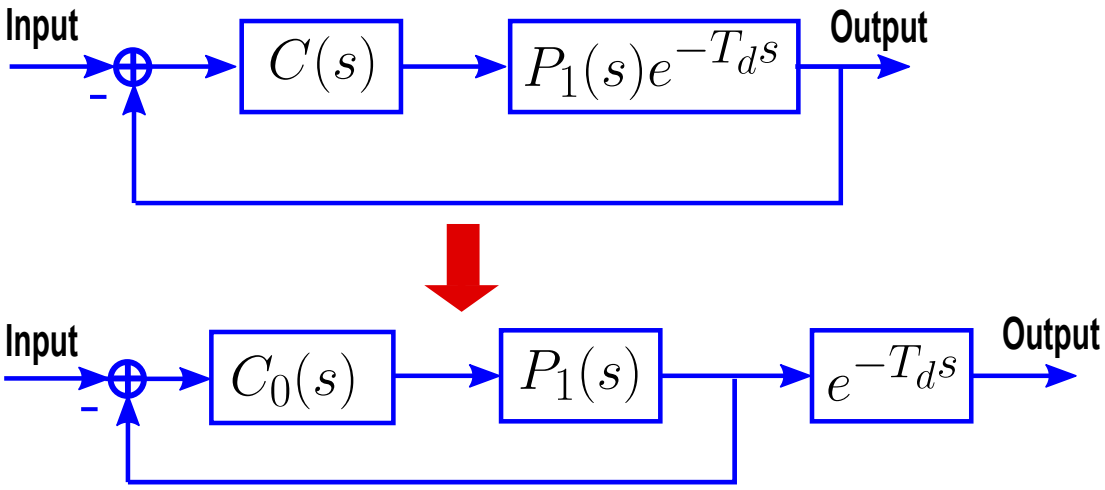

Figure 3.1: Although physically not the case, a smith predictor based controller $C(s)$, removes the time delay from the closed loop transfer function where $P_1(s)$ is delay free plant transfer function and $C_0(s)$ is a simple equivalent controller explained in later parts.

plant transfer function be,

$$P(s) = \frac{1}{Ms} e^{-T_d s} \tag{3.10}$$

Considering this transfer function, one can design either a direct closed loop position feedback system or nested position and velocity control loop structures as illustrated in Figure 1.2. Since a hierarchical closed loop feedback system can be regarded as an extension of a direct position control loop, we design both velocity and position controllers separately in this section instead of a single position controller design. To this end, a Smith Predictor based velocity controller, $C_v(s)$, is designed for the plant given by (3.10) first and then position controller $C_p(s)$ in the subsequent sections.

3.2.1 Velocity Controller Design

The main inspiration in $C_v(s)$ design is to use a copy of delay free plant transfer function and an internal controller $C_v(s)$ together in order to satisfy desired robustness and performance criteria. Hence, to get a simpler $C_v(s)$ a gain block M might be appended to controller to make plant transfer function $P_0(s) = \frac{1}{s} e^{-T_d s}$.

Then, complete controller $C_v(s)$, illustrated in Figure 3.2, can be obtained as

$$C_v(s) = \frac{C_{0v}(s)}{1 + C_{0v}(s)\left(\frac{1-e^{-T_d s}}{s}\right)}. \tag{3.11}$$

where $C_{0v}(s)$ is an internal velocity controller. Then, closed loop transfer function of velocity loop formed by $(C_v(s), P(s))$ can be obtained as

$$T_v(s) = \frac{C_{0v}(s)}{s + C_{0v}(s)} e^{-T_d s}. \tag{3.12}$$

Note that it is also possible to decompose (3.12) into $T_v(s) = T_{0v}(s)e^{-T_d s}$ where $T_{0v(s)} = {}^{C_{0v}(s)}/_{(s+C_{0v}(s))}$ is delay free closed loop velocity transfer function. To design C_{0v}, controller parametrization method explained below is employed.

- Transfer function of the delay free plant should be written in terms of coprime, rational and stable functions $N_p(s)$ and $D_p(s)$ such that

$$P_0(s) = \frac{N_p(s)}{D_p(s)}. \tag{3.13}$$

- Let the chosen $D_p(s)$ have zeros at $s = z_1, z_2, ..., z_n$. Then, another stable function $X(s)$ which satisfies $X(z_1) = {}^1/_{N_p(z_1)}, X(z_2) = {}^1/_{N_p(z_2)}, ..., X(z_n) = {}^1/_{N_p(z_n)}$ should be chosen.

- Lastly, a stable $Y(s)$ can be found by solving Bezout equation given below.

$$X(s)N_p(s) + Y(s)D_p(s) = 1. \tag{3.14}$$

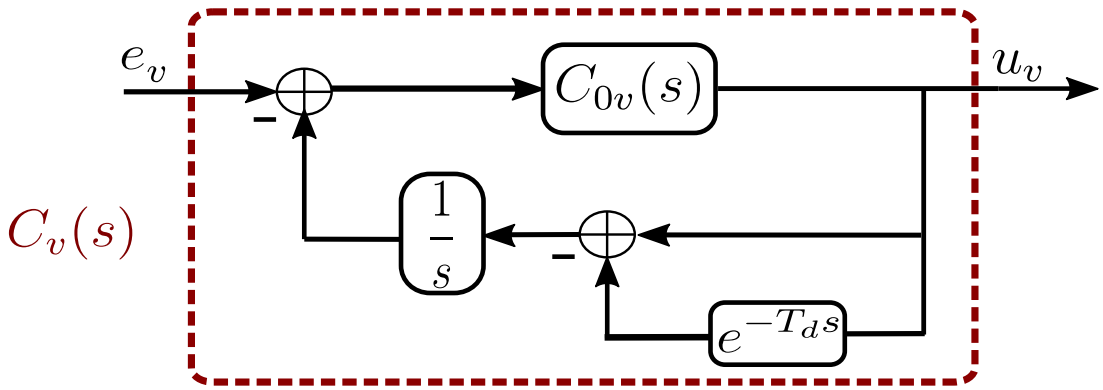

Figure 3.2: The structure of a Smith predictor based velocity controller

- Using these functions, the set of all stabilizing controllers can be written as

$$C(s) = \frac{X(s) + D_p(s)Q(s)}{Y(s) - N_p(s)Q(s)}. \tag{3.15}$$

where $Q(s)$ is proper and stable function satisfying $Q(s) \neq Y(s)N_p(s)^{-1}$. Also, it should be selected based on desired performance and robustness criterion; therefore, the minimum degree of $Q(s)$ is one less than the number of interpolation conditions. For instance, in order to obtain minimum degree controller stabilizing $P_0(s)$ when step input is applied, a particular choice might be $Q(s) = 0$ since plant has already a pole at $s = 0$. Then, for $N_p(s) = 1/(s + K_v)$, $D_p(s) = s/(s + K_v)$, $X(s) = K_v$ and $Y(s) = 1$, a candidate internal velocity controller, $C_{0v}(s)$, might be obtained such that

$$C_{0v}(s) = K_v. \tag{3.16}$$

where K_v is a free design parameter which will be determined by the pole placement method. Then, as in [38], $C_v(s)$, complete form of Smith predictor based controller and $T_v(s)$, closed loop transfer function for velocity, can be written as

$$C_v(s) = \frac{K_v}{1 + K_v\left(\frac{1-e^{-T_d s}}{s}\right)}, \tag{3.17}$$

$$T_v(s) = \frac{K_v}{s + K_v} e^{-T_d s}. \tag{3.18}$$

However, the controller given by (3.17) is only capable of step input tracking. Additionally, $Q(0) = Y(0)/N(0)$ condition should be satisfied if ramp input tracking is desired. In this case, we can simply choose $Q(s) = K_v$. Then, the transfer function of Smith predictor based controller for ramp tracking and its closed loop system become

$$C_{0v}(s) = \frac{2K_v + K_v^2 s}{s}, \tag{3.19}$$

$$C_v(s) = \frac{2s^2 K_v + sK_v^2}{s^2 + (2K_v s + K_v^2)(1 - e^{-T_d s})}, \tag{3.20}$$

$$T_v(s) = \frac{2K_v s + K_v^2}{(s + K_v)^2} e^{-T_d s}. \tag{3.21}$$

In general, one can determine the required $Q(s)$ in order to satisfy desired disturbance rejection and setpoint responses. Note that after controller parametrization

procedure is applied, the transfer function from input to output, $T_{rp}(s)$ and the transfer function from disturbance to output, T_{dp} can be acquired as below.

$$T_{rp}(s) = N_p(s)(X(s) + D_p(s)Q(s)), \tag{3.22}$$

$$T_{dp}(s) = N_p(s)(Y(s) + N_p(s)Q(s)). \tag{3.23}$$

Then, using the final value theorem, an appropriate Q(s) satisfying required conditions for desired disturbance rejection and setpoint responses can be determined. In this case steady state error, e_{ss} for a reference input $R(s)$ and disturbance $D(s)$ becomes

$$e_{ss} = \lim_{s \to 0} s[(1 - T_{rp}(s))R(s) - T_{dp}(s)D(s)]. \tag{3.24}$$

To sum up, it is possible to change controller design by simply changing $Q(s)$ and pole locations of the controller to satisfy different design requirements for a given plant transfer function.

3.2.2 Position Controller Design

Smith predictor based position controller has a very similar structure to the velocity controller given in the previous section. Distinctively, position controller, C_p, includes delay free transfer function of the velocity closed loop, T_{0v}, as in Figure 3.3. Thus, once the velocity controller is designed, same design procedure

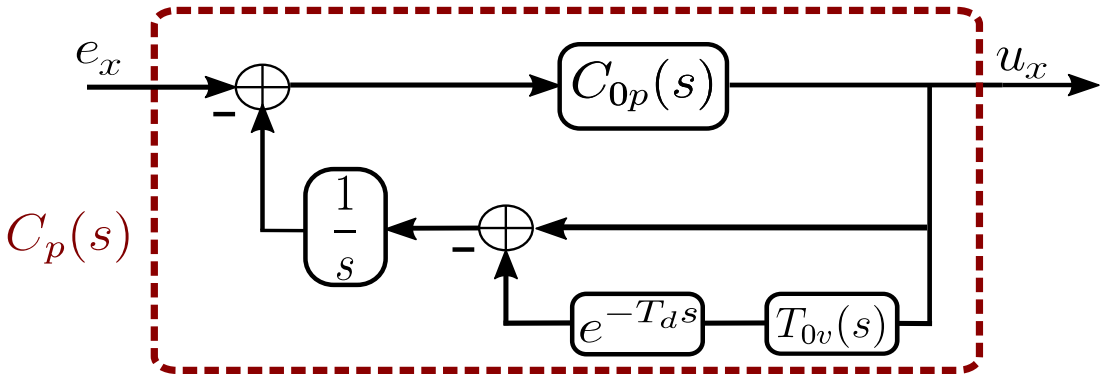

Figure 3.3: The structure of a Smith predictor based position controller

can be utilized for a position loop extension as well [38]. For step input tracking case, closed loop pole K_p can be located by again using the pole placement method. Thus, the transfer function of the controller can be given as

$$C_{0p}(s) = K_p. \tag{3.25}$$

$$C_p(s) = \frac{K_p}{1 + K_p \left(\frac{1 - T_{0v}(s) e^{-T_d s}}{s} \right)}. \tag{3.26}$$

Then, closed loop transfer function of hierarchical position system can be obtained as follows

$$\begin{aligned} T_p(s) &= \frac{K_p}{s + K_p} T_v(s) \\ &= \frac{K_p}{(s + K_p)} \frac{K_v}{(s + K_v)} e^{-T_d s}. \end{aligned} \tag{3.27}$$

Similarly, after ramp input tracking extension of velocity loop given by (3.19) and (3.21), we obtain following transfer functions for the position loop,

$$C_{0p}(s) = \frac{2K_p s + K_p^2}{s}, \tag{3.28}$$

$$C_p(s) = \frac{2K_p s^2 + K_p^2 s}{s^2 + (2K_p s + K_p 2)(1 - T_{0v}(s) e^{-T_d s})}, \tag{3.29}$$

$$T_p(s) = \left(\frac{2K_p s + K_p^2}{s^2 + 2K_p s + K_p^2} \right) T_v(s). \tag{3.30}$$

Mathematically, K_v and K_p can be set freely according to desired closed loop transfer function of the system. However, intuitively, it is generally expected that inner loop poles be larger than outer loop poles in the literature. Therefore, although it is not a strict requirement, poles of (3.27) or (3.30) may be allocated such that $K_v > K_p$. Again, the optimal pre-filter shown in Figure 1.2 can be designed to improve the transient response of the system. Certainly, more complex filter designs might be implemented for time delayed systems. For instance, Feliu-Batlle and Rivas-Perez insert inverse of the plant model inside the transfer function of the filter as in Smith-predictor based controller in [72].

Alternatively, it is possible to design a Smith predictor based position controller without a velocity control. In this case, closed loop feedback system includes

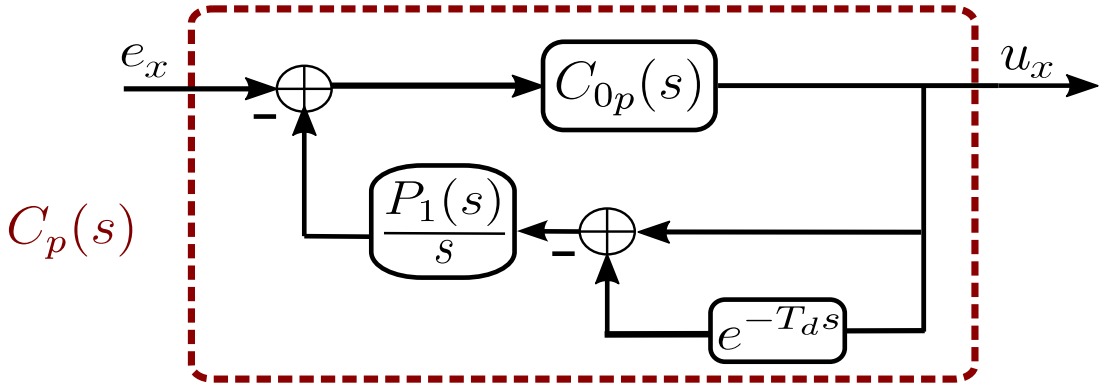

Figure 3.4: Smith predictor based position controller designed via direct approach.

only a single position loop. To this end, let $P_1(s)$ be the delay free plant transfer function. Then, using direct approach described in [61], a Smith predictor based position controller is designed such that

$$C_p(s) = \frac{C_{0p}(s)}{1 + C_{0p}(s)P_1(s)\left(\frac{1-e^{-T_d s}}{s}\right)}. \tag{3.31}$$

Then closed loop transfer function becomes as below

$$T_p(s) = \frac{C_{0p}(s)P_1(s)}{s + C_{0p}(s)P_1(s)} e^{-T_d s}. \tag{3.32}$$

Here, $C_{0p}(s)$ can be determined by appropriately chosen $Q(s)$ to satisfy design requirements and as a result general block diagram of the controller can be obtained as in Figure 3.4. For example, if it is desired that closed loop system consisting of $(C_p(s), P_1/s)$ can track step input without any steady state error, then we can simply choose $Q(s) = 0$, since the system already has a pole at $s = 0$. What is more, in order to guarantee the stability of the feedback system, the internal controller C_{0p} must stabilize the $P_1(s)/s$ and the set of all stabilizing controllers can be found again by using controller parametrization method. Lastly, an indirect controller design approach can be utilized to design a position controller in a hierarchical feedback system as in Figure 1.2. In this case, after velocity controller is designed, a position controller can be designed considering $P_1(s) = T_{0v}(s)$, see [61] for details.

Chapter 4

Simulation Results

We begin our simulations by considering different inspiring and comprehensive studies for delay free systems under LuGre friction from the literature. In these case studies, we use Matlab ode4 (Runge-Kutta) solver with 0.00001 step size.

We first recognize one degree of freedom rotary system without any elastic modes presented in [1]. For this study, required parameters are identified as given in Table 4.1. Mainly, [1], performs experiments and simulations in order to investigate the system responses to low-velocity sinusoidal position input, high-velocity sinusoidal position input and step position input. In all these experiments and simulations, model based friction compensation is utilized through feedback or feedback by considering different friction models. We repeat the simulations in

Table 4.1: Parameters used in [1]

Parameter	Notation	value	Unit
Stribeck velocity	v_s	0.01	rad/s
Stiffness coefficient	σ_0	$3.5x10^4$	$N.m/rad$
Damping coefficient	σ_1	0.1	$N.m.s/rad$
Coulomb friction	F_c	0.285	$N.m$
Stick friction	F_s	0.335	$N.m$
Viscous friction	F_v	0.018	$N.m.s/rad$
Total inertia	J	$3.8623x10^{-4}$	$kg.m^2$

[1], using Friedland-Park type and new observer instead of using fixed model based friction compensation through feedback. For this study, the position transfer function of the plant without friction can be written as below.

$$P(s) = \frac{1}{Js^2}. \tag{4.1}$$

According to [1], PD controller parameters can be computed as follows,

$$K_p = Jw_n^2, \qquad K_d = 2J\zeta w_n. \tag{4.2}$$

where w_n corresponds to the desired bandwidth of the closed loop control system and ζ is the damping coefficient. Similarly, coefficients of a PID controller can be obtained as below

$$K_p = Jw_n^2(1+2\zeta), \qquad K_d = 2Jw_n(1+2\zeta), \qquad K_i = Jw_n^3. \tag{4.3}$$

Then, aiming at low velocity sinusoidal input tracking for $\zeta = 1$ and $w_n = 36$ Hz PI and PID position controllers are designed as follows

$$C_{PD}(s) = 19.7612 + 0.1747s, \tag{4.4}$$

$$C_{PID}(s) = \frac{0.2621s^2 + 59.2836s + 4469.9}{s}. \tag{4.5}$$

In Figure 4.1, tracking performance of the controllers is presented when a reference input such that $\theta_d(t) = 0.01(1 - cos(0.8\pi t))$ is applied. For the observer, we again consider same design parameters $\zeta = 1$ and $w_n = 36$ Hz and computed $K = 72$ and $L = 1296$ by using (2.73) and (2.74). It is clear that without any friction compensation, $C_{PD}(s)$ cannot track the reference input. On the other hand, although $C_{PID}(s)$ has the same bandwidth with $C_{PD}(s)$, it manages to follow reference with some distortion. This behavior is called hunting and introduced by integral term of the controller which aggravates stick slip [9]. Furthermore, we investigate the effects of fixed torque compensation when static parameters i.e. stiction and Columb friction are identified erroneously. To this end, we positively perturbed these terms in feedback compensation such that $\hat{F}_c = 1.05F_c$ and $\hat{F}_s = 1.05F_s$ for %5 perturbation and $\hat{F}_c = 1.1F_c$ and $\hat{F}_s = 1.1F_s$ for %10 perturbation. In these cases, tracking performance of both $C_{PD}(s)$ and

$C_{PID}(s)$ deteriorate and show oscillatory response at the steady state as in Figure 4.1 B and D since there are mismatches among actual and identified friction coefficients. In fact, amplitude of these oscillations is increased for $C_{PID}(s)$ compared to $C_{PD}(s)$. Alternatively, when an adaptive observer is employed instead of fixed torque friction compensation, both of the controllers can track the reference smoothly as in Figure 4.1 A and C. Note that fixed friction compensation is a model based technique and require a precise friction parameter identification which may not always be possible. Hence, utilizing such an adaptive observer can be advantageous since it does not require a friction model and parameter identification.

Similarly, following position controllers are utilized to track a high-velocity sinusoidal position input such that $\theta_d(t) = 0.5(1 - cos(0.2\pi t))$ for the plant given in (4.1) with $\zeta = 0.85$ and $w_n = 10$ Hz. Then using (4.2) and (4.3), PD and PID controllers acquired as below :

$$C_{PD}(s) = 1.5248 + 0.0413s, \tag{4.6}$$

$$C_{PID}(s) = \frac{0.0655s^2 + 4.1169s + 95.8049}{s}. \tag{4.7}$$

Note that from (2.73) and (2.74), we compute $K = 17$ and $L = 100$ for this case.

As it can be seen in Figure 4.2, without any friction cancellation PD controller exhibit the worst tracking performance and PID controller leads to hunting at the position reversals. Furthermore, for low velocity sinusoidal position input case, fixed friction compensation with perturbed static parameters results in oscillations at position reversals. Once more, adaptive observers enhance the tracking performance for both $C_{PD}(s)$ and $C_{PID}(s)$.

Thirdly, [1] designs following controllers for square wave position tracking when $\zeta = 0.9$ and $w_n = 35$ Hz. By using (4.2) and (4.3), the designed PD and PID controllers are as given below :

$$C_{PD}(s) = 18.6786 + 0.1529s, \tag{4.8}$$

$$C_{PID}(s) = \frac{0.2378s^2 + 52.3001s + 4107.6}{s}. \tag{4.9}$$

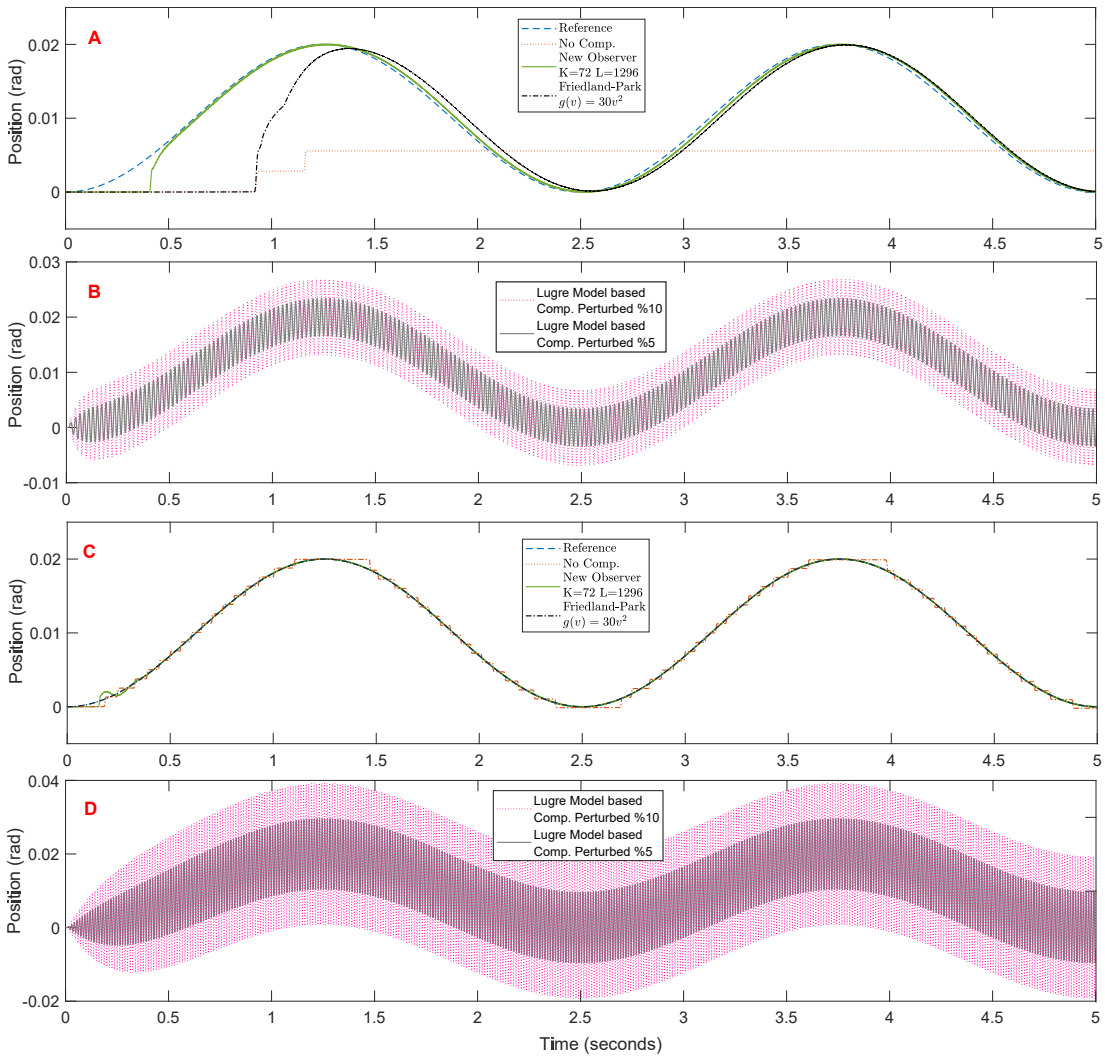

Figure 4.1: Low velocity sinusoidal position input tracking responses of $C_{PD}(s)$ and $C_{PID}(s)$. (A): Adaptive Friction compensation with $C_{PD}(s)$. (B): LuGre Model based fixed torque compensation with $C_{PD}(s)$. (C): Adaptive Friction compensation with $C_{PID}(s)$. (D): LuGre Model based fixed torque compensation with $C_{PID}(s)$.

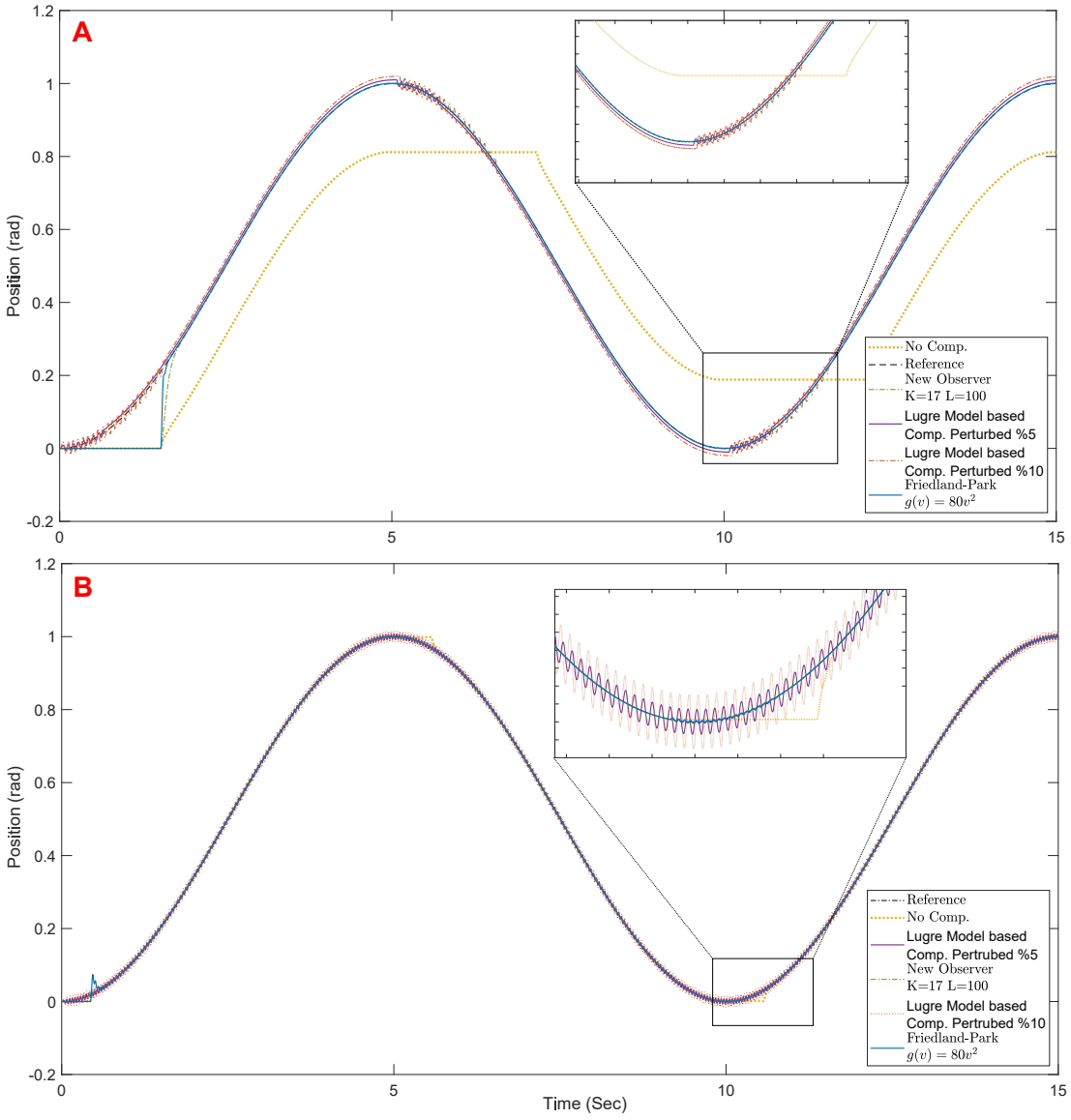

Figure 4.2: High velocity sinusoidal position input tracking responses of $C_{PD}(s)$ and $C_{PID}(s)$. (A): Friction compensation with $C_{PD}(s)$. (B): Friction compensation with $C_{PID}(s)$.

Table 4.2: Parameters used in [2]

Parameter	Notation	value	Unit
Stribeck velocity	v_s	0.001	m/s
Stiffness coefficient	σ_0	10^5	N/m
Damping coefficient	σ_1	$\sqrt{10^5}$	$N.s/m$
Coulomb friction	F_c	1	N
Stick friction	F_s	1.5	N
Viscous friction	F_v	0.4	$N.s/m$
Total mass	m	1	kg

Moreover, we employ the following reference filter $H(s)$, which is a simple low-pass filter indeed, in order to make sharp edges of the input smooth and improve the tracking performance.

$$H(s) = \frac{5}{s+5}. \tag{4.10}$$

As it can be seen in Figure 4.3, a position control system including $C_{PD}(s)$ provides a poor tracking performance without any friction compensation. Furthermore, as in previous cases, $C_{PID}(S)$ can track the square wave position input; however, at steady state, hunting is again observed. Also, $C_{PID}(S)$ having the same bandwidth with C_{PD} is more sensitive to perturbations in static parameters when model based fix torque friction compensation is applied. Consequently, adaptive observers improve the closed loop feedback system performance by eliminating friction in all three cases.

In our second case study, we consider the servo problem given in [2]. Related parameters with this study are presented in Table 4.2. Again, in our simulations, we utilize Friedland-Park type and new observer designs instead of the proposed observer in [2] and to make a fair comparison, we employ the same PID controller with $K_p = 3$, $K_d = 6$ and $K_i = 4$. Note that in this paper, an arbitrary PID controller is employed. Therefore, when there is no friction compensation, the hunting becomes evident at the steady state as in Figure 4.4. On the other hand, promoting adaptive observers with a poorly designed controller improves the tracking performances as expected.

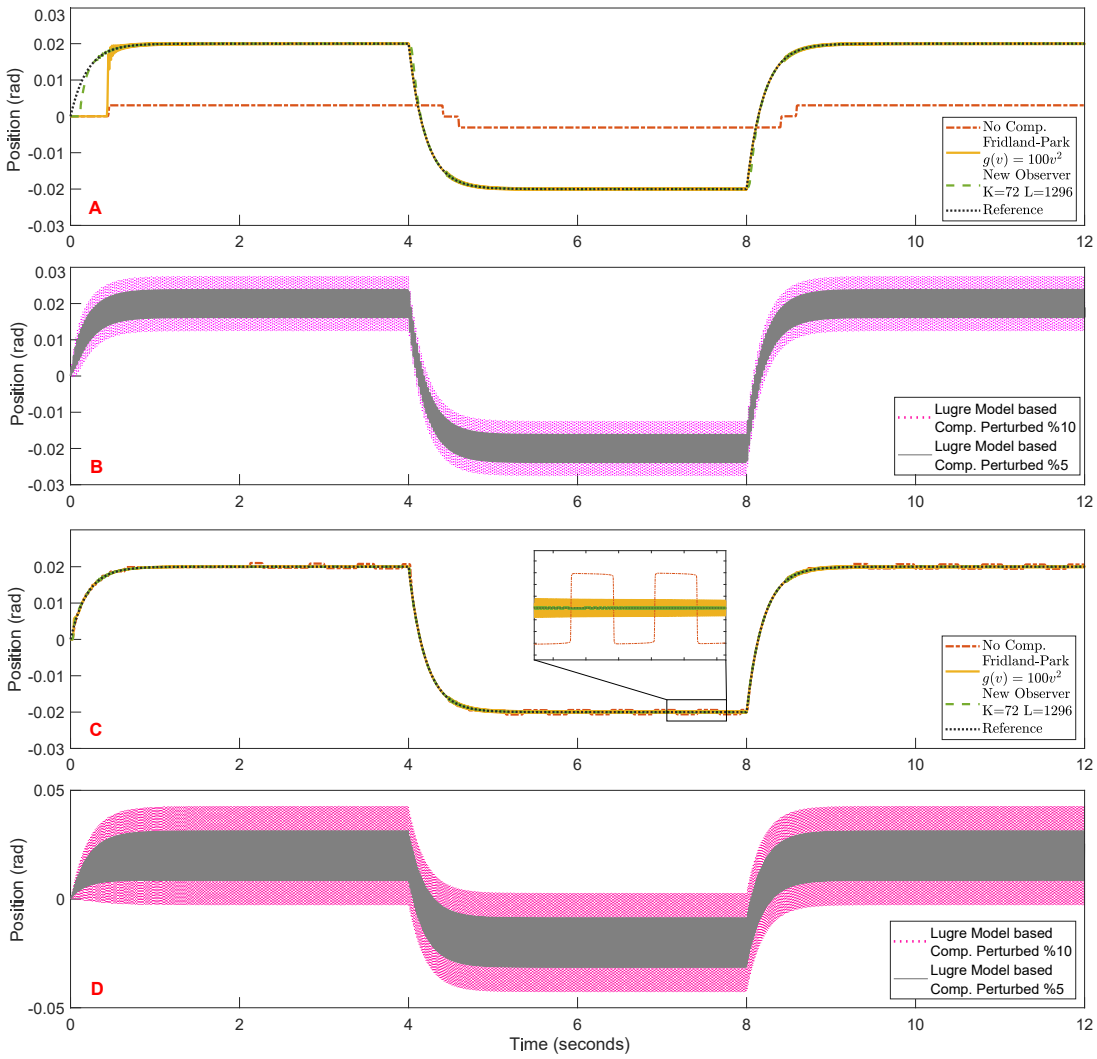

Figure 4.3: Square wave position input tracking responses of $C_{PD}(s)$ and $C_{PID}(s)$. (A): Adaptive Friction compensation with $C_{PD}(s)$. (B): LuGre Model based fixed torque compensation with $C_{PD}(s)$. (C): Adaptive Friction compensation with $C_{PID}(s)$. (D): LuGre Model based fixed torque compensation with $C_{PID}(s)$.

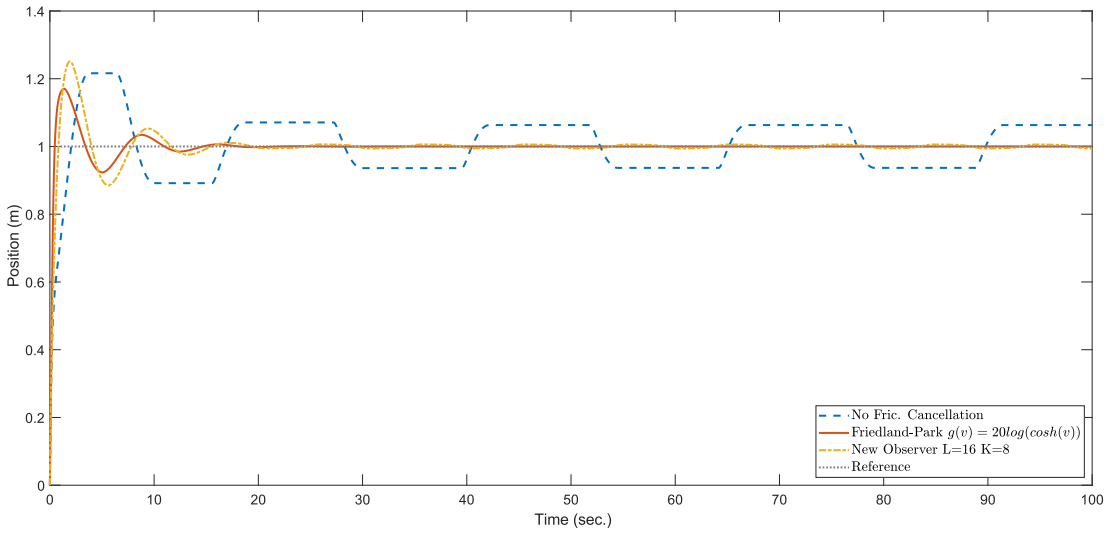

Figure 4.4: Position response of the servo system.

In our third and last case study, we consider the research presented in [3, 73]. Using the parameters given in Table 4.3, we investigate the relation between limit cycle behavior due to hunting and controller bandwidth.To this end, we perform simulation for two different PID position controllers namely $C^1_{PID}(s)$ and $C^2_{PID}(s)$. In [73], transfer functions of these controllers are given as

$$C^1_{PID}(s) = \frac{0.01196s^2 + 0.1656s + 0.4968}{s} \tag{4.11}$$

$$C^2_{PID}(s) = \frac{0.1909s^2 + 6.21s + 62.1}{s}. \tag{4.12}$$

Table 4.3: Parameters used in [3]

Parameter	Notation	value	Unit
Stribeck velocity	v_s	0.1	rad/s
Stiffness coefficient	σ_0	280	$N.m/rad$
Damping coefficient	σ_1	1	$N.m.s/rad$
Coulomb friction	F_c		$N.m$
along + direction		0.30	
along − direction		0.15	
Stick friction	F_s		$N.m$
along + direction		0.45	
along − direction		0.35	
Viscous friction	F_v	0.017	$N.m.s/rad$
Total inertia	J	0.0023	$kg.m^2$

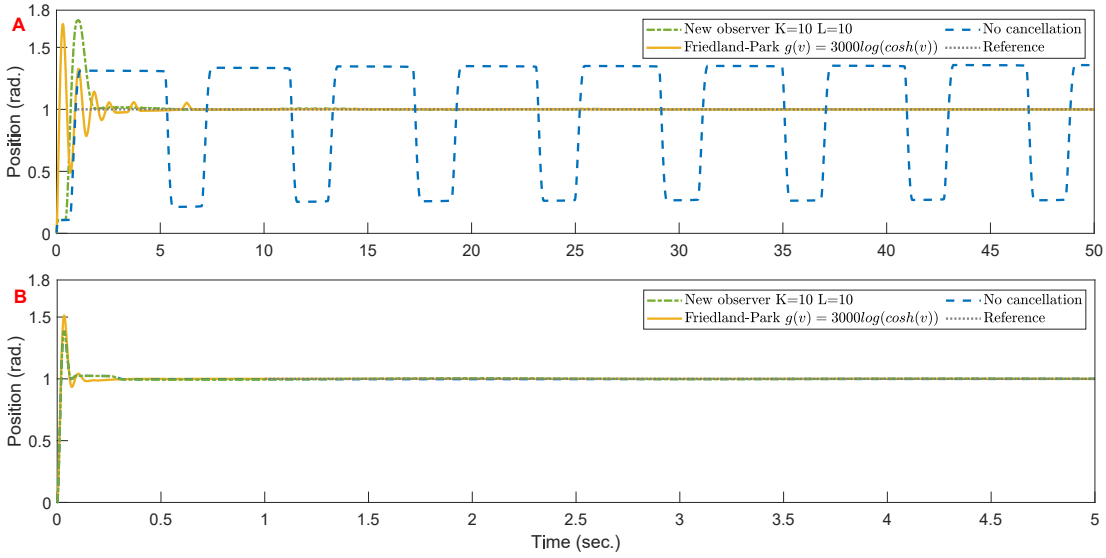

Figure 4.5: Position response of the system. (A): $C^1_{PID}(s)$ is utilized. (B): $C^2_{PID}(s)$ is utilized.

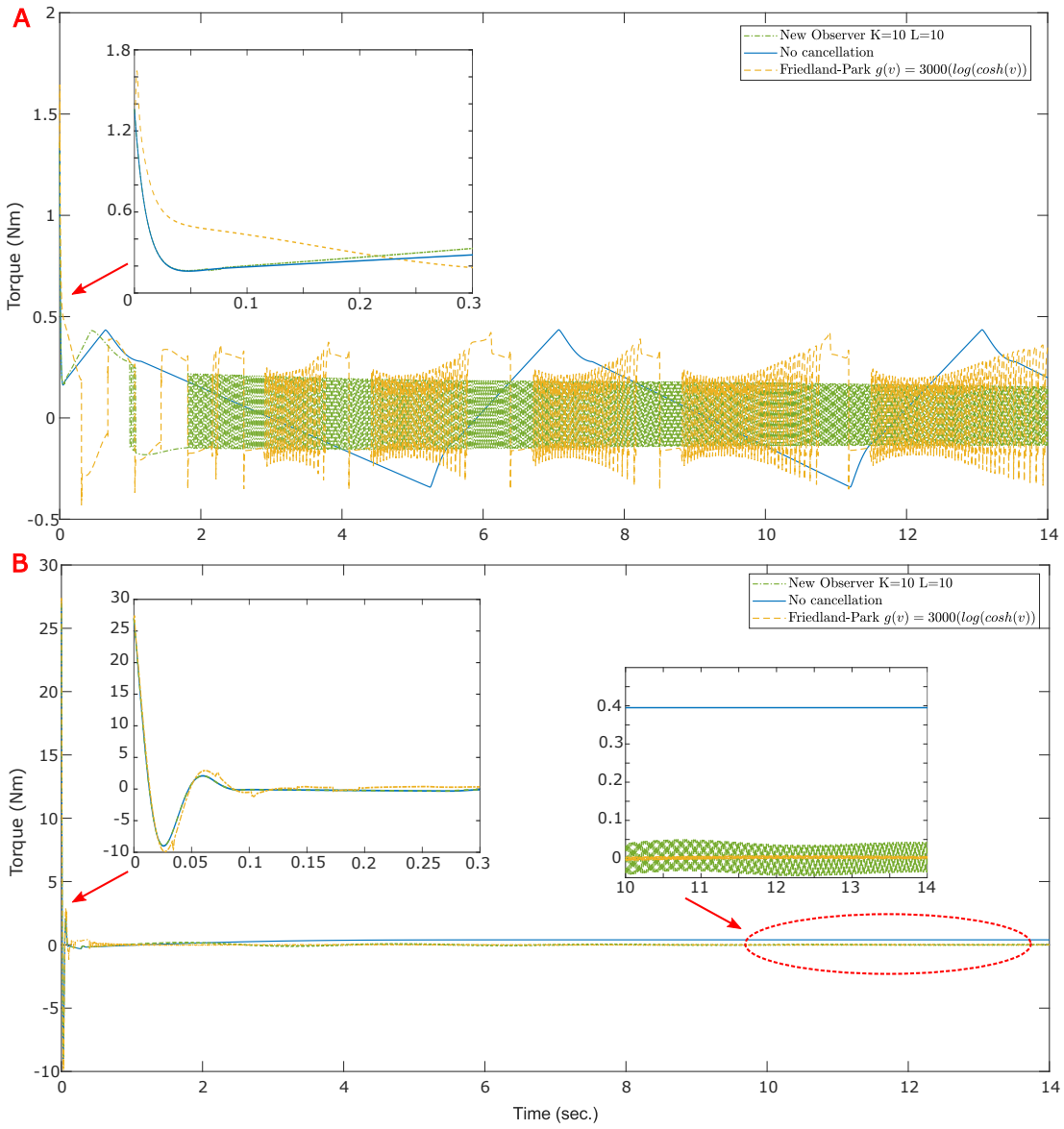

Figure 4.6: Total torque delivered to the plant for position tracking with and without friction compensation. (A): $C^1_{PID}(s)$ is utilized. (B): $C^2_{PID}(s)$ is utilized.

Note that both $C^1_{PID}(s)$ and $C^2_{PID}(s)$ are ITAE index based optimal position controllers. However, based on Figure 4.5, we can conclude that controller bandwidth should be large enough in order to prevent hunting when there is no friction compensation. Especially in this case, adaptive observers are required to track desired input. If controller bandwidth is large enough, the usage of such an adaptive observer apparently does not improve the performance significantly. However, note that one may not always employ a controller with a large bandwidth due to design constraints. Furthermore, we compare the total actuation torque of these two PID controllers delivered to the plant. As it is shown in Figure 4.6 A, since $C^1_{PID}(s)$ has a lower bandwidth, peak torque is lower compared to torque generated by $C^2_{PID}(s)$. What is more, without a friction compensation, there are oscillations at the steady state on the generated torque, which cause hunting in position response. On the other hand, at the transient, all torque characteristics are similar. Likewise, in Figure 4.6 B, transient responses are similar. However, compared to $C^1_{PID}(s)$, peak torque generated by $C^2_{PID}(s)$ is larger. In practice, this can cause some performance problems, such as saturation. Also, without a friction compensation, generated torque at the steady state is larger. On the other hand, when friction compensation generated torque is around zero. These observations show that proposed observers improve the tracking performance without causing torque generation problems.

Next, we focus on friction cancellation in the presence of measurement delay. For this purpose, we consider Coulomb friction in the first set of simulations and then LuGre friction model. The parameter set used in these simulations is presented in Table 4.4. For these set of simulations, cascaded Smith predictor based velocity and position controllers described in Section 3.2.1 and 3.2.2 are utilized.

Table 4.4: Parameters used in measurement delay simulations

Parameter	Notation	value
Stribeck velocity	v_s	0.001 m/s
Stiffness coefficient	σ_0	10^5 N/m
Damping coefficient	σ_1	$\sqrt{10^5}$ Ns/m
Coulomb friction	F_c	4 N
Stick friction	F_s	4.7 N
Viscous friction	F_v	0.4 Ns/m
Total mass	M	5 kg
Position controller design parameter	K_p	
Triangular wave tracking		4
Square wave tracking		5
Velocity controller design parameter	K_v	
Triangular wave tracking		20
Square wave tracking		15
Dead time	T_d	0.1 s
Reference filter cutoff freq.	w_{pc}	3 rad/s
Derivative filter coefficient	N	100
Observer estimation function	$g(\hat{v})$	$k.ln\,(cosh(\hat{v}))$
	$g'(\hat{v})$	$k.tanh(\hat{v})$

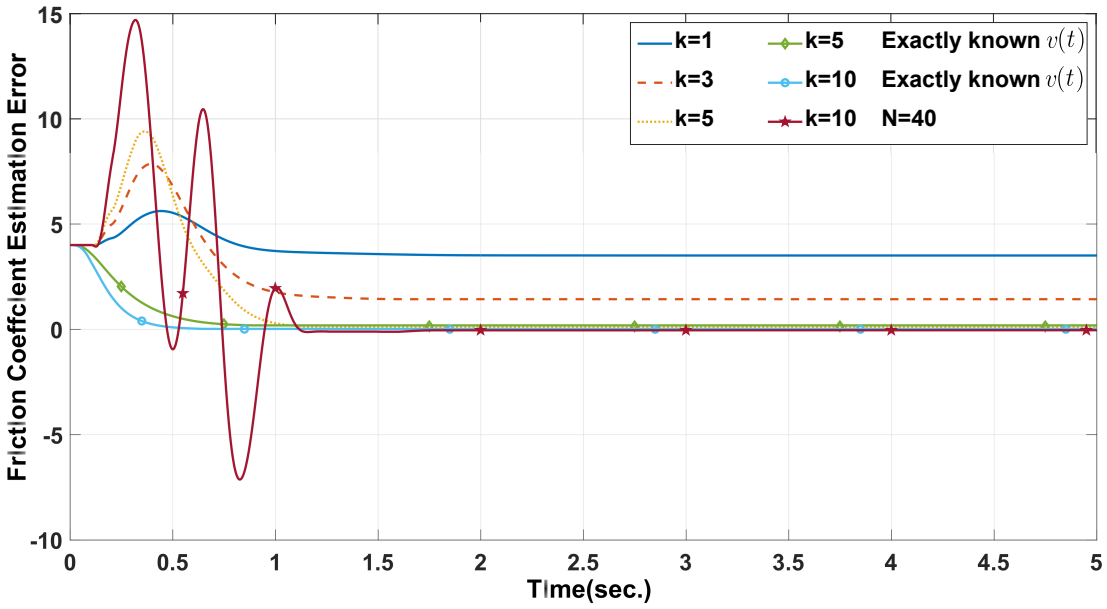

Figure 4.7: Friction estimation error, e, for unit step position tracking response with 1^{st} order inverse Pade approximant velocity prediction and Friedland-Park type observer under Coulomb Friction.

To see the efficiency of Friedland-Park type friction observer with $g(v) = k.ln\,(cosh(\hat{v}))$ and velocity estimator, we first considered position tracking response for unit step input when first order Pade approximant based velocity estimator is employed. In Figure 4.7, it is clear that when the actual velocity is known, the friction parameter estimation error e, converges to 0 for the observer gain $k = 5$ or $k = 10$. Note that this behavior is in agreement with the conclusions given in Lemma 1 and Remark 2. Also, note that when actual velocity measurement is available, increasing the observer gain k leads friction estimation to converge actual friction faster. In fact, this observation is also in agreement with Remark 3. On the other hand, the friction estimation error may not converge to zero within a reasonable duration when the observer gain is too low.

For the same observer gains, when proposed first order Pade approximant velocity predictor has adopted friction estimation under measurement delay becomes similar to the case in which the actual velocity is available. Although the velocity predictor provides a similar $e(t)$ response at the steady-state behavior as in delay free case, it may also exhibit some relatively large overshoots at the transient (e.g., for $t < 1.5$ sec), especially when the observer gain is increased. Likewise, the effect of observer gain k on the velocity prediction error e_v is presented in Figure 4.8. Again we can observe that there might be relatively large overshoots at the transient (e.g., for $t < 1.5$ sec) while e_v converges to zero at the steady-state. Again these oscillations may not be nonnegligible for large observer gains. In fact, when the actual velocity is not known and should be estimated, we observe that initial fluctuations on the velocity prediction errors may cause some undesired transient effects on the friction estimation error for large gains (see Figure 4.7). Furthermore, the last observation may also apply to the case of large time delays, since naturally, one expects a decrease in the velocity prediction performance. Hence, the selection of optimal observer gain appears to be an important problem that requires further investigation. In this respect, we also observed that decreasing N, the cut-off frequency of the low-pass filtered derivative in velocity prediction block, may also improve the transient response even for relatively large observer gains. Therefore, it may enhance both friction and

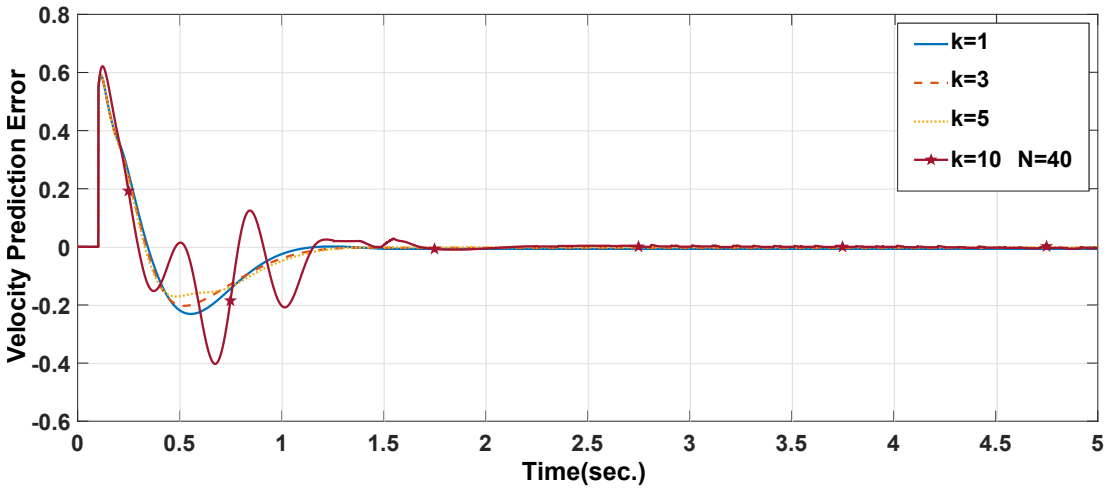

Figure 4.8: Velocity loop error, e_{vl}, for unit step position tracking response with 1^{st} order inverse Pade approximant velocity prediction and Friedland-Park type observer under Coulomb Friction.

velocity estimation performances. This approach may also be beneficial under the presence of dynamic friction (see e.g. the results given in Tables 4.5 and 4.6). To this end, the relation between k and N may be worth further investigation.

Table 4.5: Comparison of the different velocity prediction approaches in Friedland-Park type observer for $T_d = 0.1/0.2/0.3$ sec. under Coulomb Friction modelling ($N = 100$ in general except $^\bullet : N = 1$)

	Rise time (sec.)			Settling time (sec.)			Steady state value		
No friction exists	0.57	0.57	0.60	1.18	1.18	1.23	1	1	1
No friction cancellation	0.61	0.62	0.66	0.67	2.19	1.47	0.97	0.94	0.89
Observer gain $k = 1$									
Cancellation with exactly known $v(t)$	0.60	0.62	0.70	1.68	1.74	1.44	0.99	0.97	0.95
Cancellation without prediction	0.68	0.83	1.10	1.83	2.00	2.18	0.98	0.93	0.85
Euler approximation	0.65	0.74	1.10	12.04	3.05	3.72	0.98	0.95	0.92
1^{st} order Pade inverse	0.69	0.76	$0.72^\bullet$	1.84	2.28	$3.31^\bullet$	0.98	0.94	$0.89^\bullet$
Heun's method	0.60	0.71	$1.36^\bullet$	1.70	4.33	$3.34^\bullet$	0.99	0.96	$0.94^\bullet$
2^{nd} order Pade inverse	0.60	0.71	$1.36^\bullet$	1.71	4.33	$3.34^\bullet$	0.99	0.95	$0.94^\bullet$
Observer gain $k = 5$									
Cancellation with exactly known $v(t)$	0.60	0.58	0.59	1.57	1.19	1.31	1	1	1
Cancellation without prediction	0.74	1.06	1.34	1.82	1.66	2.10	1	0.97	0.95
Euler approximation	0.60	1.06	0.94	1.67	2.02	$4.56^\bullet$	1	1	$1^\bullet$
1^{st} order Pade inverse	0.66	0.85	$1.45^\bullet$	1.50	1.68	$2.24^\bullet$	1	0.99	$0.98^\bullet$
Heun's method	0.57	$1.22^\bullet$	$1.48^\bullet$	2.35	$1.95^\bullet$	$2.25^\bullet$	1	$1^\bullet$	$0.98^\bullet$
2^{nd} order Pade inverse	0.57	$1.22^\bullet$	$1.47^\bullet$	2.35	$1.95^\bullet$	$2.24^\bullet$	1	$1^\bullet$	$0.98^\bullet$

Additionally, square and triangular wave input tracking performances of the system are investigated in Figures 4.9 and 4.10 again with first order Pade approximant based velocity prediction and Coulomb friction model with $F_c = 4$. Exclusively, the reference filter can be removed for ramp input tracking case to enhance the rise time and settling time performances since velocity dynamics change slowly enough already. Position responses show that Friedland-Park type observer based cancellation improves the performance for $k = 5$ and time delay is $T_d = 0.1$ as shown in Figures 4.9 and 4.10. Thus, it can be concluded that deployed adaptive observer and velocity predictor can eliminate the friction adequately and ensure a comparable performance to no friction case. Otherwise, Smith predictor-based controllers can partially extinguish the position error; therefore, a steady state error occurs. Besides, Coulomb friction cancellation performances of different velocity prediction schemes for different time delays are presented in Table 4.5 for unit step tracking. From the table, it can be observed that in all cases, closed loop performances increase with the Friedland-Park type observer and proposed velocity predictors, as expected.

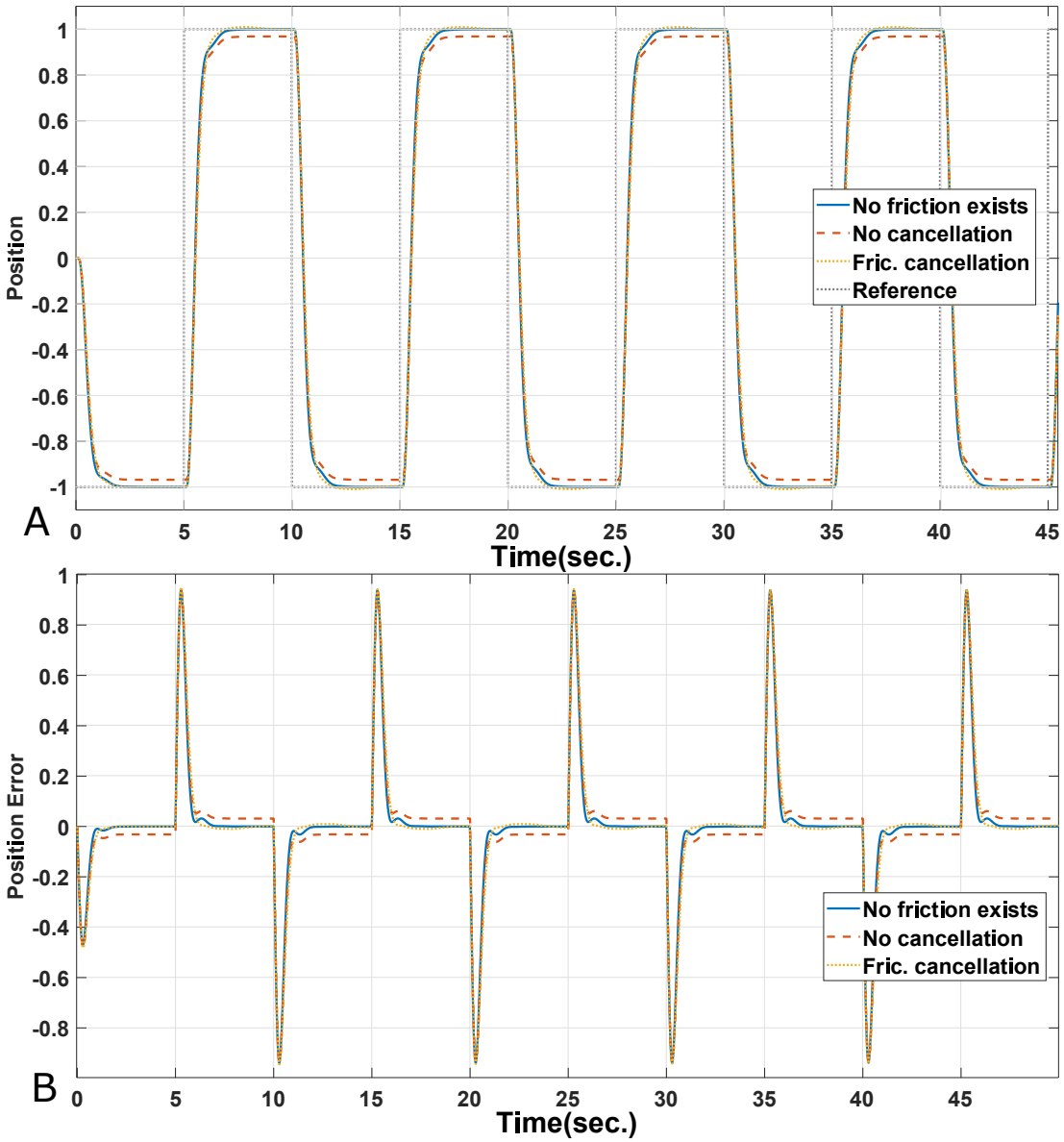

Figure 4.9: The system response for unit square wave input is applied to position control system including a 1^{st} order inverse Pade approximant based velocity predictor and a Friedland-Park type observer with $k = 5$ for $T_d = 0.1$. Without Coulomb friction compensation, steady state values for positive and negative position response are $x_{ss}^{+} = 0.968$ and $x_{ss}^{-} = -0.968$ respectively. (A) Position tracking performance. (B) Position tracking error.

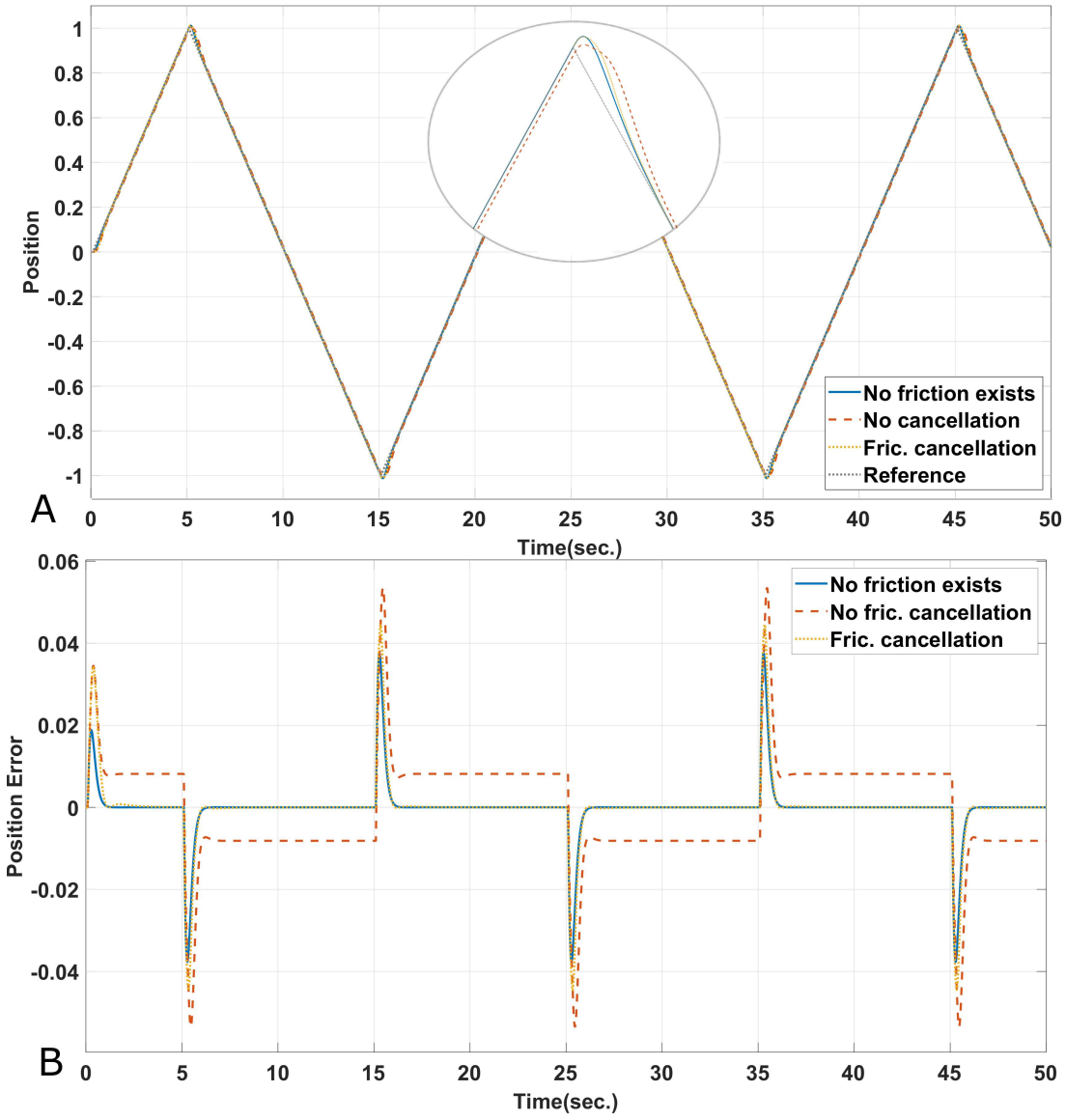

Figure 4.10: The System response for unit triangular wave input is applied to position control system including a 1^{st} order inverse Pade approximant based velocity predictor and a Friedland-Park type observer with $k = 5$ for $T_d = 0.1$. Without Coulomb friction compensation, steady state errors for positive and negative position response are $e_{ss}^{+} = 0.8\%$ and $e_{ss}^{-} = -0.8\%$ respectively. (A) Position tracking performance. (B) Position tracking error.

Also, in [26], it is claimed that the original observer design is able to estimate friction terms which are not hindered to Coulomb coefficient that is why we performed additional simulations considering LuGre friction model whose parameters are given in Table 4.4. Clearly, for a fixed observer gain k, it is required to apply filtering with lower cut-off frequencies to obtain similar position tracking errors when either observer gain or delay increases. Indeed, in all cases, Friedland-Park type adaptive observer combined with velocity predictor structure improves system performance. Among these experiments, the best estimation is achieved when actual velocity can be instantaneously measured; however, this scenario again is presented just to clarify that if we can predict velocity values so close to actual velocity values then, we can obtain friction cancellation similar to delay free measurement. Certainly, it is unreachable when there is a measurement delay within the system. From the results, it is obvious that when there is no friction compensation, the system suffers from performance degradation gradually as delay increases. It seems that all prediction methods can enhance setpoint responses to some extend. Second order methods, both Pade and Heun, provide similar results and outperform the first order approximations for the same observer gains. However, when there exists considerable time delay, they become more sensitive to velocity changes than Euler and inverse first order Pade approximant that is why it is necessary to design a derivative filter with a lower cut-off to obtain appropriate responses. As a last observation, it can be said that although they have similar structures (see Figure 2.11), Euler approximation provides faster friction but more gain sensitive estimation compared to inverse first order Pade approximant for same observer gain. This is simply due to derivative term dependent prediction coefficient c_1. Since Euler approximation updates velocity prediction with a higher c_1 (see Figure 2.11). As a result, it estimates friction better in low gains and is less sensitive to velocity changes, which may occur for high observer gains. It seems that Friedland-Park adaptive observer and designed Smith predictor based controllers for both step and ramp input tracking exhibit desired performances when both time delay and dynamic friction simultaneously exist.

Lastly, we replace Friedland-Park type observer with the recently developed new observer design and repeat square position input tracking simulation again

Table 4.6: Comparison of the different velocity prediction approaches in Friedland-Park type observer for s sec. under LuGre Friction modeling ($N = 100$ in general except $^\star : N = 10$, $^\bullet : N = 1$ and $^\dagger : N = 0.3$)

	Rise time (sec.)			Settling time (sec.)			Steady state value		
No friction exists	0.57	0.57	0.60	1.18	1.18	1.23	1	1	1
No friction cancellation	0.59	0.62	0.66	1.55	1.32	1.28	0.96	0.93	0.87
Observer gain $k = 1$									
Cancellation with exactly known $v(t)$	0.63	0.69	0.84	1.90	7.79	16.38	1	1	1
Cancellation without prediction	0.67	1.08	1.45	1.70	23.48	26.99	0.98	0.96	0.90
Euler approximation	0.66	0.81	1.71	2.30	16.69	31.48	1	0.98	0.96
1^{st} order Pade inverse	0.69	0.78	$1.80^\star$	4.37	2.22	$27.48^\star$	1	0.95	$0.96^\star$
Heun's method	0.63	0.78	$1.51^\bullet$	1.98	16.96	$29.91^\bullet$	1	0.98	$0.96^\bullet$
2^{nd} order Pade inverse	0.63	0.78	$1.51^\bullet$	1.98	16.96	$29.91^\bullet$	1	0.98	$0.96^\bullet$
Observer gain $k = 3$									
Cancellation with exactly known $v(t)$	0.60	0.63	0.71	1.59	1.29	1.41	1	1	1
Cancellation without prediction	0.76	1.06	1.81	1.79	14.07	32.05	1	0.98	0.95
Euler approximation	0.62	$0.95^\star$	$2^\dagger$	1.52	$14.81^\star$	$7.07^\dagger$	1	$0.99^\star$	$1^\dagger$
1^{st} order Pade inverse	0.69	0.87	$2.03^\dagger$	1.71	16.96	$24.18^\dagger$	1	0.98	$0.99^\dagger$
Heun's method	0.59	$1.09^\star$	$2.04^\dagger$	1.59	$4.97^\star$	$22.59^\dagger$	1	$1^\star$	$1^\dagger$
2^{nd} order Pade inverse	0.59	$1.09^\star$	$2^\dagger$	1.59	$4.97^\star$	$5.55^\dagger$	1	$1^\star$	$1^\dagger$

based on the parameters given in Table 4.4. As shown in Figure 4.11, when $K = 6$, $L = 10$ and $T_d = 0.1$, the new proposed observer exhibit similar performances with and without Euler method based velocity predictor and enhance the tracking performance. This is a reasonable result since the observer itself includes velocity error dynamics already. Thus, it can show a promising performance as if actual velocity can be measured. Note that K is a parameter directly related to e_v. Therefore, when we use $K = 3$ and $L = 10$ without a separate velocity predictor, observer friction estimation performance deteriorates for $T_d = 0.1$ and exhibits some oscillations due to poor prediction of velocities as in Figure 4.12. In this case, employing a separate Euler method based predictor improves the position tracking performance. Furthermore, for $K = 6$, $L = 10$ and slightly larger time delay such that $T_d = 0.15$, the new observer has a reduced transient performance as shown in Figure 4.13 when there is no separate velocity predictor. To conclude, although the proposed new observer improves the performance compared to the no compensation case, a separate velocity predictor may be required to obtain a good estimation performance, especially for significant measurement delays. Likewise, when parameter K is not large enough, friction estimation performance degrades in the presence of measurement delay. Also, in Figure 4.14, we compare total force delivered to the plant (controller input+observer estimation). For this

figure, total force does not change noticeably when an adaptive friction observer is adopted with a first order inverse Pade approximant velocity predictor. On the other hand, without these structures, there is a steady state error for position tracking.

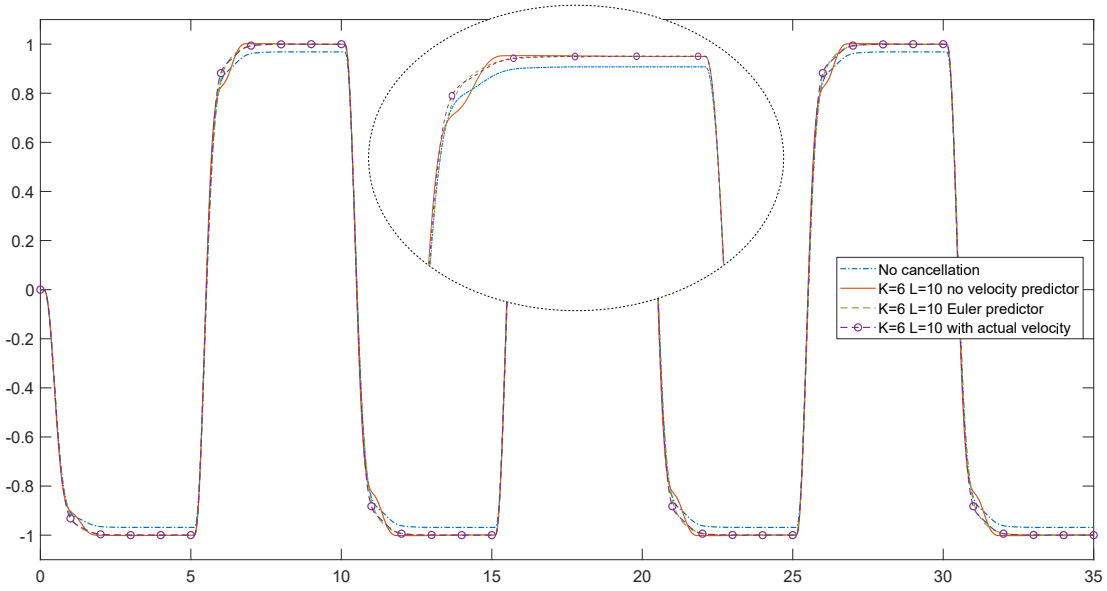

Figure 4.11: The Position response for unit square wave input with and without Euler Method based velocity prediction when the new friction observer is employed with $K = 6$, $L = 10$ for $T_d = 0.1$.

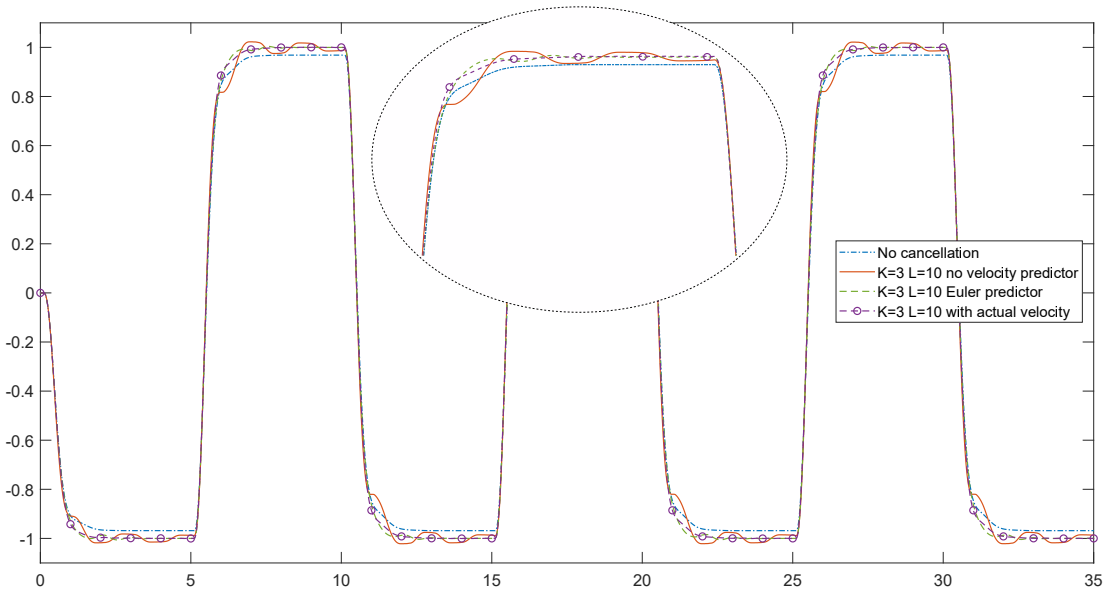

Figure 4.12: The position response for unit square wave input with and without Euler Method based velocity prediction when the new friction observer is employed with $K = 3$, $L = 10$ for $T_d = 0.1$.

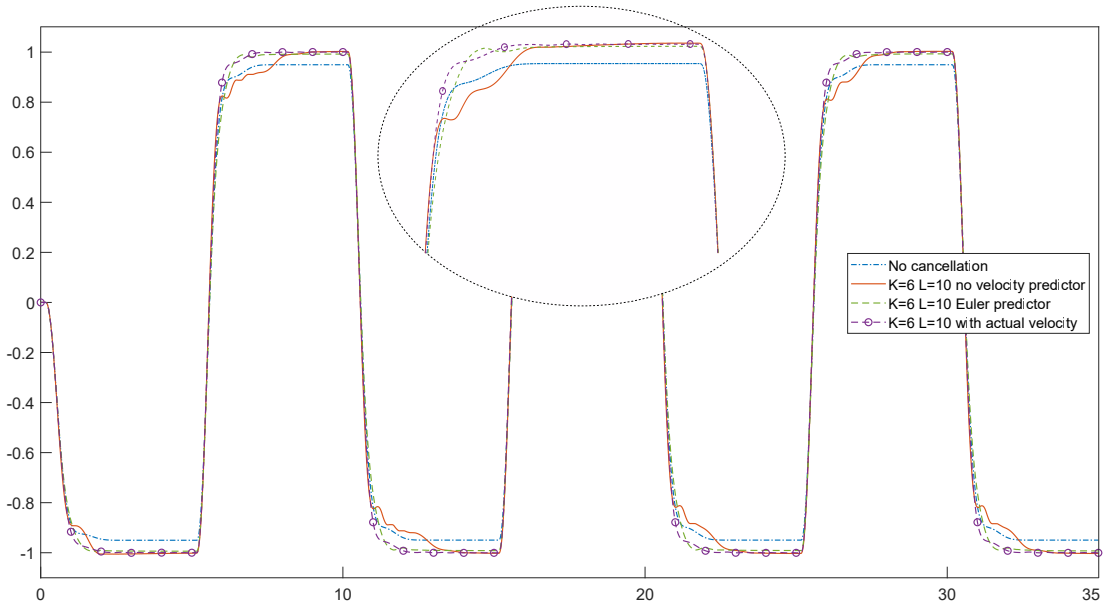

Figure 4.13: The position response for unit square wave input with and without Euler Method based velocity prediction when the new friction observer is employed with $K = 6$, $L = 10$ for $T_d = 0.15$.

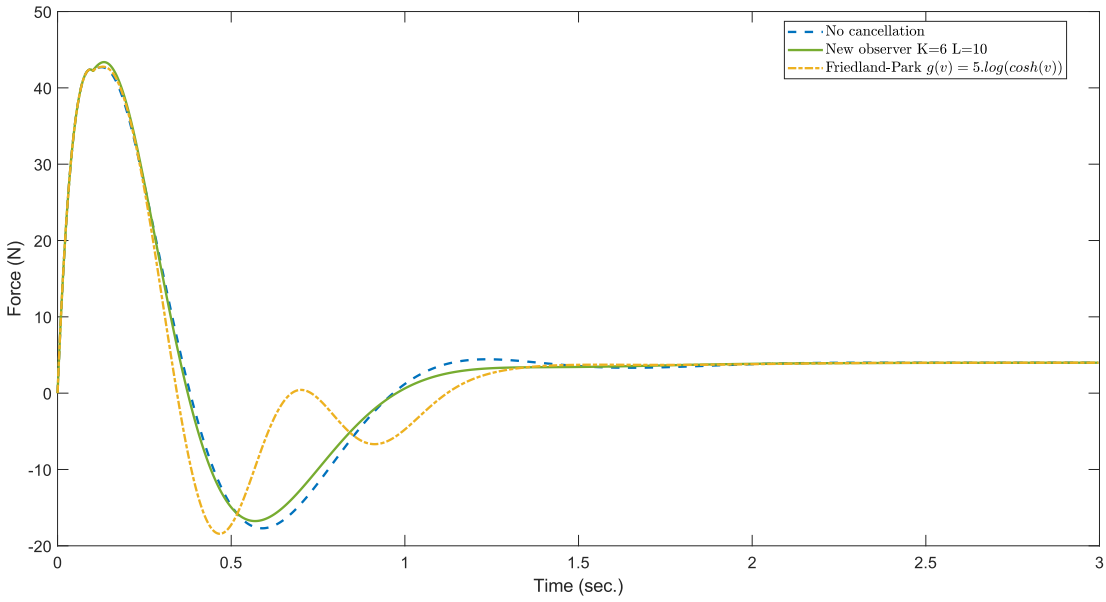

Figure 4.14: Total force delivered to the plant for position tracking with and without friction compensation with $T_d = 0.15$ *sec.* measurement delay.

Chapter 5

Experimental Results

For our experiments, we utilized an Arduino based DC motor control platform described in [74, 75]. As it can be seen in Figure 5.1, our setup simply consists of an Arduino Uno microcontroller with DC motor shield and a DC motor by Pololu, whose datasheet parameters are given in Table 5.1. As Arduino Uno Board has a limited memory capacity (32 Kbytes of Flash and 2 Kbytes of SRAM), we designed a direct position controller aiming at step input tracking instead of a hierarchical control system for simplicity. In the experiments we performed, ode3 (Bogacki-Shampine) solver with step size 0.01 is used. For the rest of Simulink settings, please refer to Appendix B.

To begin with, a second order voltage (V) to angular speed (rad/s) transfer function of a simple motor model denoted by $G(s)$ can be obtained as below [59].

$$G(s) = \frac{K_m}{(R_a + L_a s)(Js + b) + K_b K_m} \tag{5.1}$$

Table 5.1: Parameters of a 37Dx70L mm metal gearmotor with a quadrature encoder by Pololu.

Parameter	Notation	Data Sheet Value	Unit
Motor Torque	τ	-	Nm
Motor Current	i	-	A
Stall Torque	τ_{stall}	21	$kg.cm$
Stall current@12V	i_{stall}	5.5	A
No load current@12V	i_{nl}	0.2	A
Torque Constant	K_m	-	Nm/A
Back Emf Constant	K_b	-	$V.s/rad$
Input Voltage	V_{in}	-	V
Back Emf Voltage	V_b	-	V
Terminal Resistance	R_a	-	Ω
Terminal Inductance	L_a	-	H
Viscous Friction	b	-	$N.m.s/rad$
No load Inertia	J	-	$kg.m^2$
No load speed @12V	w_{max}	21	rad/s
Encoder Counts Per Revolution	CPR	3200	-

Generally, time constant due to terminal inductance is negligible; therefore, ignoring L_a, (5.1) is further simplified to a first order transfer function such that

$$G(s) = \frac{K_m}{R_a J s + R_a b + K_b K_m} \tag{5.2}$$

$$= \frac{\frac{K_m}{R_a b + K_b K_m}}{\frac{R_a J}{R_a b + K_b K_m} s + 1} \tag{5.3}$$

$$= \frac{K_1}{\tau_1 s + 1} \tag{5.4}$$

where K_1 and τ_1 are some positive constants. Unfortunately, the parameters of these type of motors can vary from production to production and some of them are not listed in the datasheets specifically. To overcome this issue, it is mandatory to perform a system identification method in open loop before designing a closed loop feedback. After applying a step reference voltage, we find $K_1 = 1.6$ and $\tau_1 = 0.12$. The missing parameters in Table 5.1 can be obtained using physical

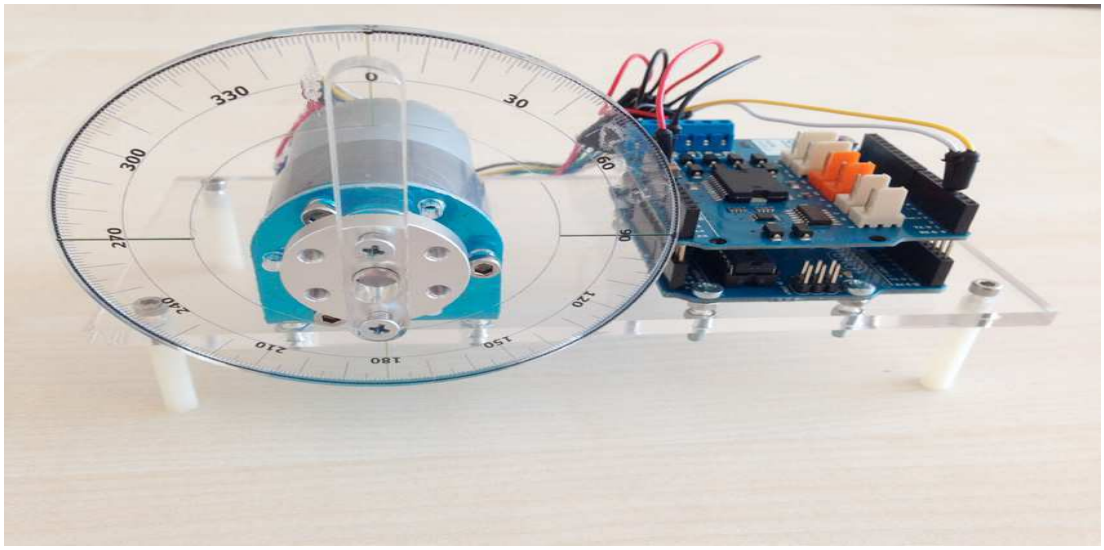

Figure 5.1: The Arduino Uno controlled DC motor platform used in experiments.

relations stated below.

$$K_m = \tau_{stall}/i_{stall}, \tag{5.5}$$

$$R_a = 12V/i_{stall}, \tag{5.6}$$

$$12V - K_b w_{max} = R_a i_{nl}, \tag{5.7}$$

$$K_1 = \frac{K_m}{bR_a + K_b K_m}, \tag{5.8}$$

$$J = \frac{\tau_1 (bR_a + K_b K_m)}{R_a}. \tag{5.9}$$

As a result, missing parameters become $K_m = 0.38\ Nm/A$, $R_a = 2.2\ \Omega$, $K_b = 0.55\ Vs/rad$, and $J = 0.01328\ kgm^2$.

Referring to Figure 2.1, adaptive observers require control input as torque command in Nm and velocity in rad/s for friction estimation. However, Arduino motor shield generates pulse width modulation (PWM) signals to drive the DC motor. In other words, it takes control input, u in volt as the desired voltage level and produces a square wave signal, whose mean equals to desired voltage level, by turning motor drive circuitry on and off repetitively. Hence, this square wave has a peak amplitude equal to supply voltage, 12 V in our case, and a switching frequency depending on u. Therefore, voltage-to-torque and torque-to-voltage conversions are required to utilize proposed friction cancellation schemes.

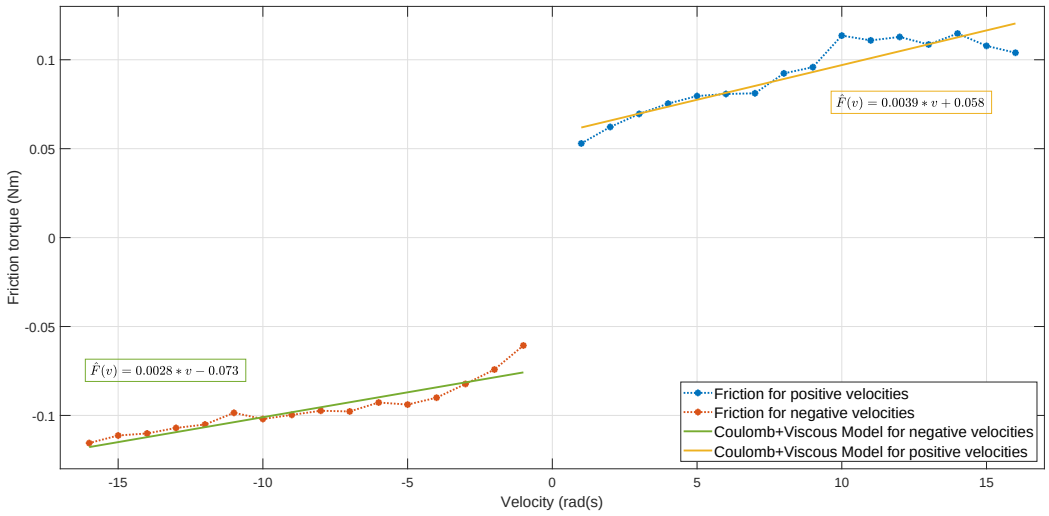

Figure 5.2: MATLAB linear curve fitting is applied to characterize velocity-torque map for friction parameter identification of DC motor.

Based on simple physics, the torque generated by a DC motor can be formulated $\tau = K_m.i$. Assuming that the motor driver circuit is ideal and there is no or low loss, this relationship can be written below.

$$\tau = K_m \frac{V_{in} - K_b w}{R_a} \tag{5.10}$$

where V_{in} is the voltage produced by motor driver. Then, using previously found motor parameters and angular velocity w, the relationship between torque and voltage can be stated as follows.

$$\tau = \frac{0.38}{2.2}(V_{in} - 0.55w). \tag{5.11}$$

Before designing a position controller, we have conducted constant speed tests on Arduino platform to identify friction parameters. Simply, in these tests, control input u becomes equal to friction torque since $\dot{w} = 0$. To this end, we first design a PI controller with $K_p = 1.25$ and $K_i = 6.25$ to obtain a zero velocity error at the steady state. Then, the total current delivered to the motor by the Arduino motor shield is measured by an onboard ADC for different velocity references. Finally, filtered ADC measurements are multiplied with K_m and linear curve fitting is applied on Matlab in order to identify friction torque. As a result,

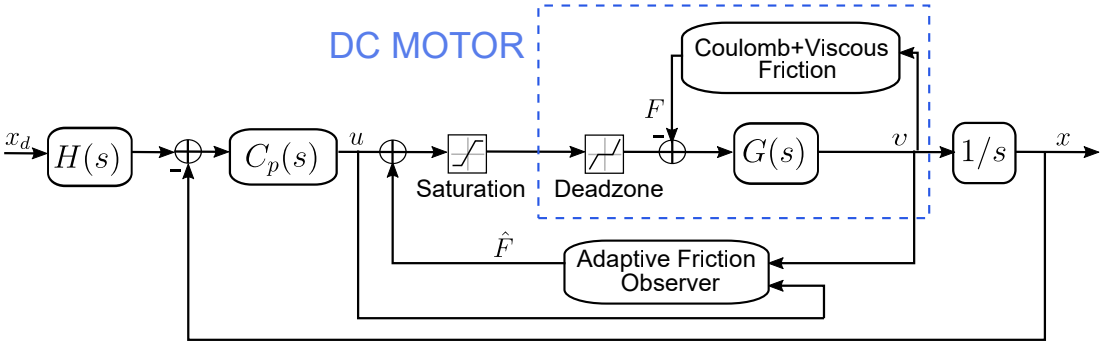

Figure 5.3: The block diagram of the DC motor position control system driven by Arduino Uno.

we can determine the parameters of Coulomb+Viscous friction model as in Figure 5.2. Note that parameters for negative and positive velocities are different. Furthermore, deadzone is a common occurrence in such kinds of motors. Inside deadzone regime, the system does not respond to the given input until the input signal reaches a particular level. Hence, starting 0.2 V, we have applied voltage to open loop system and gradually increased the level of the reference until motor shaft starts to rotate. Consequently, we comprehend that the platform has a deadzone until $1.2V$ approximately. Lastly, note that there is a sampling delay of 10 ms due to discrete time implementation with 100 Hz sampling for frequency ode3 solver. We simply ignore this microcontroller processing delay since it has a negligible effect on system dynamics. When we consider this delay, other nonlinearities become dominant and system response is degraded. Therefore, we keep our model as simple as possible, considering the computation power of Ardunio microcontroller. Based on these facts, we also did MATLAB simulations using the system model in Figure 5.3 to compare the response of Arduino Uno platform.

For our experiments, we design an optimum PID for step input position tracking based on ITAE performance index using Table 3.1. Note that (3.5) becomes slightly different for identified DC motor plant since DC motor has a pole different than zero. Using (5.4), we can find a new closed loop position transfer function as below.

$$T(s) = \frac{\frac{K_1 K_d}{\tau_1} s^2 + \frac{K_1 K_p}{\tau_1} s + \frac{K_1 K_i}{\tau_1}}{s^2(\tau_1 s + 1) + \frac{K_1 K_d}{\tau_1} s^2 + \frac{K_1 K_p}{\tau_1} s + \frac{K_1 K_i}{\tau_1}}. \tag{5.12}$$

Then, (3.6)-(3.8) can be rewritten as below for this new transfer function.

$$7.75 = \frac{K_1}{\tau_1} K_d, \tag{5.13}$$

$$2.15 w_n^2 = \frac{K_1}{\tau_1} K_p, \tag{5.14}$$

$$w_n^3 = \frac{K_1}{\tau_1} K_i. \tag{5.15}$$

We have already identified constants in plant transfer function such that $K_1 = 1.6$ and $\tau_1 = 0.12$ that is why new controller parameters can be computed as $K_p = 1.975$, $K_d = 0.384$ and $K_i = 3.216$ for $w_n = 3.5$. As a result, position controller, $C_p(s)$ and corresponding reference filter given in (3.9) can be obtained as below.

$$C_p(s) = \frac{0.384s^2 + 1.975s + 3.216}{s}, \tag{5.16}$$

$$H(s) = \frac{3.216}{0.384s^2 + 1.975s + 3.216}. \tag{5.17}$$

Then, we obtain tracking response with and without Friedland-Park observer as in Figure 5.4. It can be seen that Arduino application and Simulink results coincide pretty well.

For the same controller parameters, we also conduct experiments with the new observer. As it is shown in Figure 5.5, new observer provide a similar improvement at steady state. Compared to the Friedland-Park observer case, the new observer has similar trends in Simulink and Arduino again; however, settling time decreased this time. This may be due to the effect of velocity estimation in the new design. In both figures, there are some mismatches between the results of Arduino experiments and simulations. Possibly, these mismatches are the products of some unmodeled dynamics such as velocity noise, encoder resolution, etc. Consequently, friction cancellation using both new observer and Friedland-Park observer improve the position tracking performance for the ITAE index based PID with relatively low w_n.

Similarly, we performed experiments with another PID whose bandwidth was higher compared to the previous one. To this end, we determine $w_n = 5$ and

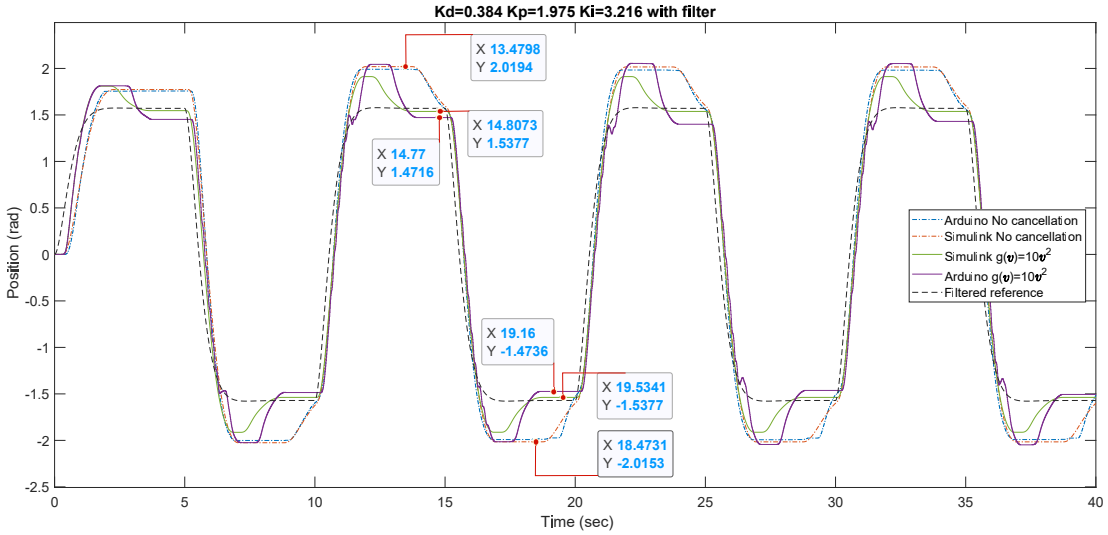

Figure 5.4: The position response comparison of Simulations and experiments with and without friction compensation when $w_n = 3.5$ and Friedland-Park observer is utilized.

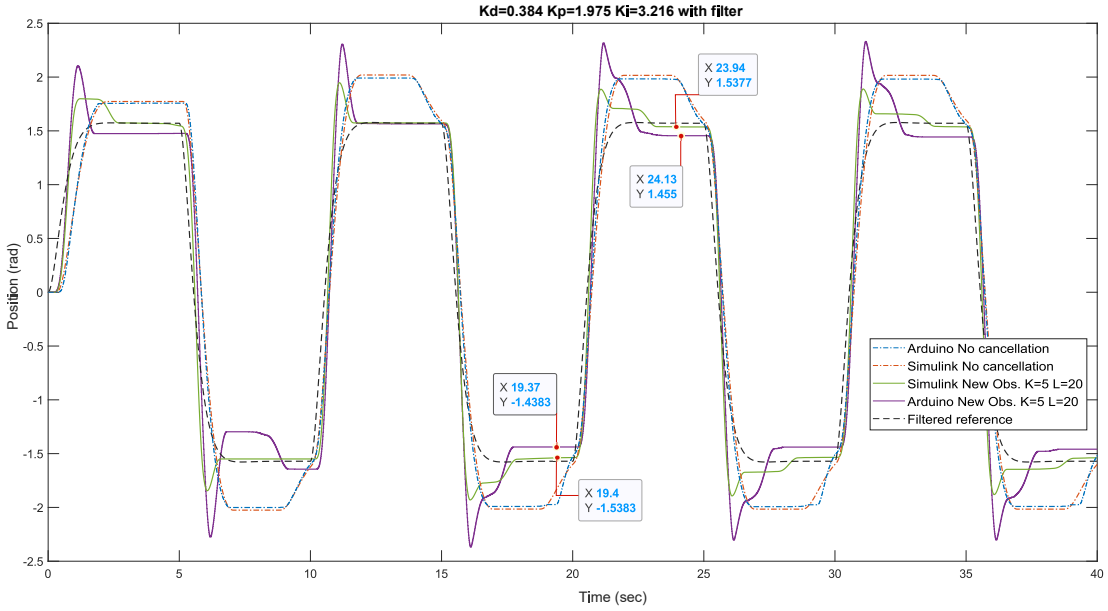

Figure 5.5: The position response comparison of Simulations and experiments with and without friction compensation when $w_n = 3.5$ and new observer is utilized.

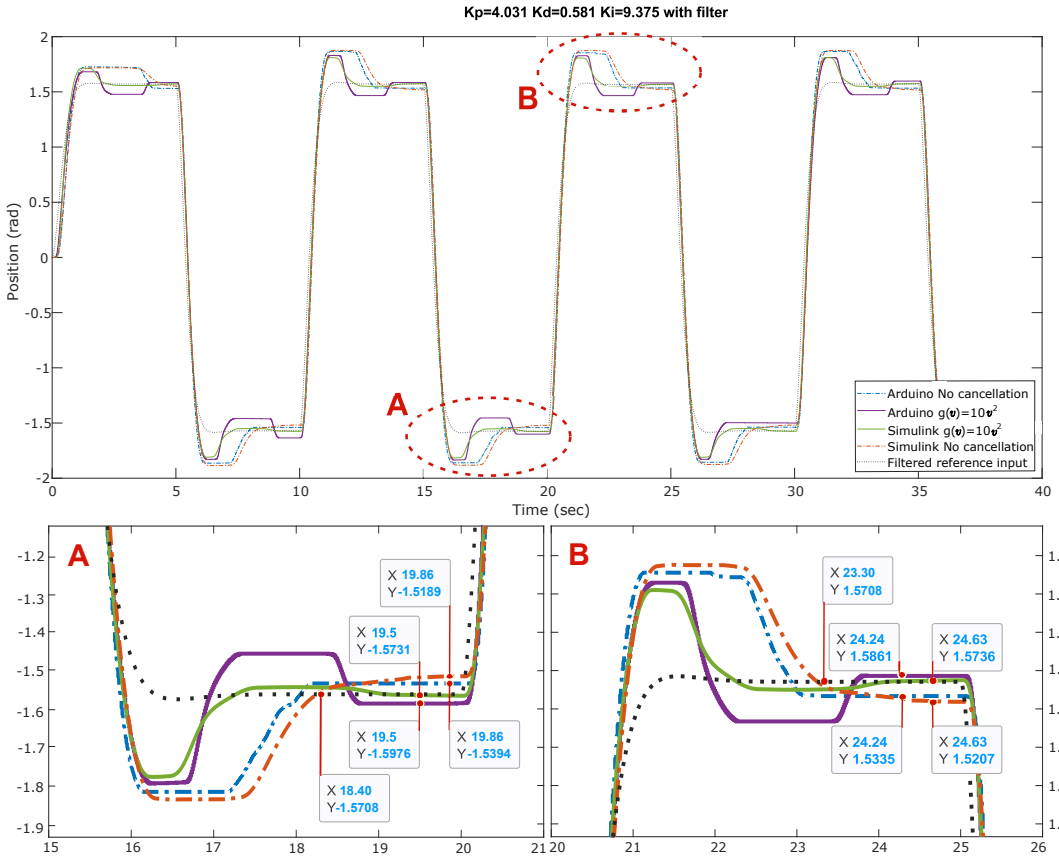

Figure 5.6: The position response comparison of Simulations and experiments with and without friction compensation when $w_n = 5$.

computed controller parameters as $K_p = 4.03$, $K_d = 0.5812$ and $K_i = 9.375$. For this case, new C_p and $H(s)$ become as below.

$$C_p(s) = \frac{0.581s^2 + 4.031s + 9.375}{s}, \tag{5.18}$$

$$H(s) = \frac{9.375}{0.581s^2 + 4.031s + 9.375}. \tag{5.19}$$

In Figure 5.6, it seems that compared to previous case, PID with higher w_n can track reference step position with a smaller steady state error even there is no friction cancellation. In this sense, observer usage slightly improves steady state response. In this sense, it becomes useless to some extent; however, it still improves transient response in both experiments and simulations.

Remark 9. *We note that the Coulomb friction is modeled by discontinuous sign*

function, which is frequently utilized in sliding mode control. Although this approach theoretically helps one to design control systems with many advantages, its practical implementations may exhibit an undesired behavior called chattering. This behavior is basically an undesired oscillation with finite frequency and amplitude, which is mainly caused by unmodeled dynamics or implementation of control laws in discrete time, see e.g. [76]. In Coulomb friction case, this may occur if velocity exhibits oscillations around zero. However, in our simulations with the parameters given in Table 4.4, we did not encounter chattering. This may be most likely because in our theoretical framework, we did not assume any unmodeled dynamics. Nevertheless, since the numerical simulation is basically a discretization, it may still be possible to encounter chattering due to numerical errors. Furthermore, although we did not observe chattering in our experiments, some other physical systems can exhibit chattering in mechanical implementations. Literature is quite rich on the subject of chattering elimination, and in such a case, suitable chattering suppression techniques should be utilized along with the methodologies presented here, see e.g. [76, 77].

Chapter 6

Conclusions

Position control of simple mechanical systems in the presence of friction is considered throughout this dissertation. Firstly, we consider a delay free system and enlarge the set of estimation functions used in well known Friedland-Park observer. To this end, we give some stability results for the extended adaptive observer structure based on standard Lyapunov stability theory. Although the primary purpose of these observers is to estimate Coulomb friction, previous studies have shown that it is also capable of more complicated friction components. Provided that actual velocity is known, one can use this estimation in order to cancel the effects of existing friction within the system and control position with a simple linear controller. To see the effectiveness of the proposed position control system, we consider some benchmark examples from the literature. Using their system parameters, we show that adaptive friction cancellation improves the position response, especially for controllers with low bandwidths. In these simulations, we also realized that PID controllers designed by using ITAE performance index could overcome PD controllers even if their bandwidths are the same.

On the other hand, if the velocity measurements are delayed, then a velocity estimator might be required to achieve a tracking performance as in a delay free system. To achieve this, we proposed various schemes and considered their effect

on the performance of the proposed control structure. Moreover, we showed that if the velocity prediction error is small, the friction parameter estimation is also small. This also shows that the proposed structure is robust to such uncertainties. Once the effect of friction is eliminated, the resulting system could be considered a linear time-invariant system with a known delay and can be controlled by utilizing classical control techniques. For such a delayed system, we provide design steps for Smith predictor based velocity and position controllers.

For velocity estimation, we considered various schemes. Consequently, it is inferred that the proposed position tracking system can be fairly utilized as long as the velocity is predicted in a small neighborhood of actual velocities. Especially when observer gain or time delay is relatively large, friction estimation is hindered due to poor velocity prediction. To overcome abrupt changes in states, reference and derivative filters are utilized to improve the prediction and estimation performances. Furthermore, we develop a new observer design as an alternative to Friedland-Park. In this new structure, we also consider the velocity error dynamics for friction estimation. It may seem to be a redundant property when the information of actual velocity is completely available. However, when there is an uncertainty or time delay on velocity measurements, it may improve the system performance without any precaution. Certainly, the proposed velocity predictor can still be utilized, especially for large time delays as well. Comparing the results of these two observers, we observe that they provide similar improvements for the position control systems not only in delay free case but also there is delay related to measurements. For the proposed new observer design, we also make a dwell time analysis. According to this analysis, velocity switching frequency should be finite such that $t_{k+1} - t_k \geq \tau_D > 0$ in order to obtain a stable observer.

To summarize, the main contributions of this thesis may be listed as follows:

- We propose two different adaptive observer schemes for friction cancellation in simple mechanical systems with and without time delay. First, we extend the update rule of the well known Friedland-Park observer to a larger set. Then, we develop a novel observer which considers velocity error for friction estimation.

- For simplicity, we design adaptive observers for a delay free system first. These observers require accurate velocity information; therefore, we also consider measurement delay and propose velocity predictors in order to improve friction estimation and position tracking responses of the system. To this end, we are inspired by different single step numerical differential equation solvers. Alternatively, we consider a rational function, which is similar to well known Pade approximation, to characterize the time delay. Using the inverse of this function, we develop a scheme to predict the actual value of velocity using delayed measurements.

- We provide stability analysis for both observers. Using the standard Lyapunov stability analysis, we provide necessary conditions for estimation function $g(v)$ in Friedland-Park type observers to achieve asymptotic stability. For the new observer design, we consider it as a switching system. Under certain regularity and assumptions regarding to switching signal, we apply LaSalle's Invariance Principle to show asymptotic stability. Furthermore, using Linear Matrix Inequalities (LMIs), we develop a Matlab code to compute the minimum dwell time and show the stability of the observer numerically as well.

- We show that proposed structures can work with different observer designs. We simply consider PD and PID controllers designed according to damping and bandwidth parameters for the delay free case. We optimize the parameters of the controller based on ITAE index. When the system includes time delay, we utilize Smith predictor based controllers.

- In addition to computer simulations, we conduct some experiments in a real application based on an Arduino Uno microcontroller and a simple DC motor. Although this is a very limited test setup and has a low computation power, acquired results seem to be compatible with theoretical simulation results.

As a future extension, it may be beneficial to consider other mechanical systems which exhibit more complex friction behaviors and time delay. Another possible

future research directive may be related to the properties of existing measurement delay. When the delay is not known, is time varying or is known with a mismatch both velocity prediction and the design of controllers that achieve closed-loop stability become challenging. What is more, in this study, we consider ITAE index based PID controllers and Smith Predictor based controllers; however, other controller designs can be utilized for position control with proposed adaptive observers. Especially, the design of repetitive controllers might be an exciting study since they regulate the system to track periodic references or reject periodic disturbances. To this end, interested readers may refer to [78, 79] and the references therein. Note that, in repetitive control, the disturbance or reference signal can be anything as long as it has a periodic characteristic. Lastly, a Kalman filter might be incorporated with a state observer in order to improve the friction estimation performance. An inspiring study for such an approach is presented in [80].

Bibliography

[1] B. Baykara, "Control of systems under the effect of friction," Master's thesis, Middle East Technical University, 2009.

[2] C. Canudas de Wit, H. Olsson, K. J. Åström, and P. Lischinsky, "A new model for control of systems with friction," *IEEE Transactions on Automatic Control*, vol. 40, no. 3, pp. 419–425, 1995.

[3] M. Gafvert, "Comparison of two friction models," Master's thesis, Lund University, 1996.

[4] H. Olsson, K. Åström, C. C. de Wit, M. Gäfvert, and P. Lischinsky, "Friction models and friction compensation," *European Journal of Control*, vol. 4, no. 3, pp. 176 – 195, 1998.

[5] D. P. Hess and A. Soom, "Friction at a Lubricated Line Contact Operating at Oscillating Sliding Velocities," *Journal of Tribology*, vol. 112, pp. 147–152, 01 1990.

[6] P. R. Dahl, "A solid friction model," tech. rep., Aerospace Corp El Segundo Ca, 1968.

[7] P.-A. Bliman and M. Sorine, "A system-theoretic approach of systems with hysteresis. application to friction modelling and compensation," in *Proceedings of the 2nd European control conference*, pp. 1844–1849, 1993.

[8] H. Olsson, *Control Systems with Friction*. PhD thesis, Department of Automatic Control, 1996.

[9] B. Armstrong-Hélouvry, P. Dupont, and C. C. de Wit, "A survey of models, analysis tools and compensation methods for the control of machines with friction," *Automatica*, vol. 30, no. 7, pp. 1083–1138, 1994.

[10] P. Lischinsky, C. Canudas de Wit, and G. Morel, "Friction compensation for an industrial hydraulic robot," *IEEE Control Systems Magazine*, vol. 19, no. 1, pp. 25–32, 1999.

[11] D. Tan, Y. Wang, and L. Zhang, "Research on the parameter identification of lugre tire model based on genetic algorithms," pp. 498–502, 2007.

[12] X. Wang and S. Wang, "High Performance Adaptive Control of Mechanical Servo System With LuGre Friction Model: Identification and Compensation," *Journal of Dynamic Systems, Measurement, and Control*, vol. 134, 12 2011.

[13] C. C. De Wit and P. Lischinsky, "Adaptive friction compensation with partially known dynamic friction model," *International Journal of Adaptive Control and Signal Processing*, vol. 11, no. 1, pp. 65–80, 1997.

[14] W.-F. Xie, "Sliding-mode-observer-based adaptive control for servo actuator with friction," *IEEE Transactions on Industrial Electronics*, vol. 54, no. 3, pp. 1517–1527, 2007.

[15] H. S. Lee and M. Tomizuka, "Robust motion controller design for high-accuracy positioning systems," *IEEE Transactions on Industrial Electronics*, vol. 43, no. 1, pp. 48–55, 1996.

[16] H. Olsson and K. J. Astrom, "Observer-based friction compensation," in *Proceedings of 35th IEEE Conference on Decision and Control*, vol. 4, pp. 4345–4350 vol.4, Dec 1996.

[17] R. H. A. Hensen, *Controlled mechanical systems with friction*. PhD thesis, Technische Universiteit Eindhoven, 2002.

[18] K. J. Åström and B. Wittenmark, *Adaptive control*. Courier Corporation, 2013.

[19] L. R. Ray, A. Ramasubramanian, and J. Townsend, "Adaptive friction compensation using extended Kalman-Bucy filter friction estimation," *Control Engineering Practice*, vol. 9, no. 2, pp. 169 – 179, 2001.

[20] J. Ishikawa and M. Tomizuka, "Pivot friction compensation using an accelerometer and a disturbance observer for hard disk drives," *IEEE/ASME Transactions on Mechatronics*, vol. 3, no. 3, pp. 194–201, 1998.

[21] O. Gomonwattanapanich, A. Pattanapukdee, and M. Mongkolwongrojn, "Compensation and estimation of friction by using extended kalman filter," in *2006 SICE-ICASE International Joint Conference*, pp. 5032–5035, 2006.

[22] Q. P. Ha, A. Bonchis, D. C. Rye, and H. F. Durrant-Whyte, "Variable structure systems approach to friction estimation and compensation," in *Proceedings 2000 ICRA. Millennium Conference. IEEE International Conference on Robotics and Automation. Symposia Proceedings (Cat. No. 00CH37065)*, vol. 4, pp. 3543–3548, IEEE, 2000.

[23] G. Palli and C. Melchiorri, "Velocity and disturbance observer for non-model based load and friction compensation," in *2008 10th IEEE International Workshop on Advanced Motion Control*, pp. 194–199, IEEE, 2008.

[24] W.-H. Chen, D. J. Ballance, P. J. Gawthrop, and J. O'Reilly, "A nonlinear disturbance observer for robotic manipulators," *IEEE Transactions on Industrial Electronics*, vol. 47, no. 4, pp. 932–938, 2000.

[25] L. Le Tien, A. Albu-Schaffer, A. De Luca, and G. Hirzinger, "Friction observer and compensation for control of robots with joint torque measurement," in *2008 IEEE/RSJ International Conference on Intelligent Robots and Systems*, pp. 3789–3795, 2008.

[26] B. Friedland and Y. Park, "On adaptive friction compensation," *IEEE Transactions on Automatic Control*, vol. 37, no. 10, pp. 1609–1612, 1992.

[27] T. Şeref, "Dynamic modelling and control of a gimballed airborne antenna platform with mass unbalance and friction," Master's thesis, Middle East Technical University, 2018.

[28] E. Sincar, "Friction identification and compensation of its effects in stabilized platforms," Master's thesis, Middle East Technical University, 2013.

[29] S. Güler and A. B. Özgüler, "Tracking and regulation control of a 2-dof robot arm with unbalance," in *2012 17th International Conference on Methods & Models in Automation & Robotics (MMAR)*, pp. 280–285, IEEE, 2012.

[30] S. Güler, "Tracking and regulation control of a two-degree-of-freedom robot arm," Master's thesis, Bilkent University, 2012.

[31] B. Friedland and S. Mentzelopoulou, "On adaptive friction compensation without velocity measurement," in *Proceedings of 1st IEEE Conference on Control Applications*, pp. 1076–1081 vol.2, 1992.

[32] H. K. Khalil, *Nonlinear systems; 3rd ed.* Upper Saddle River, NJ: Prentice-Hall, 2002.

[33] S. Sastry and M. Bodson, *Adaptive control: stability, convergence and robustness*. Courier Corporation, 2011.

[34] S. Tafazoli, C. W. de Silva, and P. D. Lawrence, "Tracking control of an electrohydraulic manipulator in the presence of friction," *IEEE Transactions Control Systems Technology*, vol. 6, no. 3, pp. 401–411, 1998.

[35] Q.-G. Wang and Y. Zhang, "Robust identification of continuous systems with dead-time from step responses," *Automatica*, vol. 37, no. 3, pp. 377–390, 2001.

[36] İ. Uyanik, M. M. Ankarali, N. J. Cowan, U. Saranli, Ö. Morgül, and H. Özbay, "Independent estimation of input and measurement delays for a hybrid vertical spring-mass-damper via harmonic transfer functions," *IFAC-PapersOnLine*, vol. 48, no. 12, pp. 298–303, 2015.

[37] C. Odabaş and . Morgül, "Observer based friction cancellation in mechanical systems," in *2014 14th International Conference on Control, Automation and Systems (ICCAS 2014)*, pp. 12–16, Oct 2014.

[38] C. Odabaş, "Observer Based Friction Cancellation in Mechanical Systems," Master's thesis, Bilkent University, 2014.

[39] C. Odabaş and Ö. Morgül, "Adaptive friction compensations for mechanical systems with measurement delay," *Transactions of the Institute of Measurement and Control*, vol. 43, no. 8, pp. 1745–1759, 2020.

[40] K. E. Atkinson, *An introduction to numerical analysis; 2nd ed.* New York: John Wiley, 1989.

[41] J. C. Butcher and N. Goodwin, *Numerical methods for ordinary differential equations*, vol. 2. Wiley Online Library, 2008.

[42] S. C. Chapra, R. P. Canale, *et al.*, *Numerical methods for engineers*. Boston: McGraw-Hill Higher Education,, 2010.

[43] A. Visioli, *Practical PID control*. Springer Science & Business Media, 2006.

[44] J. Amin, B. Friedland, and A. Harnoy, "Implementation of a friction estimation and compensation technique," *IEEE Control Systems Magazine*, vol. 17, no. 4, pp. 71–76, 1997.

[45] H. Ozbay, *Introduction to Feedback Control Theory*. Boca Raton, FL, USA: CRC Press, Inc., 1st ed., 1999.

[46] M. Vajta, "Some remarks on padé-approximations," in *Proceedings of the 3rd TEMPUS-INTCOM Symposium*, vol. 242, 2000.

[47] J. P. Hespanha, "Uniform stability of switched linear systems: Extensions of lasalle's invariance principle," *IEEE Transactions on Automatic Control*, vol. 49, no. 4, pp. 470–482, 2004.

[48] J. P. Hespanha and A. S. Morse, "Stability of switched systems with average dwell-time," in *Proceedings of the 38th IEEE conference on decision and control (Cat. No. 99CH36304)*, vol. 3, pp. 2655–2660, IEEE, 1999.

[49] A. T. Koru, A. Delibaşı, and H. Özbay, "Dwell time-based stabilisation of switched delay systems using free-weighting matrices," *International Journal of Control*, vol. 91, no. 1, pp. 1–11, 2018.

[50] F. Golnaraghi and B. C. Kuo, *Automatic control systems*. McGraw-Hill Education, 2017.

[51] A. S. Morse, "Supervisory control of families of linear set-point controllers-part i. exact matching," *IEEE transactions on Automatic Control*, vol. 41, no. 10, pp. 1413–1431, 1996.

[52] Z. Horváth and A. Edelmayer, "An algorithm for the calculation of the dwell time constraint for switched," *Acta Universitatis Sapientiae Electrical and Mechanical Engineering*, vol. 10, pp. 5–19, 2018.

[53] J. Zhang, M. Li, and R. Zhang, "New computation method for average dwell time of general switched systems and positive switched systems," *IET Control Theory & Applications*, vol. 12, no. 16, pp. 2263–2268, 2018.

[54] G. Chesi, P. Colaneri, J. C. Geromel, R. Middleton, and R. Shorten, "A nonconservative lmi condition for stability of switched systems with guaranteed dwell time," *IEEE Transactions on Automatic Control*, vol. 57, no. 5, pp. 1297–1302, 2011.

[55] P. Yan and H. Özbay, "Stability analysis of switched time delay systems," *SIAM Journal on Control and Optimization*, vol. 47, no. 2, pp. 936–949, 2008.

[56] X.-M. Sun, J. Zhao, and D. J. Hill, "Stability and l2-gain analysis for switched delay systems: A delay-dependent method," *Automatica*, vol. 42, no. 10, pp. 1769–1774, 2006.

[57] J. C. Geromel and P. Colaneri, "Stability and stabilization of continuous-time switched linear systems," *SIAM Journal on Control and Optimization*, vol. 45, no. 5, pp. 1915–1930, 2006.

[58] G. Chesi, P. Colaneri, J. Geromel, R. Middleton, and R. Shorten, "Computing upper-bounds of the minimum dwell time of linear switched systems via homogeneous polynomial lyapunov functions," in *Proceedings of the 2010 American Control Conference*, pp. 2487–2492, IEEE, 2010.

[59] R. C. Dorf and R. H. Bishop, *Modern control systems*. Pearson Prentice Hall, 2008.

[60] D. Graham and R. C. Lathrop, "The synthesis of "optimum" transient response: criteria and standard forms," *Transactions of the American Institute of Electrical Engineers, Part II: Applications and Industry*, vol. 72, no. 5, pp. 273–288, 1953.

[61] U. Taşdelen, "On Smith predictor-based controller design for systems with integral action and time delay," Master's thesis, Bilkent University, 2013.

[62] O. J. Smith, "Closer control of loops with dead time," *Chemical Engineering Progress*, vol. 53, no. 5, pp. 217–219, 1957.

[63] K. Watanabe and M. Ito, "A process-model control for linear systems with delay," *IEEE Transactions on Automatic control*, vol. 26, no. 6, pp. 1261–1269, 1981.

[64] K. J. Astrom, C. C. Hang, and B. Lim, "A new Smith predictor for controlling a process with an integrator and long dead-time," *IEEE Transactions on Automatic Control*, vol. 39, no. 2, pp. 343–345, 1994.

[65] S. Majhi and D. P. Atherton, "Obtaining controller parameters for a new Smith predictor using autotuning," *Automatica*, vol. 36, no. 11, pp. 1651 – 1658, 2000.

[66] M. R. Matausek and A. D. Micic, "A modified Smith predictor for controlling a process with an integrator and long dead-time," *IEEE Transactions on Automatic Control*, vol. 41, no. 8, pp. 1199–1203, 1996.

[67] M. R. Matausek and A. D. Micic, "On the modified Smith predictor for controlling a process with an integrator and long dead-time," *IEEE Transactions on Automatic Control*, vol. 44, no. 8, pp. 1603–1606, 1999.

[68] L. D. Cicco, S. Mascolo, and S. I. Niculescu, "Robust stability analysis of Smith predictor-based congestion control algorithms for computer networks," *Automatica*, vol. 47, no. 8, pp. 1685 – 1692, 2011.

[69] U. Taşdelen and H. Özbay, "On smith predictor-based controller design for systems with integral action and time delay," in *9th Asian Control Conference (ASCC)*, pp. 1–6, 2013.

[70] B. Francis and W. Wonham, "The internal model principle of control theory," *Automatica*, vol. 12, no. 5, pp. 457 – 465, 1976.

[71] D. Youla, H. Jabr, and J. Bongiorno, "Modern Wiener-Hopf design of optimal controllers–part ii: The multivariable case," *IEEE Transactions on Automatic Control*, vol. AC-21, no. 3, pp. 319–338, 1976.

[72] V. Feliu-Batlle and R. Rivas-Perez, "Smith predictor based fractional-order integral controller for robust temperature control in a steel slab reheating furnace," *Transactions of the Institute of Measurement and Control*, vol. 41, no. 16, pp. 4521–4534, 2019.

[73] M. Gafvert, "Comparisons of two dynamic friction models," in *Proceedings of the 1997 IEEE international Conference on Control applications*, pp. 386–391, IEEE, 1997.

[74] I. Uyanik and B. Catalbas, "A low-cost feedback control systems laboratory setup via arduino–simulink interface," *Computer Applications in Engineering Education*, vol. 26, no. 3, pp. 718–726, 2018.

[75] B. Çatalbaş and İ. Uyanık, "A low-cost laboratory experiment setup for frequency domain analysis for a feedback control systems course," *IFAC-PapersOnLine*, vol. 50, no. 1, pp. 15704–15709, 2017.

[76] H. Lee and V. I. Utkin, "Chattering suppression methods in sliding mode control systems," *Annual reviews in control*, vol. 31, no. 2, pp. 179–188, 2007.

[77] G. Bartolini and E. Punta, "Chattering elimination with second-order sliding modes robust to coulomb friction," *Journal of Dynamic Systems, Measurement, and Control*, vol. 122, no. 4, pp. 679–686, 2000.

[78] M.-C. Tsai and W.-S. Yao, "Design of a plug-in type repetitive controller for periodic inputs," *IEEE Transactions on Control Systems Technology*, vol. 10, no. 4, pp. 547–555, 2002.

[79] V. Yücesoy, *Robustly and strongly stabilizing low order controller design for infinite dimensional systems.* PhD thesis, Bilkent University, 2018.

[80] W. Lee, C.-Y. Lee, Y. H. Jeong, and B.-K. Min, "Friction compensation controller for load varying machine tool feed drive," *International Journal of Machine Tools and Manufacture*, vol. 96, pp. 47–54, 2015.

Appendix A

LMI code for a dwell time analysis

A.1: Dwell_time_main.m

```
clear all;
clc;

filename='test.mat';
m = matfile(filename, 'Writable', true); %File keeping ...
    simulation results

K=1:10000; % K vector
L=1:10000;% L vector
row=0; %Save each iteration result to a row in specified file
for i=1:length(K)
    for j=1:length(L)
        row=row+1;
        A1= [-1*K(i) -1;L(j) 0]; %Define Subsystem1
        A2= [-1*K(i) 1;-1*L(j) 0]; %Define Subsystem2
        [Tdmin]=find_dwell(A1,A2); %Find Td for corresponding ...
            iteration
        out = [K(i) L(j) Tdmin];
        m.out(row,1:3) = out; %Save Simulation results
```

```
    end
end
```

A.2: find_dwell.m

```
function [Tdmin]=find_dwell(A1,A2)
% Function Calculating the minimum dwell time for two ...
    subsystems A1 and A2

% min Td (dwell time)
%subject to
%P_{i} > 0 for all i={1,2}
%A'_{i}*P_{i}+A_{i}*P_{i} < 0 for all i
%expm(A'_{i}*Td)*P_{j}*%expm(A_{i}*Td)<P_{i} for all i!=j

I=eye(2);
eps =1e-4; % the relative accuracy of the solution
Tdmax=50; % the upper limit of the interval
Td=Tdmax; % the step size (midpoint)
b=Tdmax; % the initial upper limit of the interval
a=0; % the initial lower limit of the interval
i=0; % iteration index

    while (b-a)>eps % check whether the new interval reached ...
        the accuracy
    Td = a+(b-a)/2; % interval-halving
    i = i+1;

    setlmis([]); % define the system of LMI-s
    P1 = lmivar(1, [2, 1]);
    P2 = lmivar(1, [2, 1]);

    % constructing the system of the LMI-s
    % for subsystem 1
    lmiterm([1, 1, 1, P1], 1, A1, 's');
    % LMI #1: A'_{1}*P_{1} + P_{1}*A_{1}
    lmiterm([2, 1, 1, P2], expm(Td*A1)', expm(Td*A1));
    % LMI #2: expm(Td*A'_{1})*P_{2}*expm(Td*A_{1})
    lmiterm([2, 1, 1, P1], -1, 1);
```

```
33      % LMI #2: P_{1}
34
35      % for subsystem 2
36      lmiterm([3, 1, 1, P2], 1, A2, 's');
37      % LMI #3: A'_{2}*P_{2} + P_{2}*A_{2}
38      lmiterm([4, 1, 1, P1], expm(Td*A2)', expm(Td*A2));
39      % LMI #4: expm(Td*A'_{2})*P_{1}*expm(Td*A_{2})
40      lmiterm([4, 1, 1, P2], -1, 1);
41      % LMI #2: P_{2}
42
43      %for P_{i}>0
44      lmiterm([-5, 1, 1, P1], 1, 1);
45      lmiterm([-6, 1, 1, P2], 1, 1);
46
47      lmiterm([-7, 1, 1, P1], -1, 1); % LMI #2: -Zj
48      lmiterm([-7, 1, 1, 0], P2); % LMI #2: Yq
49
50      lmis = getlmis; % obtaining the system of LMI
51      [tmin,xfeas] = feasp(lmis); % calling function of feasibiliy.
52
53      Ps1 = dec2mat(lmis,xfeas,P1);
54      Ps2 = dec2mat(lmis,xfeas,P2);
55  % decision vector xfeas since tmin < 0
56  % checking constraints of feasibility. That is that if % tmin ...
        < 0.
57      if tmin ≥ 0
58          a = Td; % the minimum is changed to the Td
59      else
60          b = Td; % iteration is continued the minimum
61          Tdm = b; % Save Tdmin for this iteration
62      end
63      end
64  Tdmin = Tdm; % Final Tdmin is obtained
65  end
```

Appendix B

Simulink settings for the Arduino Experiments

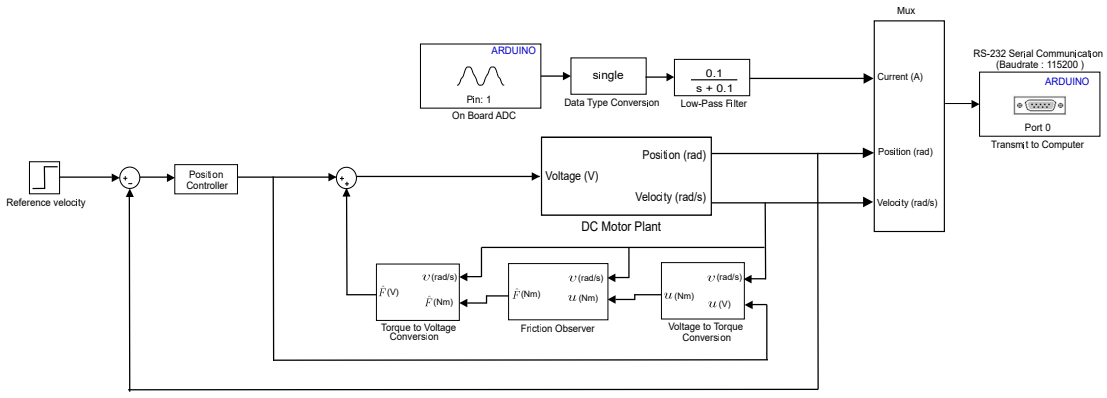

Figure B.1: An example for closed loop feedback system runnig on Arduino Uno

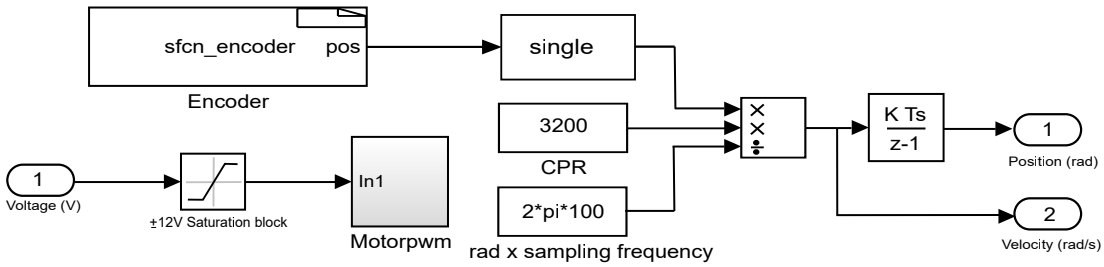

Figure B.2: Sublock diagram of DC Motor Plant

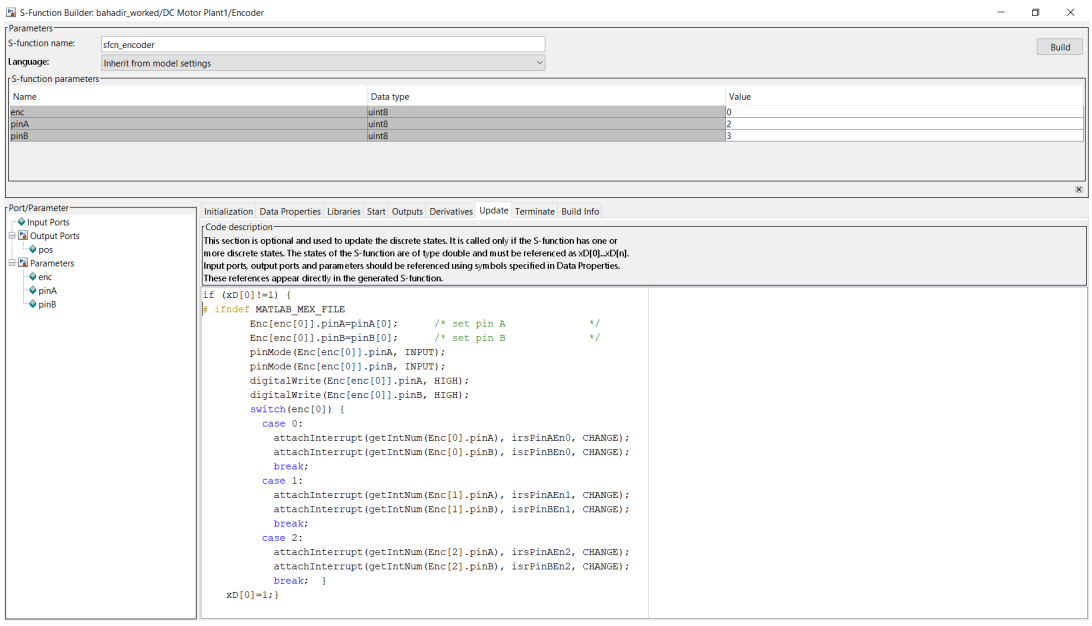

Figure B.3: The S-Function block settings for the encoder.

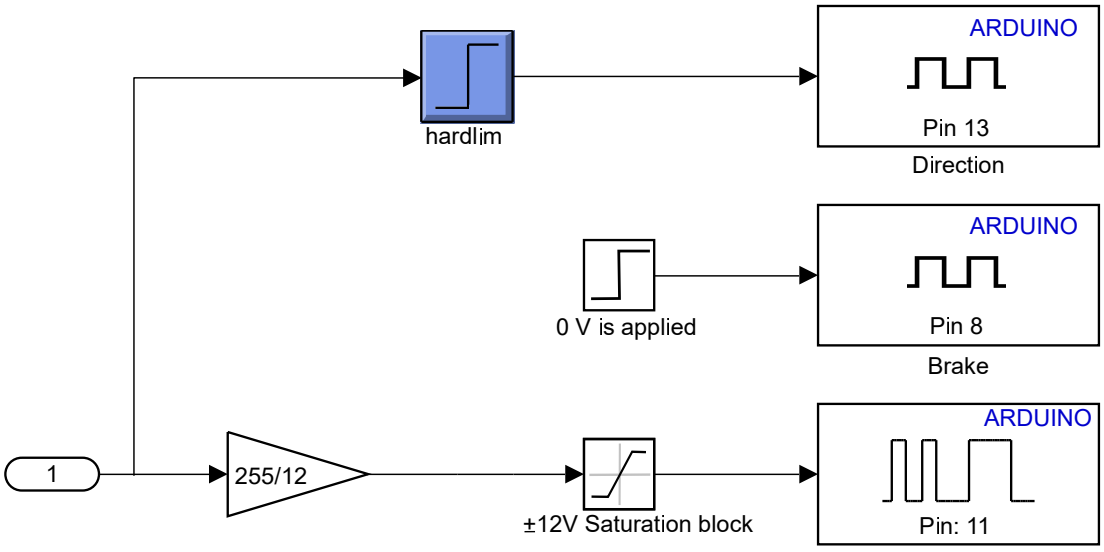

Figure B.4: The Matlab Simulink Pulse width modulation (PWM) implemenation on Arduino.

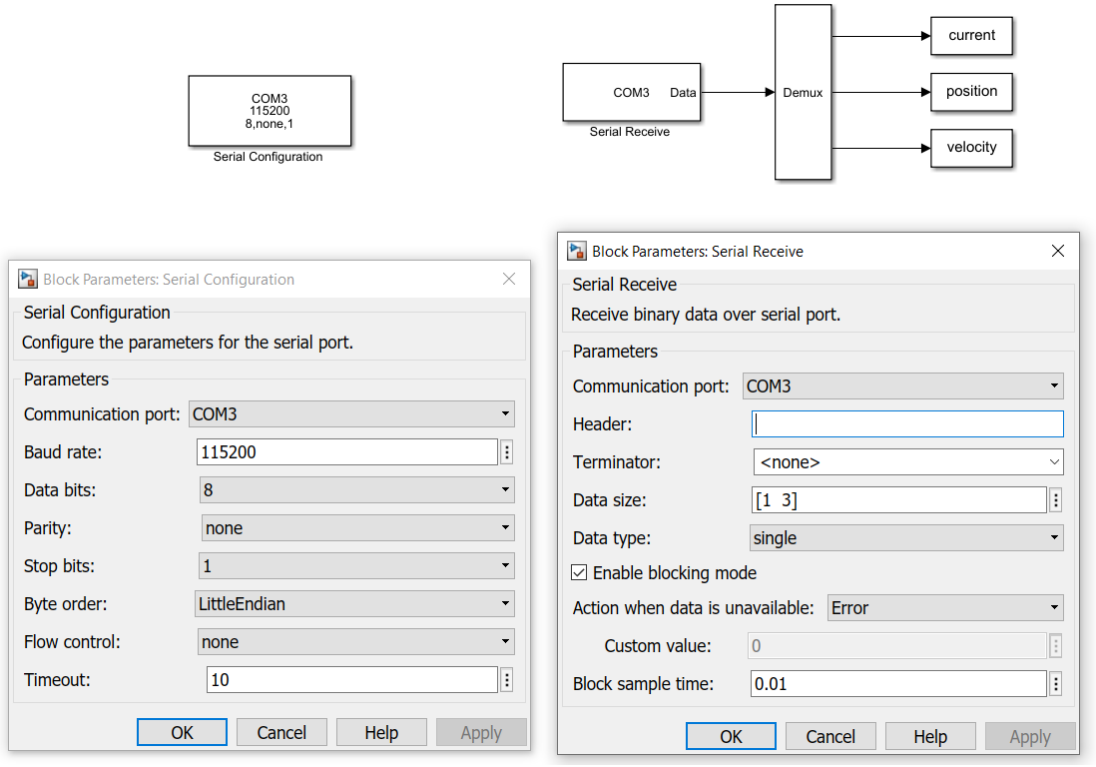

Figure B.5: The Matlab Simulink serial port reading settings.